

A Method for Measuring Formation Pressure

by

Laura Alexis Montalvo

B.S., Mechanical Engineering (1999)
Massachusetts Institute of Technology

Submitted to the Department of Mechanical Engineering in Partial
Fulfillment of the Requirements of the Degree of

Master of Science in Mechanical Engineering

at the

MASSACHUSETTS INSTITUTE OF TECHNOLOGY

June 2000

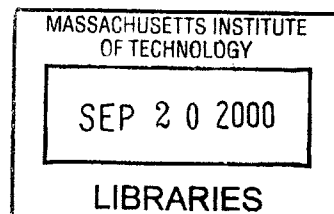
© 2000 Laura Alexis Montalvo. All rights reserved.

The author hereby grants MIT permission to reproduce and
distribute publicly paper and electronic copies of this thesis document
in whole or in part.

Author.....
Department of Mechanical Engineering
May 19, 2000

Certified by.....
Ernesto E. Blanco
Adjunct Professor of Mechanical Engineering
Thesis Supervisor

Accepted by.....
Ain A. Sonin
Chairman, Department Committee on Graduate Students



ENG

A Method for Measuring Formation Pressure

by

Laura Alexis Montalvo

Submitted to the Department of Mechanical Engineering on May 10, 2000,
in partial fulfillment of the requirements for the degree of
Master of Science in Mechanical Engineering

Abstract

This thesis presents the development of a new method for measuring formation pressure for Schlumberger, Ltd., a leader in the oil well service industry. This project was part of the Engineering Internship Program at the Massachusetts Institute of Technology, and all of the research took place on site at Schlumberger's Sugar Land Product Center (SPC) in Sugar Land, Texas.

Currently, in the oil well service industry, the methods for obtaining pressure measurements involve a drawdown technique, which can often times, take several hours for obtaining one measurement. The goal of this thesis is to determine the feasibility of a new concept for measuring formation pressure downhole. The new method for measuring formation pressure, called the Nozzle Concept, was developed and tested as a part of this thesis. As well, an experimental apparatus was built to test the Nozzle concept.

Experimental testing proved the Nozzle Concept to be a feasible method for measuring formation pressure. The results from the Nozzle Concept tests showed that formation pressure can be measured through a small orifice nozzle by creating a seal with the mudcake layer. The experimental data showed that the nozzle concept measures maximum formation pressure quickly, dissipates to a lower formation pressure very slowly, and the mudcake seals the nozzle only if the nozzle is initially at the face of the formation.

Thesis Supervisor: Ernesto E. Blanco
Title: Adjunct Professor of Mechanical Engineering

Acknowledgements

First and foremost, I would like to express my sincere appreciation to my Schlumberger advisor, Wayne Sundquist, whose mentorship and friendship made this thesis project not only an incredible learning experience, but also an enjoyable one.

On an academic level, I would like to thank my MIT advisor Professor Ernesto Blanco, Karl Reid, and Leslie Regan whose support of the Engineering Internship Program made this thesis project at Schlumberger a success.

On a professional level, I would like to thank the entire Reservoir Sampling and Pressure Department and Aaron Flores, “my work family”, for supporting this program and my project. Special thanks to Andrew Kurjian, Mario Flores, Joe Nahas, Lin Moore, Michelle Tesciuba, Cecilia Prieto, Lennox Reid, Sony Tran, and Ben Kovar without whose guidance and abundant technical help, this project would have never been possible. I would also like to express my appreciation to Mark Brady, Paul Sehgal, and Andrew Werner whom provided their technical expertise whenever needed. To everyone at the Schlumberger Sugar Land Product Center, I would like to say thank you for a well organized, finely run product development center that made this project possible.

Table of Contents

Abstract	3
Acknowledgements	4
Table of Contents	5
List of Figures	7
List of Tables.....	9
1 Introduction	11
1.1 Schlumberger	11
1.2 Background and Motivation	13
1.3 Thesis Summary.....	14
2 Formation Pressure.....	15
2.1 Importance of Measuring Formation Pressure.....	15
2.1.1 Determining Mud Weight.....	15
2.1.2 Flow Performance of the Reservoir.....	17
2.2 Current Methods of Measuring Pressure Down hole.....	17
2.2.1 Draw-Down Method.....	18
2.2.1.3 Customer Concern's of Draw-Down Method	20
2.2.2 The Modular Formation Dynamics Tester (MDT) TM	20
2.3 Cone Penetrometer Technology (CPT).....	21
2.3.1 CPT Applications	22
2.3.2 Piezo-Cone Penetrometer	23
2.3.3 ASTM Standards	24
3 Wellbore Conditions During Reservoir Development.....	27
3.1 The Effects of Drilling Fluids on the Formation	27
3.1.1 Particulate Invasion from Drilling Fluid	27
3.1.2 Bridging Agents and Mudcake Properties.....	28
3.2 Drilling Fluid Effects on Pressure Measurements	29
3.3 Advances in Drilling Fluid Technology	29
3.3.1 STARDRILL Fluid.....	31
4 The Nozzle Concept.....	33
4.1 F&H Nozzle.....	33
4.2 Nozzle Probe Assembly.....	34
5 The Formation Pressure Tester	37
5.1 Stickance Tester	38
5.2 Design of Formation Pressure Tester.....	39
5.2.1 Modified Parts	41
5.2.2 Designed Parts	41
5.2.3 Other Components of the Apparatus	41
5.3 Experimental Setup.....	42
6 Experimental Testing and Results.....	45
6.1 Core Analysis.....	45
6.1.1 Mudcake Analysis	45
6.1.2 Permeability Analysis.....	45
6.1.3 SEM Analysis	47

6.2 Nozzle Concept Tests and Results.....	47
Test 01	48
Test 02	49
Test 03	50
Test 04	51
Test 05	52
Test 06	53
Test 07	54
Test 08	56
Test 09	56
Test 10	57
Test 12	58
Test 13	59
Test 14	60
Test 15	61
Test 16	62
Test 17	63
Test 18	64
Test 19	64
Test 20	65
Test 21	67
Test22	68
Test 23	69
Test 24	70
Test 25	71
Test 26	72
Test 27	73
Test 28	74
Test 29	75
Test 30	76
Test 31	77
Test 32	78
7 Conclusions and Recommendations.....	81
7.1 Conclusions.....	81
7.2 Recommendations for Future Work.....	84
References	85
Appendix A	87
A.1 F&H Nozzles and Retaining Nuts.....	87
A.2 Cores and Disc Filters	89
A.2.1 Capstan Stainless Bronze Disk Filters	89
A.2.2 Mott Corporation Steel Disk Filters	91
Appendix B	92
B.1 Fann Instrument Company	92

List of Figures

Figure 1.1: Logging Tool in wellbore.	11
Figure 1.2: Schlumberger Logging Tools.	12
Figure 2.1: Hydrostatic Pressure vs. Depth.	15
Figure 2.2: Blowout due to under balance of mudweight in borehole.	17
Figure 2.3: Schlumberger's Modular Dynamic Formation Tester Probe.	19
Figure 2.4: The Modular Formation Dynamic Tester Tool.	20
Figure 2.5: Experimental Assembly for testing the MDT probe.	21
Figure 2.6: Schematic of Cone Penetrometer.	23
Figure 2.7: Reference Piezocone Penetrometer.	24
Figure 3.1: Illustration of Drilling Fluid-Formation Interaction.	27
Figure 3.2: Mud damage zone in open hole.	28
Figure 3.3: STARDRILL Drill-In Fluid vs. Conventional System.	30
Figure 3.4: STARDRILL fluid leaves no-skin mudcake on formation.	31
Figure 4.1: Nozzle Concept.	33
Figure 4.2: F&H Nozzles and Retaining Nuts.	34
Figure 4.3: F&H Nozzle and Retaining Nut Assembly.	34
Figure 4.4: F&H Nozzle and shaft assembly.	35
Figure 5.1: Schematic of Formation Pressure Tester.	37
Figure 5.2: Dowell Ball Stickance Tester.	39
Figure 5.3: Schematic of the Nozzle Concept Experimental Setup.	40
Figure 6.1: Mudcake build up on core from STARDRILL fluid.	45
Figure 6.2: Berea Sandstone Core before and after mudcake build up.	47
Figure 6.3: Pictures of Nozzle Concept Test 1.	49
Figure 6.4: Pressure vs. Time graph of Nozzle Concept Test 2.	50
Figure 6.5: Picture of core from Nozzle Concept Test 2.	50
Figure 6.6: Pressure vs. Time graph of Nozzle Concept Test 3.	51
Figure 6.7: Pictures of Nozzle Concept Test 3.	51
Figure 6.8: Pressure vs. Time graph of Nozzle Concept Test 4.	52
Figure 6.9: Pictures of Nozzle Concept Test 4.	52
Figure 6.10: Pressure vs. Time graph of Nozzle Concept of Test 5.	53
Figure 6.11: Picture of Nozzle Concept Test 5.	53
Figure 6.12: Pressure vs. Time graph of Nozzle concept Test 6.	54
Figure 6.13: Pictures of Nozzle Concept Test 6.	54
Figure 6.14: Pressure vs. Time graph of Nozzle Concept Test 7.	55
Figure 6.15: Pictures of Nozzle Concept Test 7.	55
Figure 6.16: Pressure vs. Time Graph of Nozzle CoNcept Test 8.	56
Figure 6.17: Pictures of Nozzle Concept Test 8.	56
Figure 6.18: Pressure vs. Time Graph of Nozzle Concept Test 9.	57
Figure 6.19: Pictures of Nozzle Concept Test 9.	57
Figure 6.20: Pressure vs. Time Graph of Nozzle Concept Test 10.	58
Figure 6.21: Pictures of Nozzle Concept Test 10.	58
Figure 6.22: Pressure vs. Time graph of Nozzle Concept Test 12.	59
Figure 6.23: Pictures of Nozzle Concept Test 12.	59

Figure 6.24: Pressure vs. Time Graph of Nozzle Concept Test 13.....	60
Figure 6.25: Pictures of Nozzle Concept Test 13.....	60
Figure 6.26: Picture of core from Nozzle concept Test 14.	61
Figure 6.27: Picture of core from Nozzle concept Test 15.	61
Figure 6.28: Pressure vs. Time graph of Nozzle concept Test 16.....	62
Figure 6.29: Pictures of Nozzle Concept Test 16.....	62
Figure 6.30: Pressure vs. Time graph of Nozzle Concept Test 17.....	63
Figure 6.31: Pictures of Nozzle Concept Test 17.....	63
Figure 6.32: Pressure vs. Time graph of Nozzle Concept Test 18.....	64
Figure 6.33: Pictures of Nozzle Concept Test 18.....	64
Figure 6.34: Pressure vs. Time graph of Nozzle Concept Test 19.....	65
Figure 6.35: Pictures of Nozzle Concept Test 19.....	65
Figure 6.36: Pressure vs. Time Graph of Nozzle Concept Test 20.....	66
Figure 6.37: Pressure Decay vs. Time graph of Nozzle Concept Test 20.....	67
Figure 6.38: Pictures of Nozzle Concept Test 20.....	67
Figure 6.39: Pressure vs. Time graph of Nozzle Concept Test 21.....	68
Figure 6.40: Pressure decay vs. Time graph of Nozzle Concept Test 22.	69
Figure 6.41: Pressure Decay vs. Time graph of Nozzle Concept 23.	70
Figure 6.42: Pressure Decay vs. Time graph of Nozzle Concept Test 24.....	71
Figure 6.43: Pressure vs. Time Graph of Nozzle Concept Test 25.....	72
Figure 6.44: Pressure vs. Time graph of Nozzle Concept Test 26.....	73
Figure 6.45: Pressure vs. Time graph of Nozzle Concept Test 27.....	74
Figure 6.46: Pressure vs. Time Graph of Nozzle Concept Test 28.....	75
Figure 6.47: Pictures of Nozzle Concept Test 28.....	75
Figure 6.48: Pressure vs. Time graph of Nozzle Concept Test 29.....	76
Figure 6.49: Pictures of Nozzle Concept Test 29.....	76
Figure 6.50: Pressure vs. Time Graph of Nozzle Concept Test 30.....	77
Figure 6.51: Pictures of Nozzle Concept Test 30.....	77
Figure 6.52: Pressure vs. Time Graph of Nozzle Concept Test 31.....	78
Figure 6.53: Pictures of Nozzle Concept Test 31.....	78
Figure 6.54: Pressure vs. Time graph of Nozzle Concept Test 32.....	79
Figure 6.55: Pressure Decay vs. Time Graph of Nozzle Concept Test 32.....	80
Figure 6.56: Pictures of Nozzle Concept Test 32.....	80
Figure 7.1: Nozzle pressure measures Maximum Water Pressure quickly.....	81
Figure 7.2: Dissipation Rate of nozzle pressure to a lower formation pressure.....	82
Figure 7.3: Dissipation rate to a lower water pressure.....	82
Figure 7.4: Dissipation Rate to a lower water pressure.....	83
Figure 7.5: Capillary Pressure effects on nozzle pressure (non existent)	83

List of Tables

Table 2.1: Density Differences 16
Table 6.1: Permeability test results for a berea sandstone core. 46

1 Introduction

1.1 Schlumberger

Schlumberger, the leading oilfield services company in the world [1], provides Reservoir Evaluation, Reservoir Development and Reservoir Management to the petroleum industry. Services range from seismic data acquisition to drilling and completion, evaluation, reservoir monitoring and control, and data services and software. Many of these services are implemented using oil well tools. Schlumberger has a complete product line of oil well tools specialized for functions varying from monitoring pressures of fluids to controlling the flow of fluids. These tools have an elongated, cylindrical shape to fit inside the borehole of the oil well [2] as demonstrated in Figure 1.1. A picture of common oil well logging tools is shown in Figure 1.2.

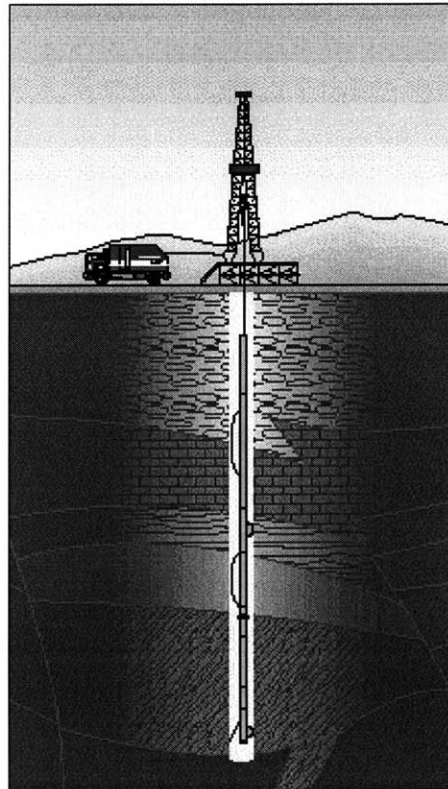


Figure 1.1: Logging Tool in wellbore.

Down-hole logging and sampling tools allow Schlumberger to deliver accurate, detailed reservoir data and cost-effective well completion and testing. Research and engineering efforts are focused on developing methods to provide a more detailed image of the reservoir and to produce oil and gas reserves most economically. Schlumberger has several research and development facilities whose goals are to provide the most technically advanced products available [3].



Figure 1.2: Schlumberger Logging Tools.¹

Schlumberger's Sugar Land Product Center (SPC) focuses on the improvement of existing tools as well as the development of new, innovative tools for the advancement of oilfield services. Every new project at Schlumberger undergoes concept, feasibility, development, field and testing, and commercialization phases.

¹ Picture taken from the Schlumberger internal website.

Concept phase, the initial phase of a project, provides the scientific, conceptual basis for a proposed product. In this phase, all scientific limitations, risks, and alternate technologies are identified. In addition, concept phase establishes the likelihood of the project meeting significant market needs. If market needs are met then the concept phase includes the development of a strategy to obtain an exclusive position in the relevant technology [4].

This thesis work, conducted at Schlumberger's Sugar Land Product Center, entails the evaluation of a new concept for measuring formation pressure. The new method, which from here on out will be referred to as the Nozzle Concept, measure formation pressure using a small orifice nozzle to penetrate through the mudcake layer to the face of the formation, form a seal with the mudcake, and communicate with the formation. Work involved fully investigating and understanding the concept, and the design and fabrication of a test set-up to test and evaluate the Nozzle Concept. The main goal of the project was to verify the feasibility of this method of measuring pressure down-hole. The focus of this project is on the concept of measuring pressure down hole, and is in no part related to any specific logging tool.

1.2 Background and Motivation

Oil and gas companies around the world are always seeking new ways to optimize the performance of their reservoirs and to maximize recovery of their resources [3].

Reservoir characterization helps them do so by providing knowledge of the dynamics of the well at hand. Schlumberger provides logging and sampling data for characterization of reservoir dynamics. Important reservoir characteristics that Schlumberger provides the client include anisotropic permeability, static (annulus, hydrostatic) pressure, resistivity, temperature, permeability, fluid and gas samples, as well as formation samples. With this data, Schlumberger can put together the puzzle of exactly what production performance to expect from a particular well and whether or not it is worth producing. Some of these measurements can be taken while in the process of drilling the well, while others cannot be taken until the well has been cased with steel piping. However, the earlier these measurements can be made, the better the job can be done to ensure optimization of a

reservoir. Schlumberger's research and product centers are focused on the advancement of what they can offer the oil industry.

1.3 Thesis Summary

The first part of this thesis introduces the importance of measuring formation pressure, current methods for measuring formation pressure down hole, technologies used for measuring pressure in other applications, and wellbore conditions during reservoir development. The second part of this thesis presents a new concept for measuring formation pressure, the test apparatus and method used to prove feasibility of the concept, and the results of the concept.

The Nozzle Concept is based on the cone penetrometer technology developed for geotechnical investigations [11] and advancements in drilling fluid technology. Information on penetrometer technology was gathered from several sources, including the U.S. Department of Energy, ASTM standards, and geotechnical companies such as Fugro, Pagani, and several Geotechnical theses [11], [5], [6], [7], [8], [9]. (References noted in this thesis are publicly available).

To implement this technology, a small orifice nozzle from F&H Nozzle Specialists, Inc. was used to penetrate through the mud cake layer of the formation. In theory, if the ratio of the mud cake's particle size to the nozzle's tip diameter is great enough, the nozzle will penetrate through the mud cake, form an effective seal around the nozzle, and be exposed to formation pressure. As well, the ratio of the nozzle orifice size to the mud particle size will determine whether or not the nozzle will clog. This technique is similar to the fluid mechanics of a syringe drawing blood. It penetrates the skin, does not clog when puncturing the skin, and draws out blood through the needle rather than spurting out around it.

Reservoir formation and drilling fluid properties were researched in order to understand the conditions in which the Nozzle Concept method would be implemented. Furthermore, SEM (scanning electron microscopy) analysis and permeability tests were performed in situ of this study to understand this interaction for testing purposes.

2 Formation Pressure

2.1 Importance of Measuring Formation Pressure

Pressure measurements are important in evaluating the reservoir at all stages of well development. Knowing the formation pressure can help determine an appropriate drilling fluid weight for the well, and flow performance and production capabilities of the reservoir.

2.1.1 Determining Mud Weight

When drilling a borehole, the rock removed from the well must be replaced with an equivalent weight (hydrostatic pressure) for stability. Drilling fluid, more commonly known as mud, is used to stabilize the formation during reservoir evaluation and development by compensating for the weight loss from the removed formation.

As illustrated in Figure 2.1, there is a linear relationship between the hydrostatic pressure and vertical depth of a column of fluid, such that the pressure gradient of the fluid can be calculated.

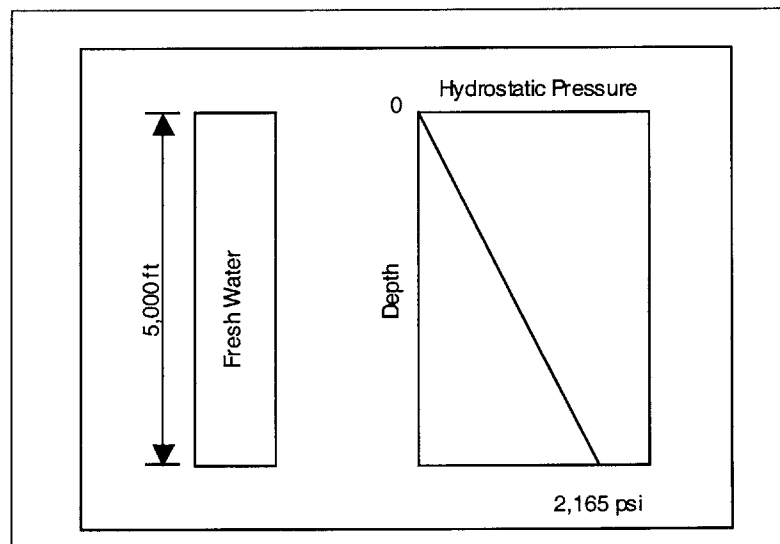


Figure 2.1: Hydrostatic Pressure vs. Depth.²

² Taken from a Schlumberger Wireline and Testing Manual Report on Pressure.

However, when dealing with the formation, which is a combination of rock, oil, gas, and water in various amounts at different vertical depths, calculating this pressure gradient is not so simple and is by no means constant. The densities of the different fluids as well as their contribution per depth must be taken into account when calculating the mud weight. The density of oil, salt water and mud are shown in Table 2.1 for comparison.

Table 2.1: Density Differences ²

Fluid Type	lbm/gal	lbm/cu.ft.
Mud	12.68	94.9
Saltwater	8.96	67.0
Oil	6.88	51.5

Drilling fluids are designed to accommodate the pressure gradient differences in the well bore, but their accuracy is highly dependent on the estimations of the original formation pressures. Knowing the formation pressure in the early stages of well development, would improve the mud performance.

2.1.1.1 Mud Weight Overbalance

If there is an over balance in the mud weight, such that the mud weight is much greater than the formation pressure, $P_{\text{mud}} \gg P_{\text{formation}}$, the drilling mud will invade the formation causing significant damage to the reservoir that could reduce production capabilities of the well. At worst, if the formation rock has a relatively high permeability and porosity, the invasive drilling fluid could completely block any passage of flow out of the well, destroying all production capabilities at the well site.

2.1.1.2 Mud Weight Under-Balance

If there is an under balance in the mud weight, such that the formation pressure is greater than borehole pressure, $P_{\text{formation}} > P_{\text{mud}}$, a blow out could occur causing an uncontrollable, unrecoverable loss of hydrocarbons from the well. A blow not only causes production losses, but several safety and environmental problems as well. Figure 2.2 depicts the catastrophe that occurs from a blow out.



Figure 2.2: Blowout due to under balance of mudweight in borehole.³

Knowing the formation pressure at early stages of development can help determine the appropriate drilling fluid weight needed for a particular well and could possibly prevent damage to the formation and blowouts.

2.1.2 Flow Performance of the Reservoir

The flow rate of hydrocarbons in a reservoir is dependent upon reservoir size, shape, and location, and the formation pressure, permeability, and porosity. Knowing the formation pressure can help determine flow performance of the reservoir such as how fast the well will produce and the amount it will produce. With this information, the rate of production can be set according to the maximum number of barrels of oil per day that the well is capable of producing. By knowing the formation pressure at an early stage of development, better efforts can be made to produce the well most efficiently.

2.2 Current Methods of Measuring Pressure Down hole

Currently, methods for obtaining pressure measurements are limited to systems that involve taking measurements in the open hole using wireline conveyed tools after the drill pipe has been removed. Often times these tools get stuck in the borehole because of

³ Figure 1.2 is a Photo of a blow out taken in 1992 by Schlumberger Dowell in Kuwait.

the time it takes to obtain each pressure measurement. (Reason's for tool sticking will be discussed in more detail in 5.1 Stickance Tester). From the customer's standpoint, it would be desirable to obtain accurate formation pressure measurements while drilling to minimize the risk of a blow out, formation damage, and any early stage problems that could compromise the productivity of the reservoir.

2.2.1 Draw-Down Method

The current technique used to measure formation pressure in both Schlumberger's formation testers and in the competitions' tools, known as the "draw-down method", has been utilized for decades. A formation tester tool is typically comprised of a donut-shaped rubber packer pushed against the borehole wall in order to isolate a small area of rock face as illustrated in Figure 2.3. Then a hydraulically powered piston is withdrawn and the pressure within this volume of mud is reduced significantly below the formation pressure. As time passes, fluid flows from the rock into the tool and the measured pressure converges to the actual formation pressure.

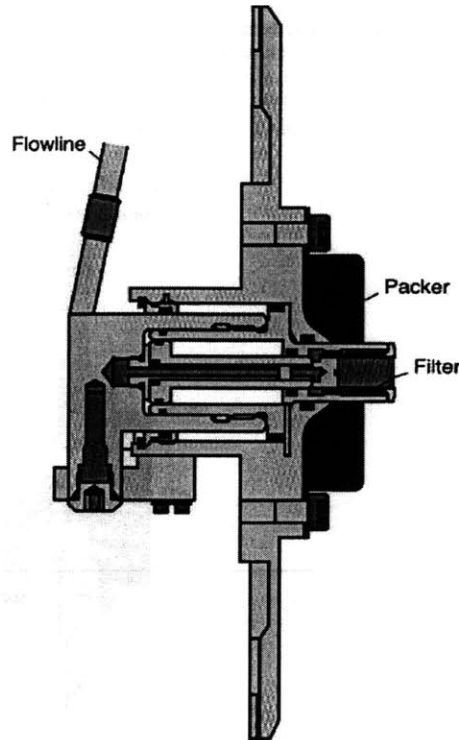


Figure 2.3: Schlumberger's Modular Dynamic Formation Tester Probe.⁴

2.2.1.1 Advantages of Draw-Down Method

The advantages of using the drawdown technique are that it already exists and is thoroughly understood, customers accept it as a “standard procedure”, and it is successful in a wide variety of formations [10].

2.2.1.2 Disadvantages of Draw-Down Method

The disadvantages of the draw-down technique are that it takes too long in low permeability formations (leads to tool sticking), creates large pressure imbalances (leads to packer failures), it requires hydraulic-power (leads to high maintenance), tends to require large and heavy tools, does not work well in unconsolidated formations (due to the high packer stresses), and tends to plug the tool with formation sands [10].

MDT™ Mark of Schlumberger

⁴ MDT™ Probe illustration taken from “Schlumberger Wireline Formation Testing and Sampling” book (SMP-7058).

2.2.1.3 Customer Concern's of Draw-Down Method

From customer analysis, the main concerns of making formation pressure measurements using the drawdown method are fear of sticking, cost of service, and reliability [10].

2.2.2 The Modular Formation Dynamics Tester (MDT)TM

The Modular Formation Dynamics Tester shown in Figure 2.4, better known as the MDTTM, is Schlumberger's wireline conveyed tool that has a module for sampling and measuring pressure down hole.

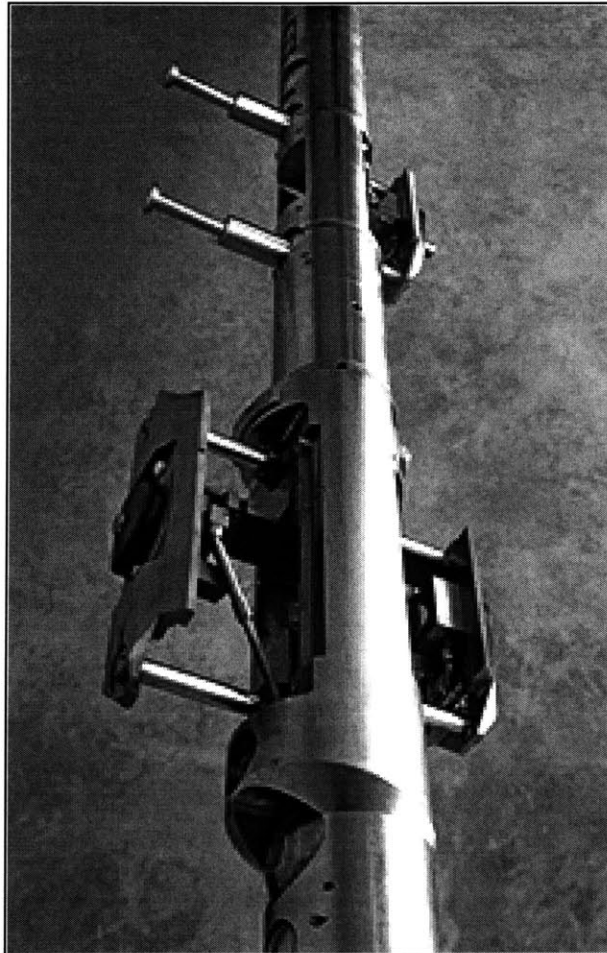


Figure 2.4: The Modular Formation Dynamic Tester Tool.⁵

The MDT takes pressure measurements using the draw down method previously described. The MDT pressure-sampling module creates a seal with the borehole wall and

⁵ Taken from Schlumberger MDT review. SMP-5124/January 1996.

“draws back:” by changing the volume with in the flow line of the tool. This in turn creates a pressure drop between the formation and the sample chamber and a fluid sample is taken. Because there is a drop in pressure, the sample taken is initially at lower pressure than the formation pressure. The pressure then overcompensates and increases to some pressure above formation pressure, and gradually equilibrates to formation pressure. As discussed in Section 2.2.1, this method can take anywhere from a few minutes to days depending on the porosity and permeability of the formation being sampled.

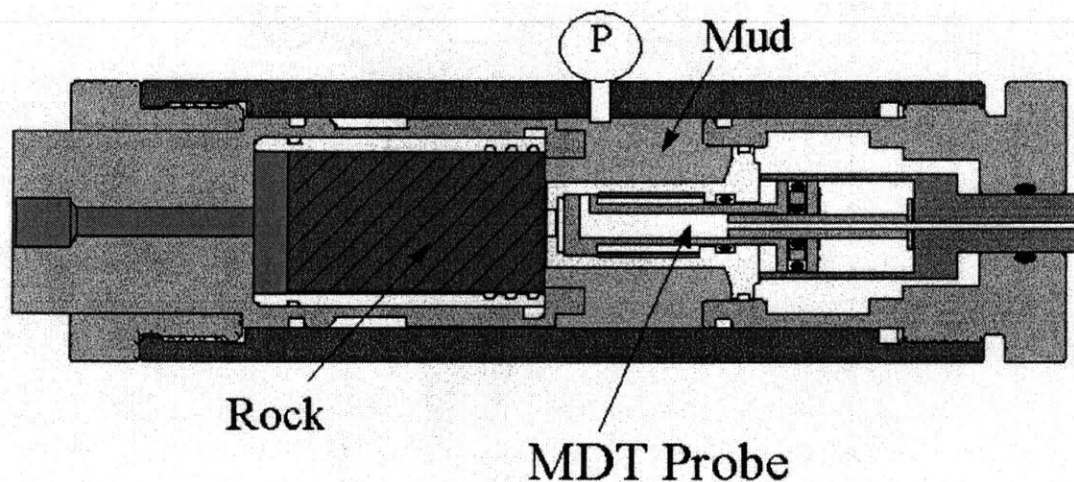


Figure 2.5: Experimental Assembly for testing the MDT probe.⁶

Figure 2.5 shows an experimental assembly with the MDT probe installed. The MDT typically uses a packer to seal the area to be tested, but is not needed for this test set up, since the area is of comparable size to the internal volume in the packer.

2.3 Cone Penetrometer Technology (CPT)

A major part of this project was researching methods used to measure pressure in other applications. One of the more promising technologies researched was the Cone Penetrometer Technology (CPT). Information on cone penetrometer technology was

⁶ Picture taken from Ken Havlinek’s report on “Obtaining Formation Pressure using an Ultra-Sonic Horn”[10].

gathered from the U.S. Department of Energy (DOE), Fugro Geotechnical Company, Pagani Geotechnical Equipment, and Cone Penetrometer ASTM standards.

2.3.1 CPT Applications

Cone Penetrometer Technology provides real-time data for use in the characterization of the subsurface, and can be adapted for new sensors to measure various types of chemical contaminants and other physical characteristics of the subsurface [11].

The cone penetrometer consists of a steel cone that is hydraulically pushed into the ground while in situ measurements are continuously collected and transported to the surface for data interpretation and visualization. Standard cone penetrometers collect stratigraphic information using sensors for cone tip pressure and sleeve friction. The ratio of the tip resistance to the sleeve friction provides information that can be used to classify soil type.

Other sensors available include two-axis inclinometers, acoustic cone (for identification of soil type), temperature, pH, radioactivity (gamma), and geophones for measurement of pressure, P , and shear waves (surface to borehole seismic), S . [11] A schematic of a cone penetrometer used for radiation detection is illustrated in Figure 2.6.

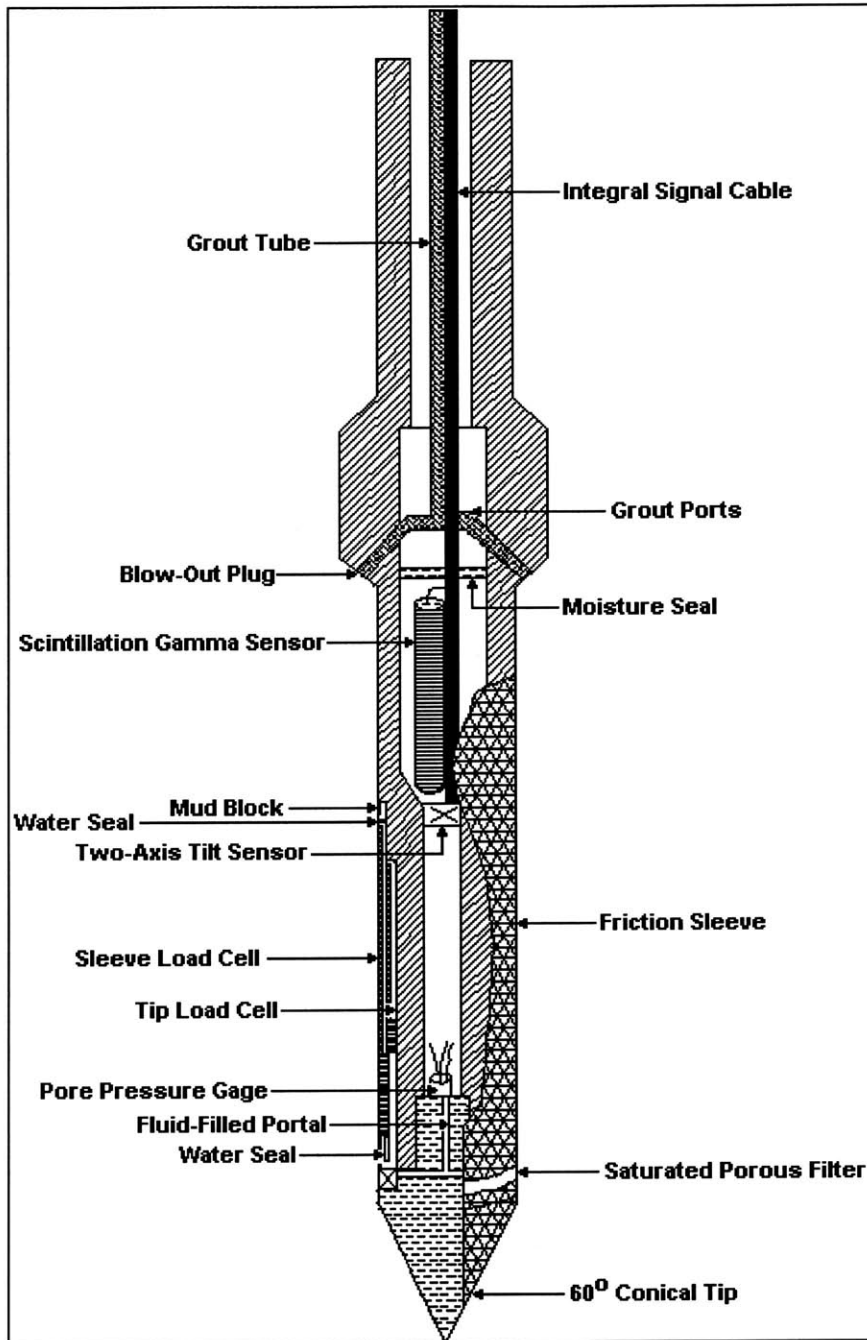


Figure 2.6: Schematic of Cone Penetrometer.⁷

2.3.2 Piezo-Cone Penetrometer

As mentioned in Section 2.3.1, Cone penetrometer technology can be used for a variety of applications just by changing the internal components of the probe. Fugro has

⁷ Schematic taken from U.S. Department of Energy Innovative Technology Summary Report: Cone Penetrometer. April 1996 (DOE/EM-0309).

developed a piezo-cone test that takes continuous measurement of cone resistance (q_c), sleeve friction (f_s) and pore pressure (u) using a piezo-cone penetrometer. The piezo-cone penetrometer is an electrical measuring instrument for piezo cone penetration (CPTU). These measurements improve the interpretation quality of the soil conditions.

As well, the piezo-cone penetrometer can take measurements of the dissipation of the transient pore pressure by interrupting the penetration of the probe. The transient pore pressure can be significant for some low-permeability soils [6].

2.3.3 ASTM Standards

ASTM Standard D5778-95, “Standard Test Method for Performing Electronic Friction Cone and Piezocone Penetration Testing of Soil,” is a test method used to determine pore pressure development during push of a piezocone penetrometer [5]. A standard piezocone penetrometer is shown in Figure 2.7.

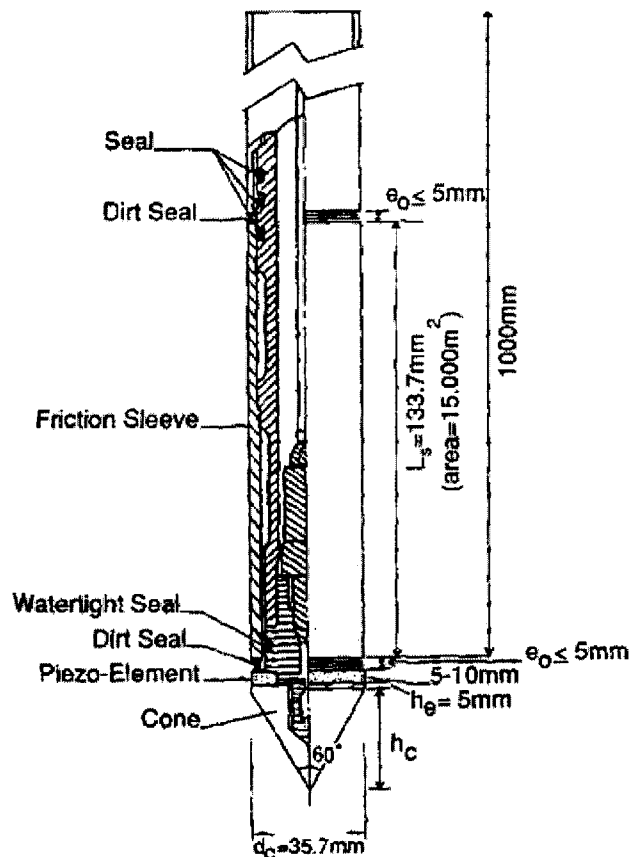


Figure 2.7: Reference Piezocone Penetrometer.

In general, electronic piezocone penetrometers can contain porous element(s), pressure transducer(s), and fluid filled ports connecting the elements to the transducer to measure pore water pressure. The pore pressure measurement locations of the porous element are limited to the face or tip of the cone, directly behind the cylindrical extension of the base of the cone, or behind the sleeve. The electronic piezocone penetrometer tip measures pore water pressure on the exterior of the penetrometer tip by transferring the pressure through a de-aired fluid system to a pressure transducer in the interior of the tip [5].

The information gathered on Piezocone Penetrometer Technology had a great influence on the Nozzle concept development in this thesis; specifically the porous conical tip of the penetrometer that is used to communicate with the fluid.

Several studies have also been done on rock penetration and indentation. This information was useful in the selection of a concept for measuring formation pressure, however all information gathered is confidential to Schlumberger.

3 Wellbore Conditions During Reservoir Development

Measuring formation pressure down hole is a challenging task considering the complexity of the conditions of the down hole environment during reservoir development. Not only does the formation contain different geological properties, but it is also exposed to a series of fluids and operations that change these properties.

3.1 The Effects of Drilling Fluids on the Formation

3.1.1 Particulate Invasion from Drilling Fluid

During development, drilling fluids are pumped into the wellbore to stabilize the formation. These drilling fluids damage the reservoir such that there is a physical reduction in pore or pore throat size and a relative permeability reduction of the formation. The damage to the near-wellbore formation, called the skin damage zone, is the area of extra pressure drop around the wellbore as shown in Figure 3.1.

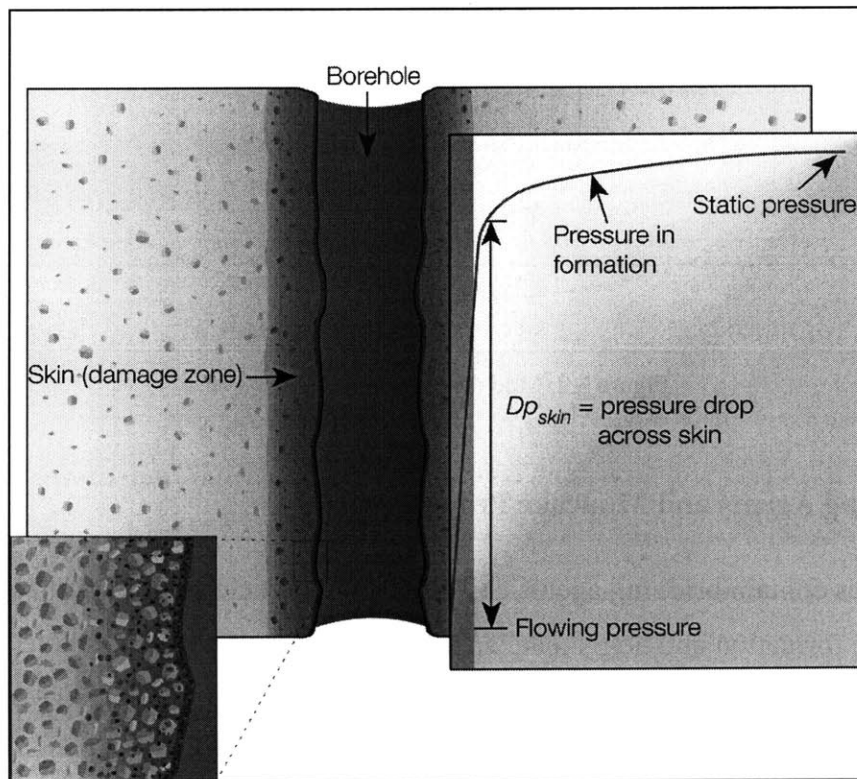


Figure 3.1: Illustration of Drilling Fluid-Formation Interaction.

This area of formation damage can be measured in terms of the skin factor, S , such that:

$$S = (k / k_d - 1) \ln(r_d / r_w) \quad (1)$$

where, k is the permeability of the formation, k_d is the permeability of damaged region, r_d is the radius of the damaged region, and r_w is the radius of the wellbore as depicted in Figure 3.2. When $S > 0$, the formation is damaged, when $S = 0$, there is no damage, and if $S < 0$, there is enhanced production of the reservoir such that the well produces better after using drilling fluids. Hence, the skin factor and radial depth of the skin damage zone is highly dependent upon the properties of the drilling fluid [12].

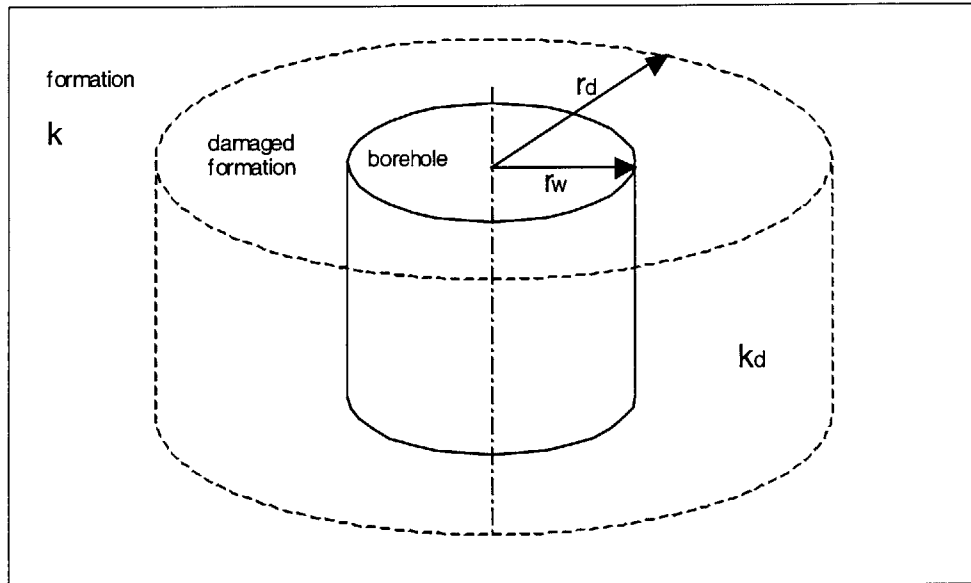


Figure 3.2: Mud damage zone in open hole.

3.1.2 Bridging Agents and Mudcake Properties

Drilling fluids contain bridging agents and other solid particles that minimize invasion of fluid into the formation and help create an effective seal around the borehole wall. This seal, known as mudcake, creates a highly concentrated differential pressure layer between the formation and the mud in the borehole. The thickness of the mudcake layer is

dependent upon the pressure difference between the drilling fluid and the formation as well as the properties of the mud.

A key property of mudcakes is the void ratio, e , which is defined as the ratio of fluid volume to solid volume. For compressible mudcakes, e is a continuously varying function of distance from the borehole wall, asymptotically approaching a value that is characteristic of the mud. There is no sharp mud-to-mudcake boundary, but typical differential pressures tend to highly compact the base of the cake near the borehole wall. It is in this “boundary layer” where most of the pressure drop across the cake occurs. Thus, in practice, the mudcake can be considered to have a time-dependent thickness,

$$\delta = \beta t^{1/2} \quad .(2)$$

where β is a mudcake thickness parameter [13].

Optimally, the mudcake layer would form an effective seal at the face of the formation layer such that there would be no particulate invasion into the formation ($S=0$). To minimize damage of the formation, bridging agents in the drilling fluid should be greater than the pore throat diameter to block at the surface of the formation [12], mudcake thickness should be minimized, and mud pressure overbalance should be minimal.

3.2 Drilling Fluid Effects on Pressure Measurements

Drilling fluid invasion will affect formation pressure measurements taken near the wellbore. However, if the pressure drop across the skin damage zone can be minimized such that there is little variation between actual formation pressure and measured formation pressure, then a pressure measurement taken on the radial surface of the formation is acceptable. Advances in drilling fluid technology have improved the performance of drilling fluids such that measuring pressure with minimal penetration through the formation could be an acceptable method of measuring formation pressure [14].

3.3 Advances in Drilling Fluid Technology

Recent advancements in engineered drill-in fluids have proved it possible to deliver no-skin wells as noted in well development offshore Gabon, Africa in 1998[15]. In the wells

developed offshore Gabon, Schlumberger's STARDRILL™ drill-in and completions fluid was specially formulated to optimize production. STARDRILL™ fluid is a carbonate-based drill-in fluid system with a scleroglucan viscosifier that is designed to create a thin external mudcake to protect the production zone during drilling and completion procedures. As seen in Figure 3.3, to achieve a thin cake with low leak off, the filter cake grains are coated with polymers (A). The lack of grain-to-grain contact leaves the formation with little damage for maximum return permeability (B). Conventional carbonate mud systems provide either grain-to-grain contact or a thicker filter cake (C), which results in lower return permeability (D).

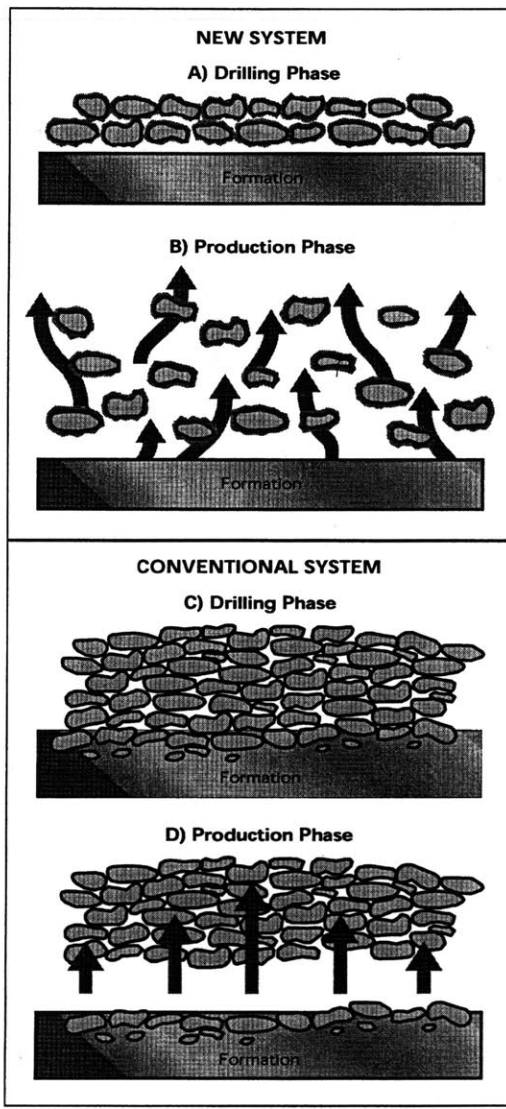


Figure 3.3: STARDRILL Drill-In Fluid vs. Conventional System.

Figure 3.4, shows the filter cake layer built up on the formation, proving it possible to develop a well with zero skin ($S=0$) using STARDRILL fluid [15].

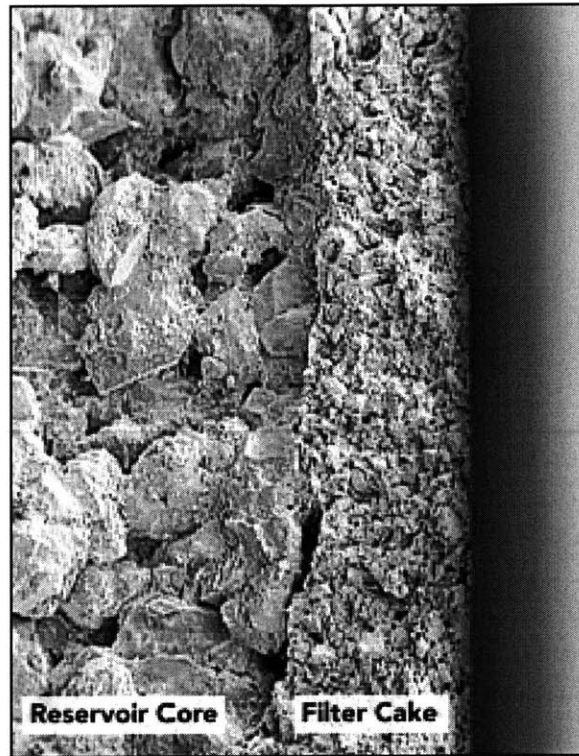


Figure 3.4: STARDRILL fluid leaves no-skin mudcake on formation.

3.3.1 STARDRILL Fluid

STARDRILL drilling fluid minimizes formation damage by maintaining correct particle size distribution, monitoring filter cake properties, and controlling clay solids buildup. This result in zero internal filter cake, thin, external cake with low spurt loss, and minimum filtrate and solids invasions [16].

4 The Nozzle Concept

The new concept developed to measure formation pressure in this thesis project is called the Nozzle Concept. This concept was selected based on information gathered from piezo-cone penetrometer technology, formation characteristics during well development, advances in drilling fluid technology, and confidential research, reports, and theories to Schlumberger.

Conceptually, the nozzle concept uses a small orifice probe to penetrate through the mudcake layer, without clogging. The mudcake forms a seal around the nozzle allowing the nozzle to communicate with the formation pressure, rather than mud pressure (bore hole pressure) as illustrated in Figure 4.1.

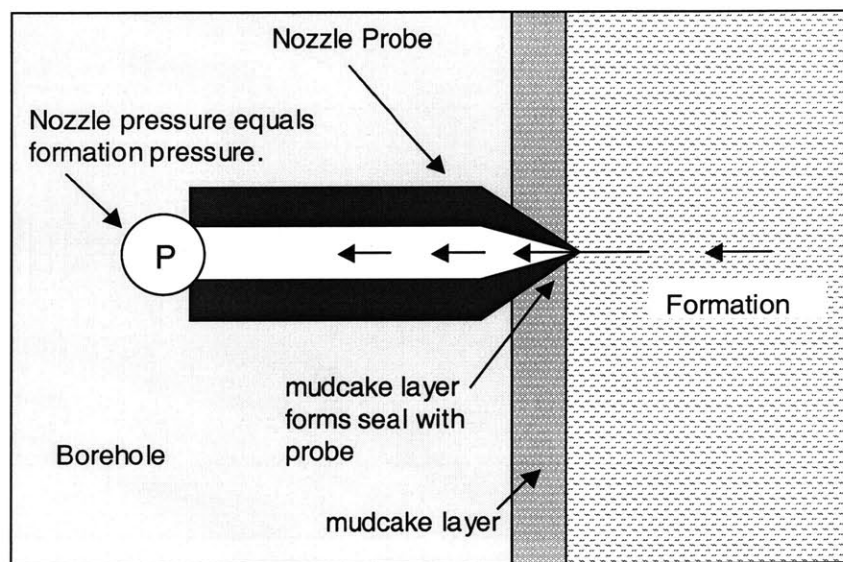


Figure 4.1: Nozzle Concept.

4.1 F&H Nozzle

The Nozzle concept was implemented and tested using small orifice nozzles from F&H Company. F&H nozzles, designed and used for releasing compounds in glue guns, were perfect for testing the feasibility of the Nozzle Concept. The nozzles, held by a retaining

nut, vary in shape and orifice size as seen in Figure 4.2 and Figure 4.3. A complete list of all the F&H nozzles is shown in Appendix A.1.

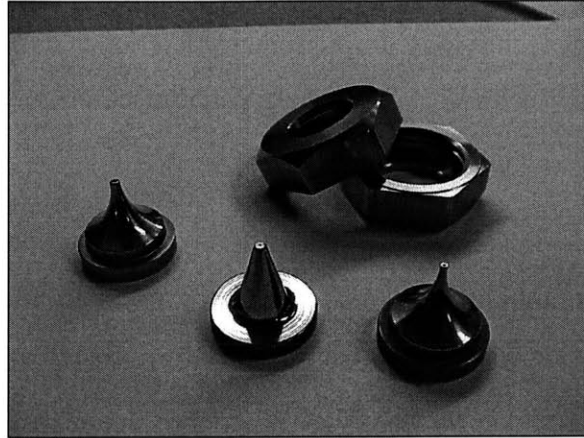


Figure 4.2: F&H Nozzles and Retaining Nuts.

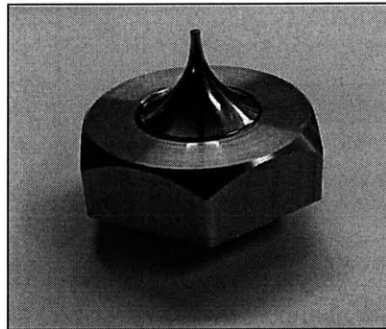


Figure 4.3: F&H Nozzle and Retaining Nut Assembly.

4.2 Nozzle Probe Assembly

The nozzle probe used to test the Nozzle concept was designed to accommodate a variety of F&H nozzles and a modified test apparatus described in the following chapter. The probe consists of an F&H nozzle, retaining nut, a hollow shaft (previously designed), a nozzle adapter to connect one end of the shaft to the retaining nut, and a second adapter to connect the other end to a pressure gauge. A picture of this assembly can be seen in Figure 4.4.

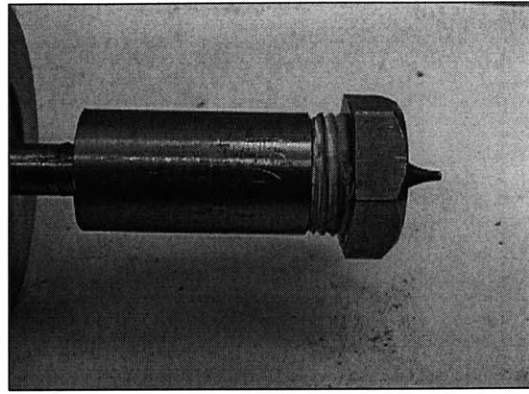
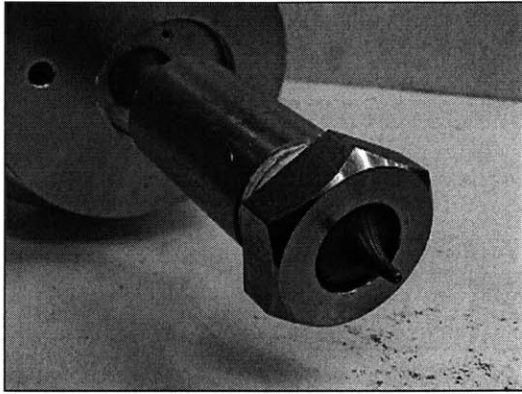


Figure 4.4: F&H Nozzle and shaft assembly.

5 The Formation Pressure Tester

An experimental setup was designed and built as part of this project to test the feasibility of the Nozzle Concept. The experimental apparatus, called the Formation Pressure Tester, was designed to accommodate variations of the Nozzle concept and simulate the buildup of mudcake along the borehole wall that is created from the differential pressure between the mud and the formation as would normally be seen in the field. An illustration of the Formation Pressure Tester can be seen in Figure 5.1.

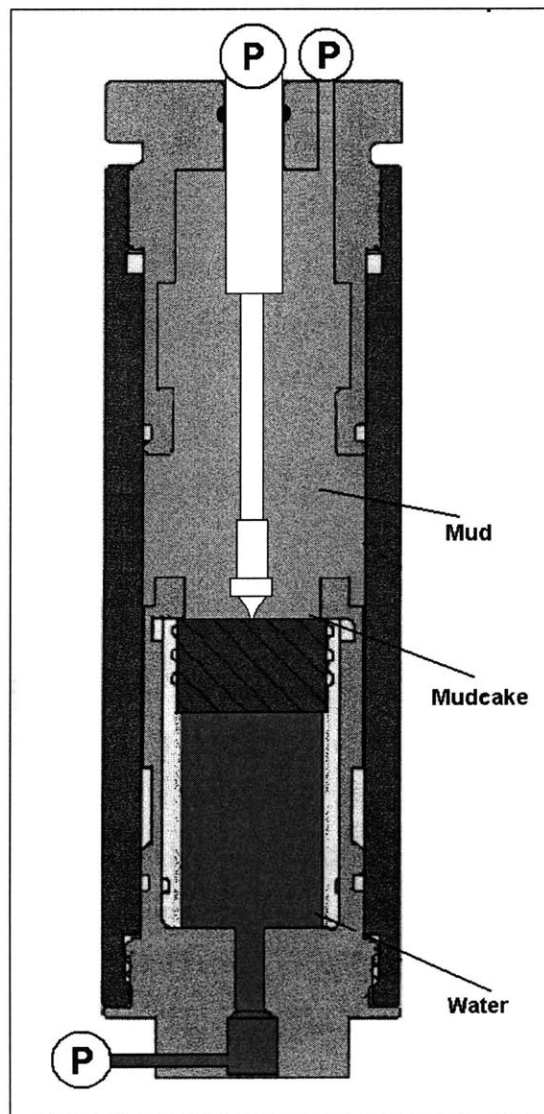


Figure 5.1: Schematic of Formation Pressure Tester.

Since the nozzle concept had not been previously studied in the laboratory, but rather only in theory (this information is Confidential to Schlumberger), there were no previous experimental setups designed to test the concept. However, Schlumberger has done extensive experimental testing on down hole tool sticking [17], [18], and the filtration properties of drilling fluids, which also involve recreating the pressure differential down hole.

5.1 Stickance Tester

Schlumberger has designed and used several testers for measuring stickance and the filtration properties of drilling fluids. Sticking occurs when the logging tool gets stuck to the mudcake layer of the borehole wall and is generally caused by leaving the tool stationary down hole too long or by a high, pressure differential within the mudcake layer.

A typical ball-stickance tester consists of a cylindrical pressure vessel with a top that houses a ball-shaft assembly, and a bottom that holds a filter and opens to the atmosphere through a small tube. The vessel is filled with drilling mud and pressurized (to a pressure greater than atmospheric), so that the mud builds up a mudcake on the filter. The filtrate from the mud drips out through the small tube at the bottom, just as it would seep into the formation. The filtration from the mudcake in itself is another property that is often measured.

The top of the pressure vessel houses a ball-shaft assembly that can be twisted back and forth. A low friction seal, retains the pressure inside the vessel, as torque is applied to the shaft in the vessel. Lowering the ball-shaft assembly to the mudcake layer simulates what happens to the tool when it is stuck to the side of the bore hole wall. The ball is then twisted free from the mudcake and the force required to do so can be measured. The force required to remove the object from the mudcake is known as the stickance force; a property inherent of the mud that often times causes tool sticking. A schematic of a ball stickance tester designed and used by Schlumberger can be seen Figure 5.2.

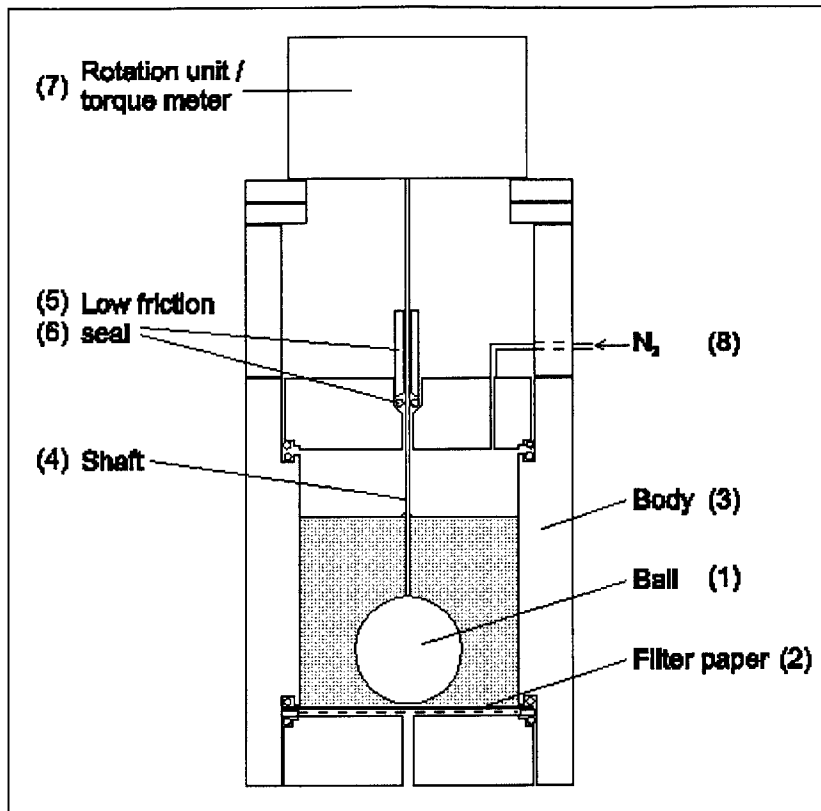


Figure 5.2: Dowell Ball Stickance Tester.

The stickance apparatus in Figure 5.2, shows the basic apparatus used to build up a mudcake to measure stickance. Notice, that the setup is relatively simple, and only takes into account the pressure differential created by the drilling fluid that cause down hole sticking (not temperature related properties). Many of the problems that occur in drilling service applications are due to the differential pressure created in the borehole, not necessarily the extremity of the temperature conditions. Hence, to simplify the problem of measuring formation pressure or properties there of, thermal conditions of the down hole environment are often times ignored in these types experiments.

5.2 Design of Formation Pressure Tester

The fundamental conditions required to measure stickance are basically the same as those to measure formation pressure, and mud filtration properties. Because of this similarity, the experimental setup needed to test the Nozzle concept did not have to be designed from scratch, but rather was a modification of an existing “mudcake-making” tester.

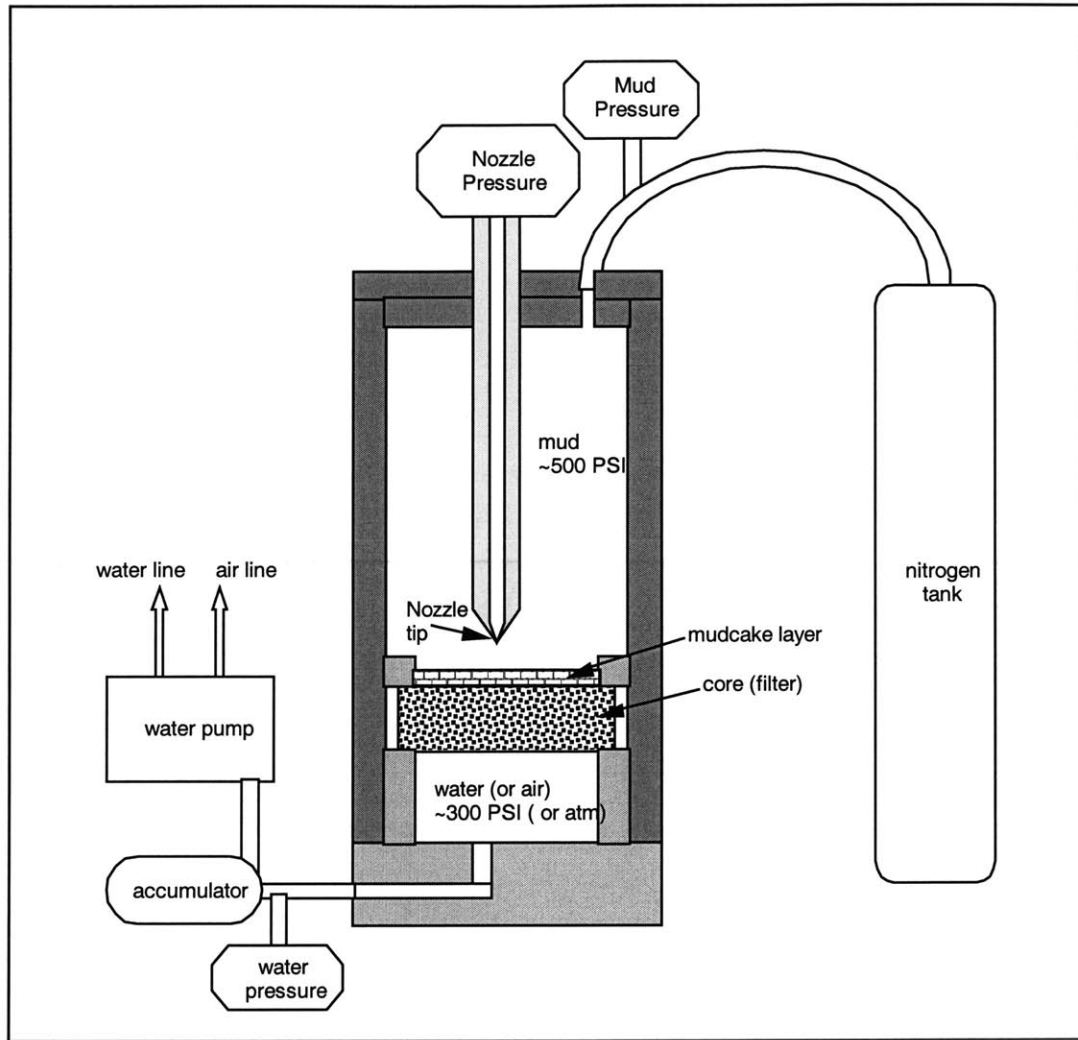


Figure 5.3: Schematic of the Nozzle Concept Experimental Setup.

The Formation Pressure Tester designed to test the Nozzle concept, was designed in accordance with modifications that were made to a stickance tester designed by Cecilia Prieto at Schlumberger [19] and a dynamic filtration system from Fann Instrument Company (see Appendix B).

The stickance tester designed by Prieto was an MIT master thesis project and was designed at the Schlumberger Sugar Land Product Center in Sugar Land, Texas. Her design was first implemented using parts of the Fann Model Dynamic Filtration System for a prototype. A schematic of Prieto's stickance tester prototype and the Fan Model 90 Dynamic Filtration System can be seen in Appendix B. This stickance tester measures

pull force rather than torsional force described in Section 5.1. This push-pull design made an ideal setup for the nozzle concept.

5.2.1 Modified Parts

Only a few modifications had to be made to the stickance tester prototype.

The modification included redesigning:

- The shaft - to accommodate a variety of nozzle shapes and sizes.
- The core holder – so that the lower pressure would be distributed evenly on the bottom and sides of the core rather than to just the outer sides of the hollow core.

5.2.2 Designed Parts

Additional parts that had to be added to the apparatus included:

- A shaft Adapter – to accommodate several nozzle shapes and sizes while retaining a connection to the hollow shaft.
- A connector- to connect the shaft to the pressure gauge used to measure the nozzle pressure

The original drawings of the Stickance Tester prototype and Fann Instrument filtration parts along with the modifications that were made can be seen in Appendix B.

5.2.3 Other Components of the Apparatus

Once the necessary modifications were made and the new parts were designed, other parts of the setup were ordered or provided by the laboratories at Schlumberger's Sugar Land Product center to accommodate the necessary testing on the Nozzle Concept.

Parts of the setup that had to be ordered include:

- Gaskets to hold the core in place (Fann Instruments)
- Nozzles (F&H Nozzle Company)
- Retaining Nuts (F&H Nozzle Company)
- Cores (Mott Corporation, Capstan Permaflow, Stimlab)
 - Bronze disc filters
 - Metal disc filters
 - Berea Sandstone cores
- Large Digital Display Pressure Gauges (Omega)
- Accumite 1 gallon Accumulator
- Win wedge Software

Parts of the setup provided by the Reservoir Sampling and Pressure Laboratory include:

- A nitrogen tank
- A water pump
- Fittings and Quick-release connectors
- Drilling Fluid (STARDRILL)
- Pressure lines
- Pressure Gauges

5.3 Experimental Setup

Given that the goal of the project was to merely determine the feasibility of the Nozzle Concept, rather than its implementation on a specific logging tool, concept testing was sufficient using the simplistic apparatus that was designed.

A schematic shown in Figure 5.3 shows the complete experimental setup used to test the Nozzle Concept. Because down hole reservoir conditions vary greatly, the setup was designed so that several parameters could be changed. These parameters include the drilling fluid (mud), the core filters (simulating the formation), and the pressure differential. The setup also allowed for different nozzle geometries to be tested by simply changing one part of the setup. The apparatus was setup to record the mud pressure, the nozzle pressure, and the formation pressure during a test. As well, visual observations of the tests were recorded.

The experimental setup simulated the mudcake build up on the borehole wall by creating a pressure differential between the drilling fluid and a cylindrical core. The differential pressure was created using a pressure vessel. The vessel was separated into two chambers by a core that was held in place by the core clamp. A nitrogen tank was used to pressurize the mud side of the pressure chamber, and the backside of the chamber was pressurized with water using an accumulator and a pump. The different pressure on each side of the core creates a pressure differential within the core. This pressure differential is what builds up the mudcake layer on the mud side of the core. Once the mudcake begins to form, there is an obvious separation between the three layers of the setup: the mud in the chamber acting as the mud in the borehole, the mudcake layer, and the backside of the core, which resembles the formation. It is noted that the bottom-side of the core and the core have the same pressure.

Tests were conducted in the Reservoir Sampling and Pressure Laboratory at the Sugar Land Product Center in Sugar Land, Texas. The laboratory contained all necessary pressure equipment needed to pressurize the apparatus including a water source, an air source, pressure valves, quick connects, pressure gauges, a nitrogen tank, and other necessary tools.

Two digital pressure gauges with RS-232 port connectors were used to monitor pressure conditions of the Needle Point probe and the mud pressure in the chamber. WinWedge Software was used to monitor the pressures from the digital gauges and store the data files needed to analyze the results of the tests.

6 Experimental Testing and Results

6.1 Core Analysis

6.1.1 Mudcake Analysis

Before testing the Nozzle concept, experimental testing was done to understand the interaction between the drilling fluid and the formation. Using the Formation Pressure Tester, mudcake was built up on a core with STARDRILL drilling fluid. The results of the tests proved that the mudcake is completely removable from the core as shown in Figure 6.1.

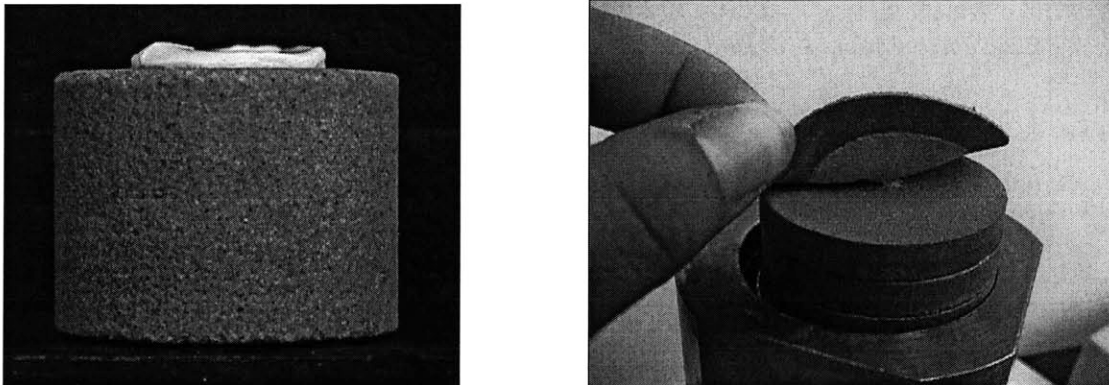


Figure 6.1: Mudcake build up on core from STARDRILL fluid.

Although it was proven that the mudcake is removable from the core, observation also noted that the core-drilling fluid interaction varies greatly. The resultant mudcakes varied in thickness (0.05” to 0.15”) and ease of removal from the core. Some mudcakes were not removable at all, while others could be “peeled” off the core.

6.1.2 Permeability Analysis

To understand the property changes made to the core from building up a mudcake, a liquid permeability test was conducted on a Stimlab Berea Sandstone Core (300-400 millidarcy in air). A Hassler cell was used to run the permeability test.

First, a permeability test was performed on the core soaked in KCl Brine and kerosine was run through the core for the permeability test. Next, a mudcake was built up on the core for 2hours using a filtration cell. The pressure differential was held at 400psi at room temperature (68 deg F). After the cake was built up, a second perm test was done on the core, using kerosine again. Kerosine is filtered through the core for the perm test because it is very similar to the oil in a reservoir.

Table 6.1: Permeability test results for a berea sandstone core.

Permeability Test on Berrea Sanstone Core Using Stardrill Drilling Fluid				
Plug Length (cm)	2.588	1.019		
Area of Plug (cm ²)	6.120			
Plug Diameter (cm)	2.791	1.099		
Sat. Weight (g) =	0.000			
Dry Weight (g) =	0.000			
Bulk Volume (cc)	15.840			
Initial Permeability				
Flow Rate (cc/min)	Pressure (psig)	keros. Perm (md)	Temperature (deg F)	Viscosity (cp)
50.00	73.00	176.66	68.0	2.4900
100.00	135.00	191.06	68.0	2.4900
150.00	194.00	199.43	68.0	2.4900
		AVG:	189.05	
Final Permeability				
Flow Rate (cc/min)	Pressure (psig)	Water Perm (md)	Temperature (deg F)	Viscosity (cp)
50.00	70.00	184.24	68.0	2.4900
100.00	115.00	224.29	68.0	2.4900
150.00	167.00	231.67	68.0	2.4900
		AVG:	213.40	
RETURN PERMEABILITY:		112.9%		

The results of the test, shown in Table 6.1, show that the permeability of the core actually improved after mudcake buildup. The initial liquid permeability of the core was 191.58 millidarcy, the 5mL/min flow initiation permeability (after mud cake buildup) was 99.20

md, and the return permeability average was 213.40 md. Improvement in permeability is rare, but possible with the advancements in drilling fluid technology. Tests were conducted at a Dowell Schlumberger laboratory at the Sugar Land Product Center.

6.1.3 SEM Analysis

Scanning electron microscopy has been employed to great advantage in visualization studies of filter cakes and formation damage [20]. SEM Analysis was performed on the Berea Sandstone cores to see the result of the mudcake invasion into the core. Analysis was done on a Berea sandstone core before and after mudcake build up. The results are shown in Figure 6.2.

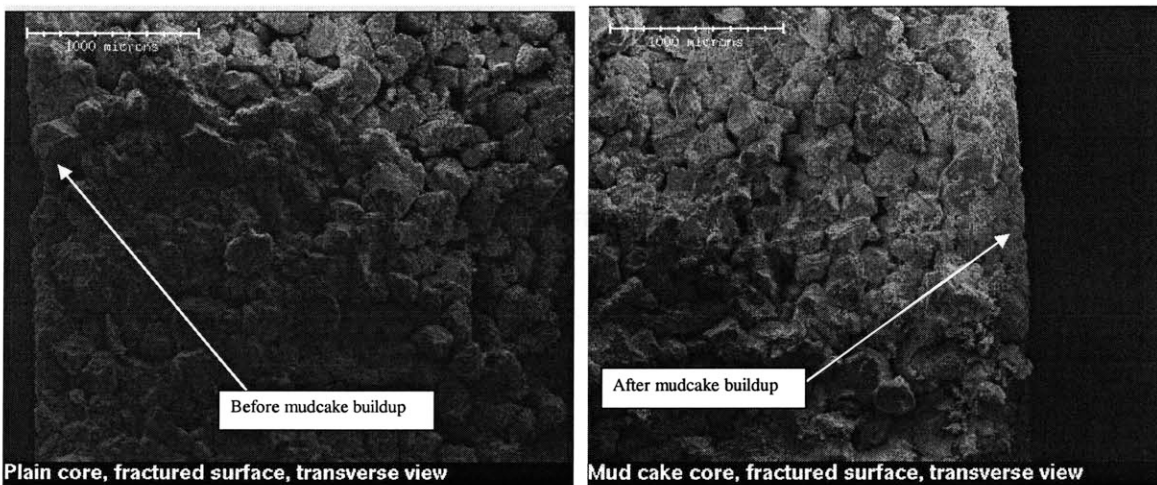


Figure 6.2: Berea Sandstone Core before and after mudcake build up.

The SEM analysis shows on a microscopic level that there is very little damage to the Berea sandstone core due to mudcake. The elemental breakdown was also determined from the SEM tests. The Berea sandstone cores are mostly silica with some carbonates and assorted clays. SEM analysis was conducted at the Schlumberger Reservoir Completions center in Rosharon, Texas.

6.2 Nozzle Concept Tests and Results

Nozzle concept tests were conducted using the Formation Pressure Tester. STARDRILL drilling fluid, formulated in lab for consistency, was used to build up mudcake for all the

tests. Berea sandstone cores, bronze disk filters, and metal disc filters were used to simulate the formation and vary the permeability and porosity conditions. The mud pressure for the tests varied from 200 to 700 PSI, water (or air) pressure varied from 0 to 300 psi, and a pressure differential between the two was anywhere from 100 and 400 PSI. The time to build up a mudcake was varied as well.

Different F&H nozzles were used for testing. Some tests used the same nozzle and the initial setup conditions of the test were varied instead. Initial setup variants included starting point of the nozzle, initial contents in the nozzle shaft, and penetration depth.

The mud pressure and nozzle pressure were monitored using two large digital display pressure gauges (measure from 0-1000 psi). The water pressure was monitored using a pressure gauge as well. Data was recorded using Win Wedge data acquisition software and graphically displayed using Excel charts. Pictures of the setup were also used to analyze the results of the test.

The main goal of this testing was to determine feasibility of the Nozzle concept, and to gain an understanding of what determined success or failure of the concept by varying the conditions of the test. About 30 experimental tests were done to test the Nozzle concept. All tests were conducted in the Reservoir Sampling and Pressure laboratory at Schlumberger's Sugar Land Product Center in Sugar Land, Texas. The setup and results of each test are shown in the following sections.

Test 01

Results: Failure to do clogging.

F&H Nozzle: L2-75

Berea Sandstone Core

Mud Pressure: ~500psi

Water Pressure: ~300 psi

Nozzle Pressure was recorded

Observations: The nozzle pressure never reached the water pressure. It always remained at mud pressure. There was clogging at the nozzle tip due to the mud. The resultant mudcake was removable from the core and had a hole where the nozzle tip penetrated the core. It slightly indented the core. From looking at the core, it seems as though the cake

did not seal around the core, but rather invaded the indentation area. The results of the test method are inconclusive since the tip was clogged during part of the test. This clogging, and attempt to remove clogging skewed the actual data. It is still not understood why the nozzle pressure at some time was about 300psi greater than the mud pressure and 500 psi greater than the water pressure.

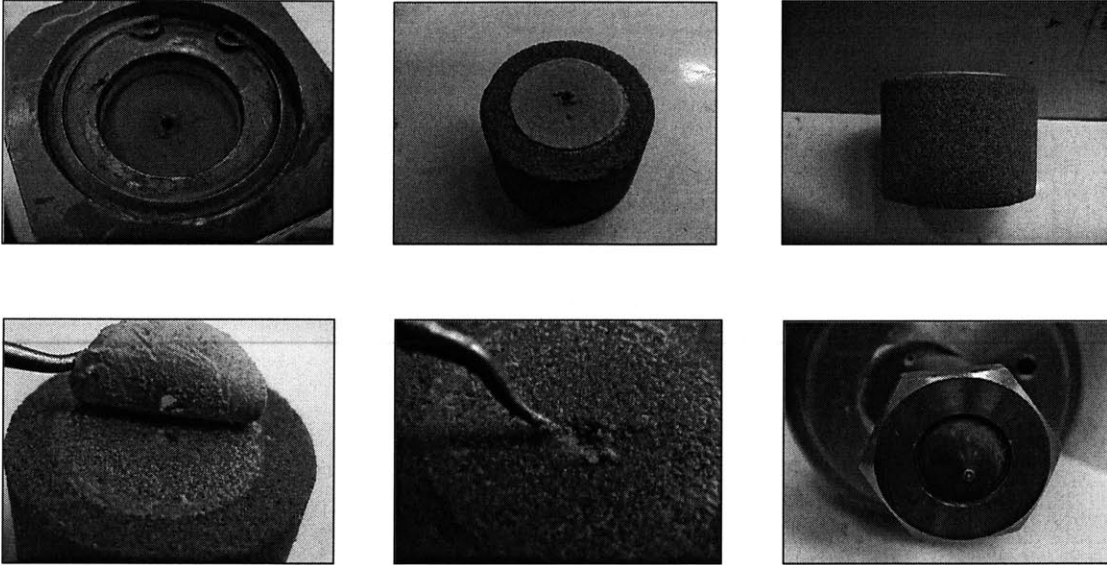


Figure 6.3: Pictures of Nozzle Concept Test 1.

Test 02

Results: failure due to improper sealing of core.

Berea Sandstone Core

Water Pressure: Approx 300psi

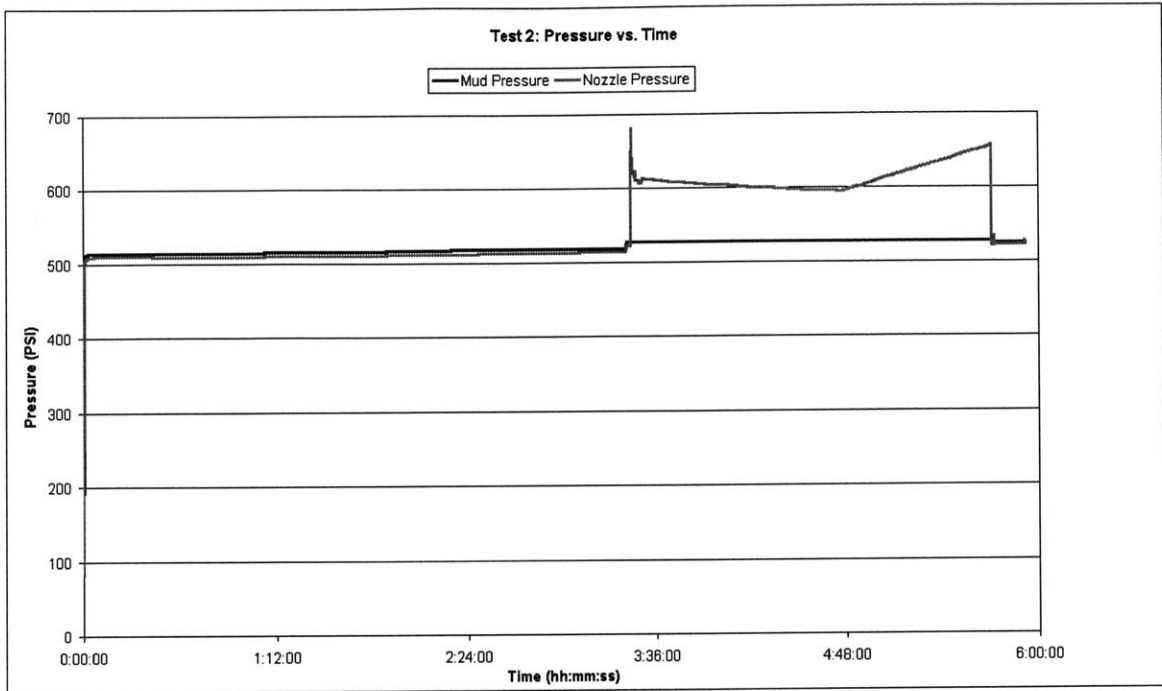


Figure 6.4: Pressure vs. Time graph of Nozzle Concept Test 2.

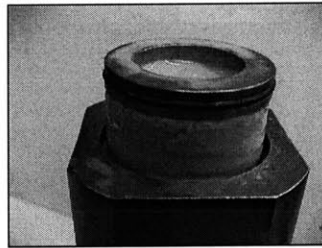


Figure 6.5: Picture of core from Nozzle Concept Test 2.

Test 03

Results: Failure due to core fracture.

Berea Sandston Core

Mud Pressure: ~520psi

Water Pressure: ~400psi

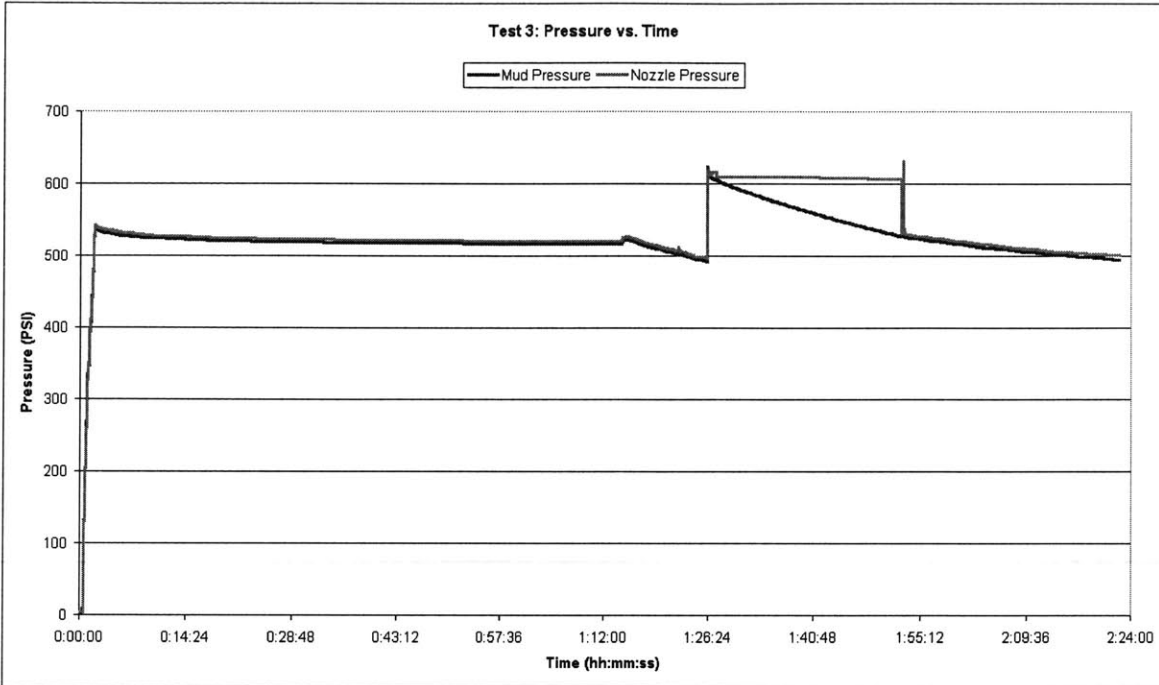


Figure 6.6: Pressure vs. Time graph of Nozzle Concept Test 3.

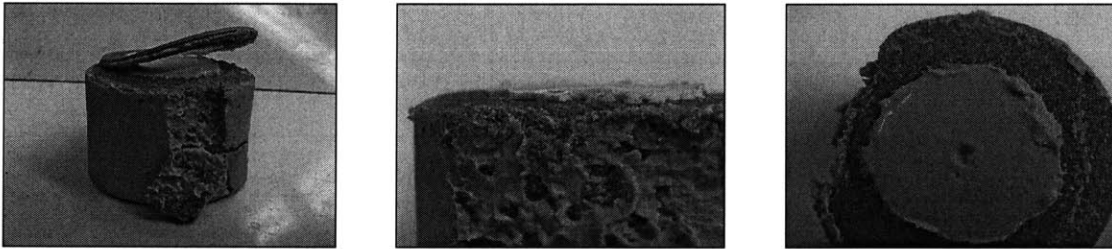


Figure 6.7: Pictures of Nozzle Concept Test 3.

Test 04

Result: Failure due to cracked core.

F&H Nozzle: VAL
Berea Sandstone Core

Observations: The mud pressure was held between 500 and 600psi. and a mudcake was built up for 2 hours prior to adding a back water pressure of 300psi. Once the nozzle was lowered to the face of the core, it cracked the core, and the water pressure instantly rose to the mud pressure. The water pressure was drained several times, only to again reach the mud pressure. The entire container of mud filtered through the core, and out through the pump. The core plugged the nozzle so that the nozzle pressure was actually higher than the mud or water pressure. When the setup was disassembled, the mudcake that touched the outside of the nozzle was stuck to the nozzle, and a hole was cut out from the

center of the mudcake on the core face. The crack on the core was directly on the centerline of the core. The mudcake built up was considerably thick considering the equalization of the pressures. This thickness was probably built up during the initial two hours prior to the actual test. Pictures of the test and resultant core can be seen in Test 4 pictures.

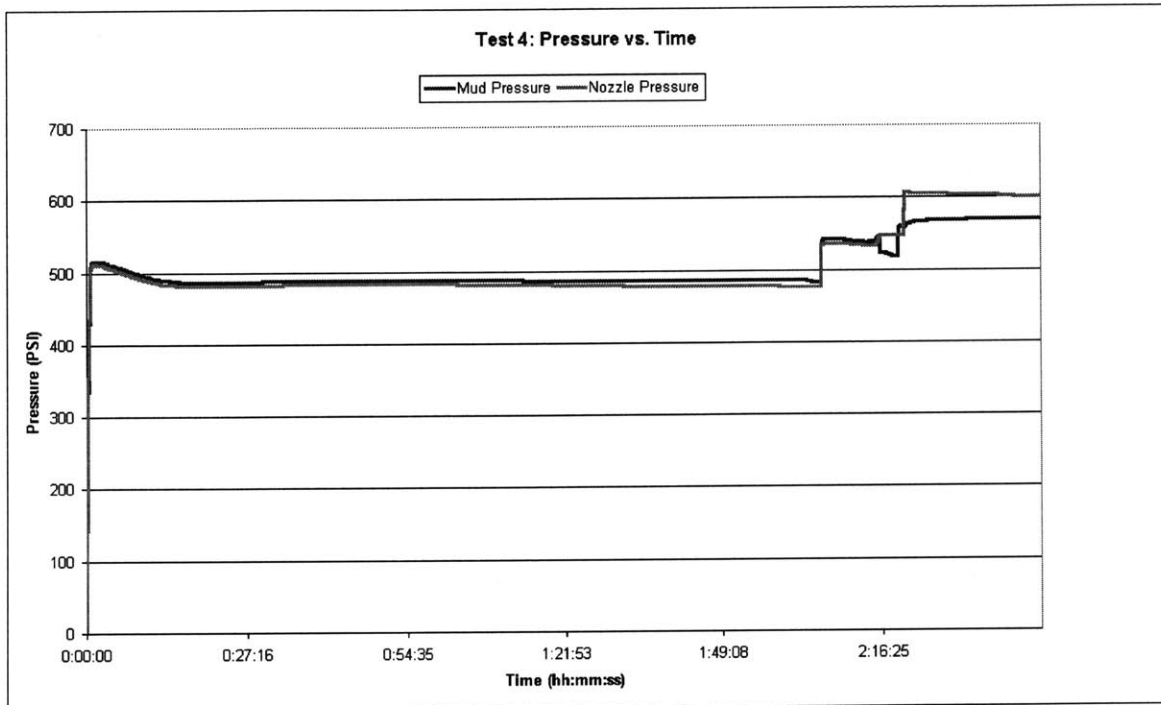


Figure 6.8: Pressure vs. Time graph of Nozzle Concept Test 4.



Figure 6.9: Pictures of Nozzle Concept Test 4.

Test 05

Result: Failure due to no differential pressure from rock cracking

F&H Nozzle: C1 77

Metal disk filters: 3 Permaflow F40 filters

Observations: Mud Pressure and Nozzle pressure remained the same during the entire test. The nozzle was put at the face of the filter at the start of the test. The water pressure started at about 350psi and eventually reached 420psi during the test. Filtration through the filters or setup is probable cause. Mud cake did not filter through filters. Mud was only seen on top layer of the first filter.

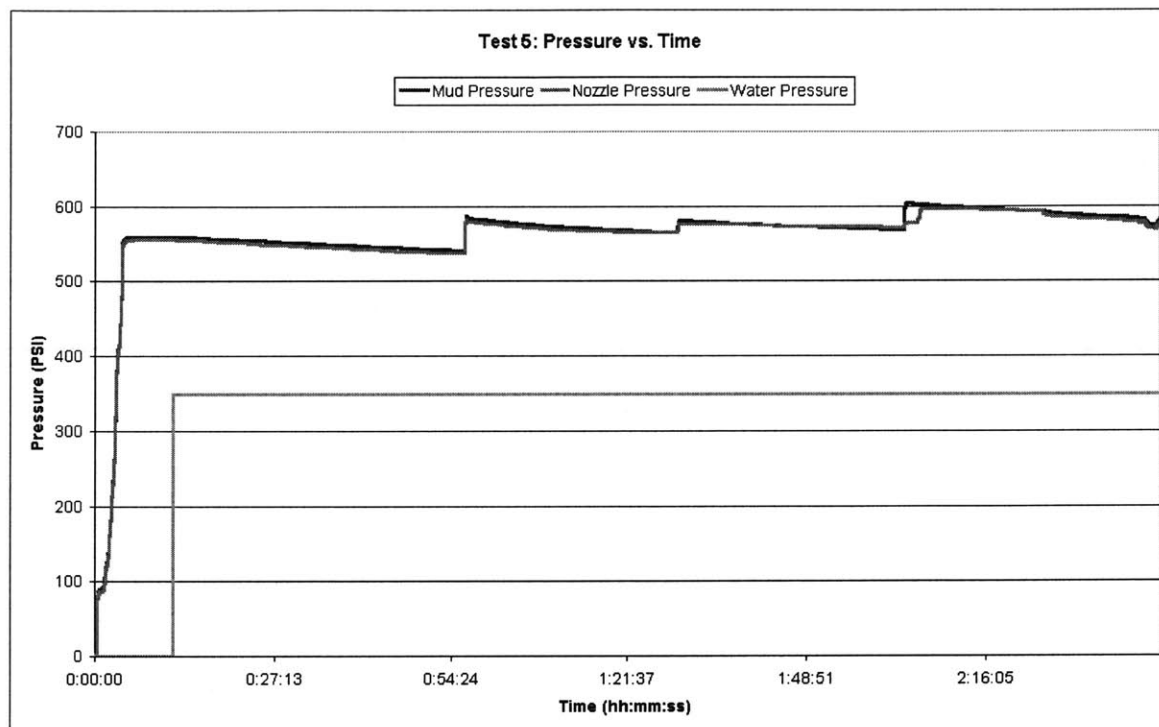


Figure 6.10: Pressure vs. Time graph of Nozzle Concept of Test 5.



Figure 6.11: Picture of Nozzle Concept Test 5.

Test 06

Result: Successful. Demonstrates time decay to reach nozzle pressure once it has been exposed to mud/borehole pressure.

F&H Nozzle C1 77

Disk Filters: 3 permaflow disk filters – F60

Started Test with nozzle at face of filter.

Built up mudcake for approx. 2 hours.

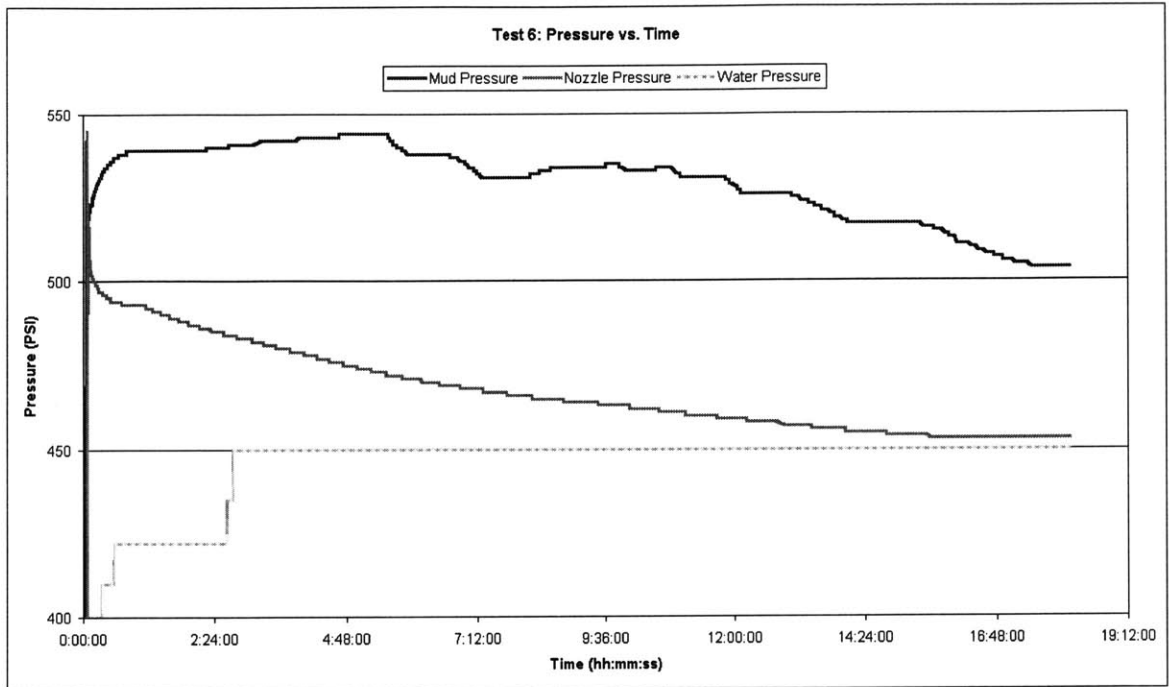


Figure 6.12: Pressure vs. Time graph of Nozzle concept Test 6.

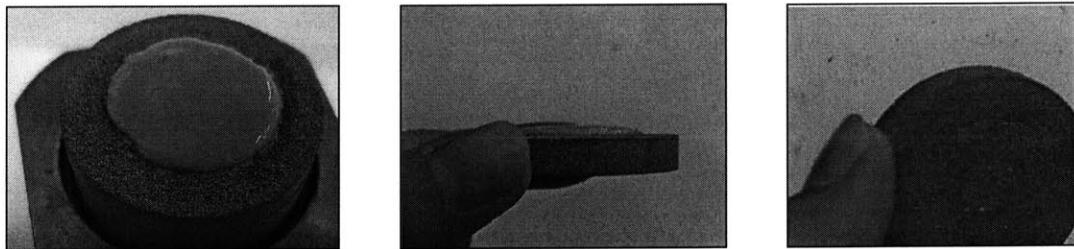


Figure 6.13: Pictures of Nozzle Concept Test 6.

Test 07

Result: Failure

F&H Nozzle: LS 75

Disc Filters: 3 Permaflow Bronze filters F100

Starting test with nozzle at face of filter

Observation: Ended test due to nozzle plugging up. It had a very small orifice diameter. Water pressure was maintained at about 350- 400psi. The mudcake was completely removable from the filter (except for the part of the cake that was touched by the nozzle.)

The filters had a very low permeability and small pore size. This is why the mudcake was so thick and removable once the test was disassembled.

The nozzle plugged up. Perhaps if a wider nozzle were used, this setup would have worked. Will try this in test 8. The reason for failure is that the nozzle cut away part of the top filter. When the centerpiece of the mudcake was removed using a probe, the mudcake was also built up in the crevice made by the nozzle digging into the filter. Therefore, there was never a perfect seal between the mudcake layer and the formation (filter) and the probe.

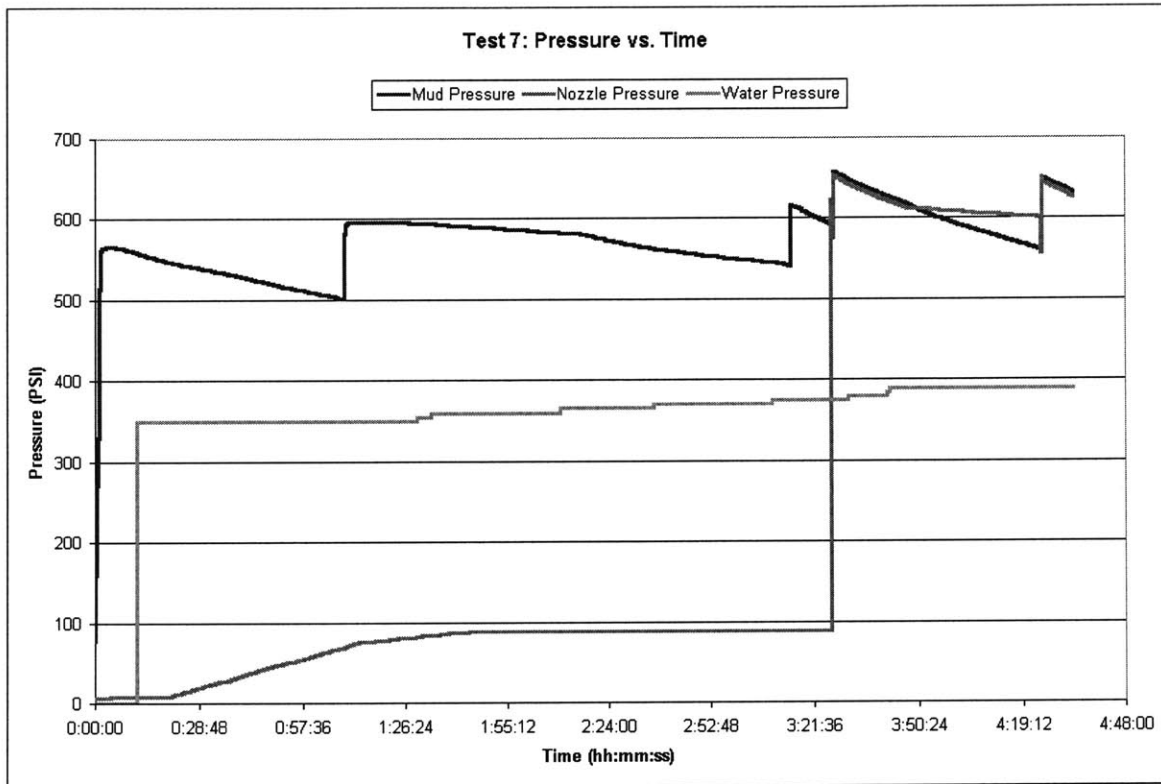


Figure 6.14: Pressure vs. Time graph of Nozzle Concept Test 7.



Figure 6.15: Pictures of Nozzle Concept Test 7.

Test 08

Result: Failure

F&H Nozzle: C1 (same as in Test 5 and 6)

Disc Filters: Used two Permaflow bronze disk filters F100

Starting test with nozzle at face of filter

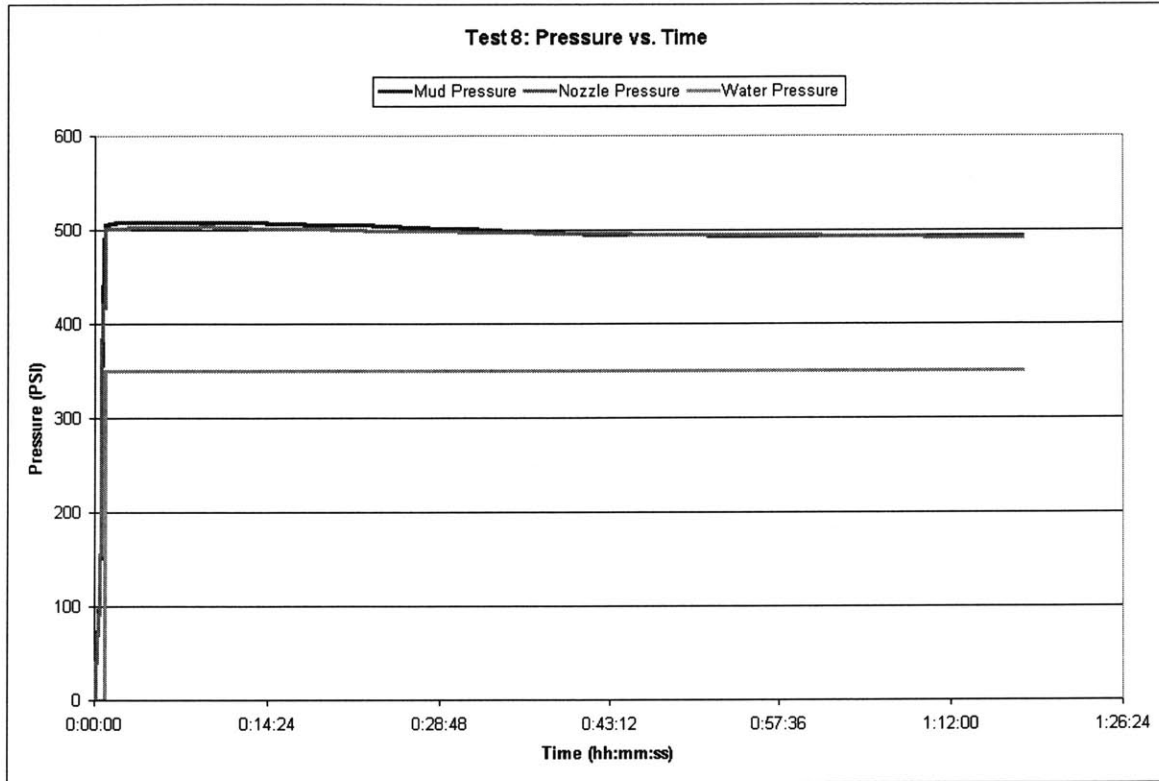


Figure 6.16: Pressure vs. Time Graph of Nozzle Co0ncept Test 8.



Figure 6.17: Pictures of Nozzle Concept Test 8.

Test 09

Result: Successful. Demonstrates time decay to reach nozzle pressure once nozzle has seen mud pressure.

F&H Nozzle (Unlabeled, but shown in pictures. 0.70mm orifice size)
Disk Filters: Used 2 Permaflow Bronze disk filters - F60
Started test with the nozzle to the face of the filter.

Observations: Every so often during the test the mud pressure was slightly increased to account for any leakage in the system. This should not affect the nozzle pressure if it is actually reading formation (water) pressure.

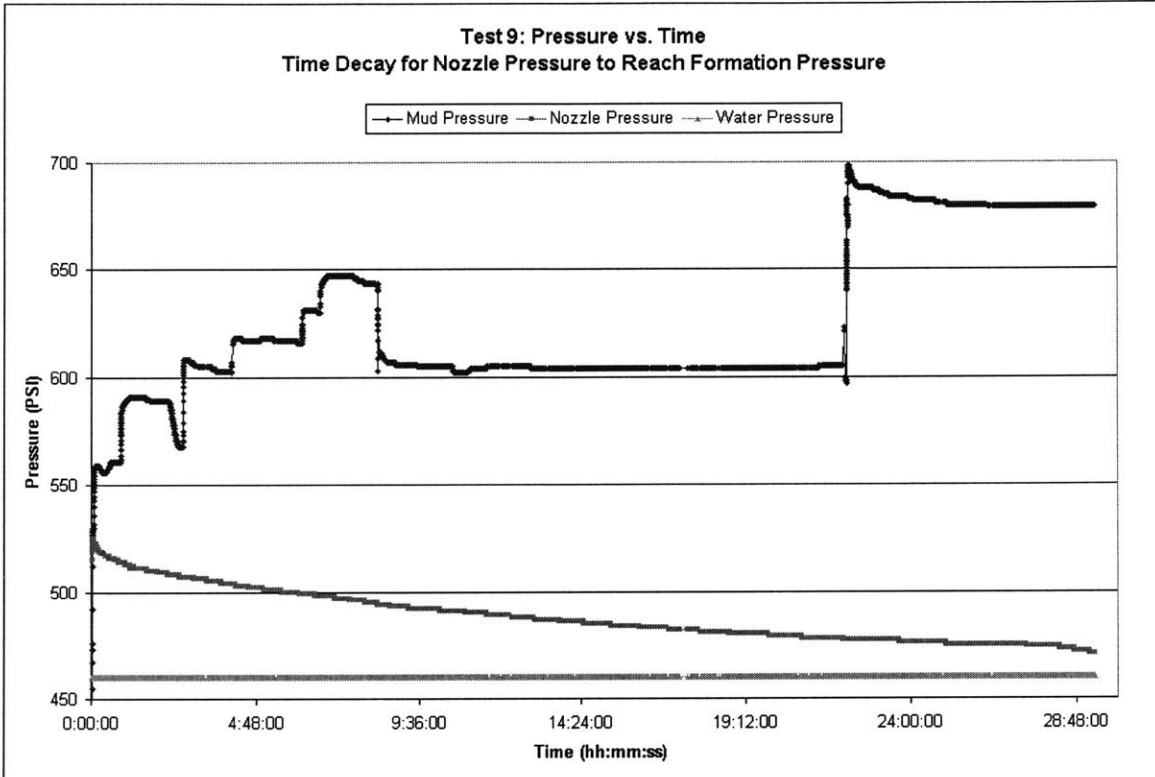


Figure 6.18: Pressure vs. Time Graph of Nozzle Concept Test 9.

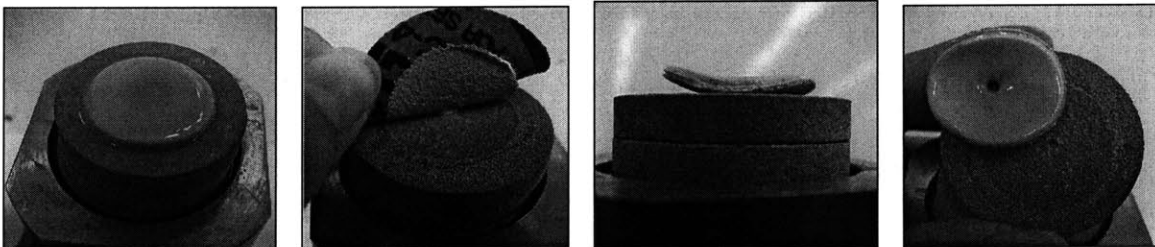


Figure 6.19: Pictures of Nozzle Concept Test 9.

Test 10

Result: Failure due to nozzle plugging

F&H Nozzle: C1-SS (#60)
Disk Filters: 2 Permaflow disk filters - F60
Starting test at Face of filter
Water Pressure: 0psi (atmospheric)
Mud pressure: ~200 psi

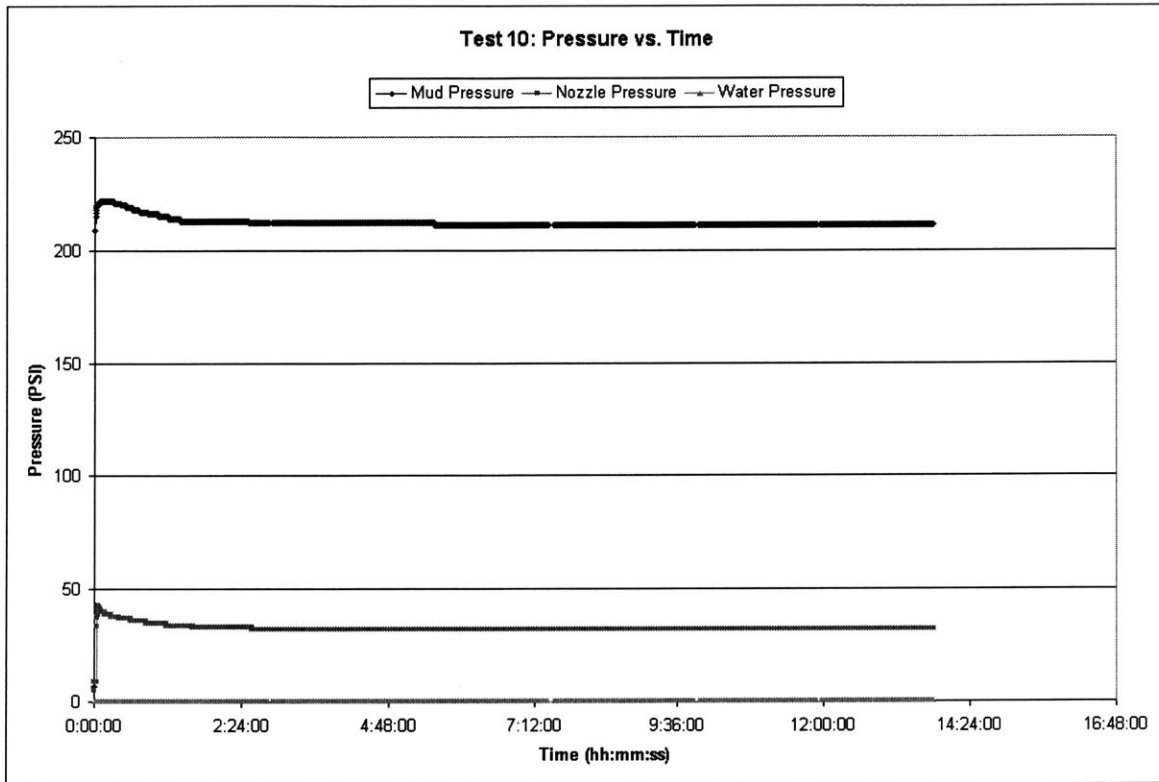


Figure 6.20: Pressure vs. Time Graph of Nozzle Concept Test 10.

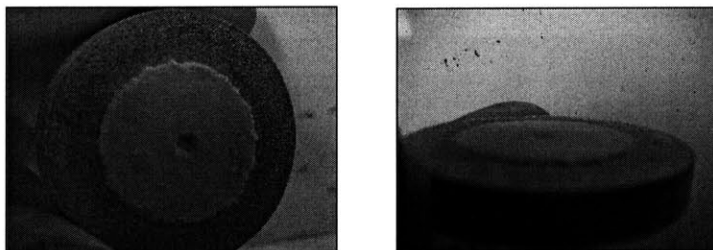


Figure 6.21: Pictures of Nozzle Concept Test 10.

Test 12

Result: Successful

F&H Nozzle (long nozzle)- Modified to .067" ID and .171" OD

Disc Filters: Used 2 permaflow disc filters - F60
 Start test with nozzle at face of core
 Mud pressure: ~200 psi
 Water pressure: 0psi

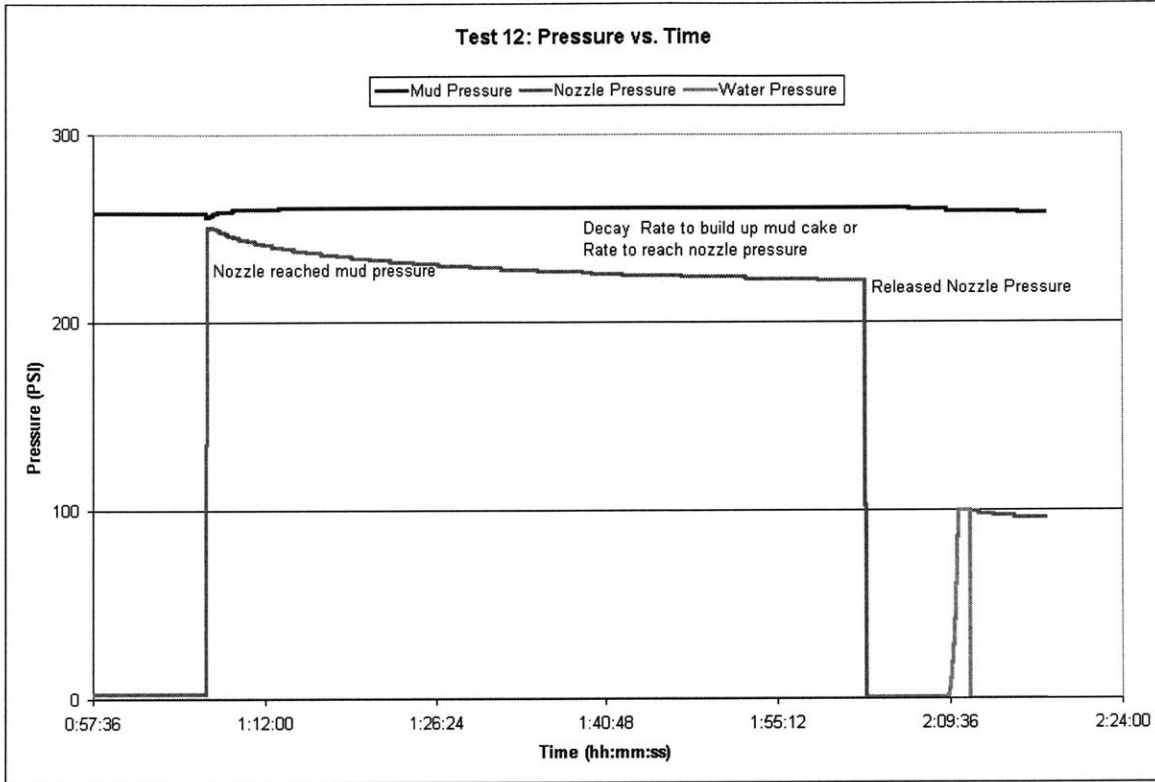


Figure 6.22: Pressure vs. Time graph of Nozzle Concept Test 12.

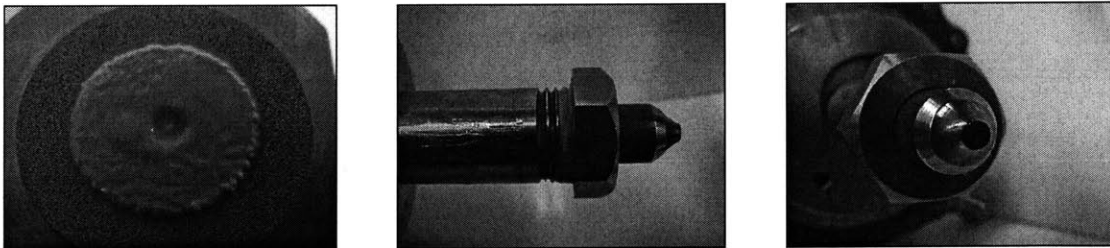


Figure 6.23: Pictures of Nozzle Concept Test 12.

Test 13

Result: Failure

F&H Nozzle: same nozzle as in Test 12
 Disc Filters: Used 2 permaflow disc filters – F60
 Mud pressure: ~250psi

Water pressure: (starting at 0 psi), varied throughout test
Start test with nozzle at face of filter

Observation: Water pressure shown in the chart is just an estimation of what occurred.
Unsure of actual water variation.

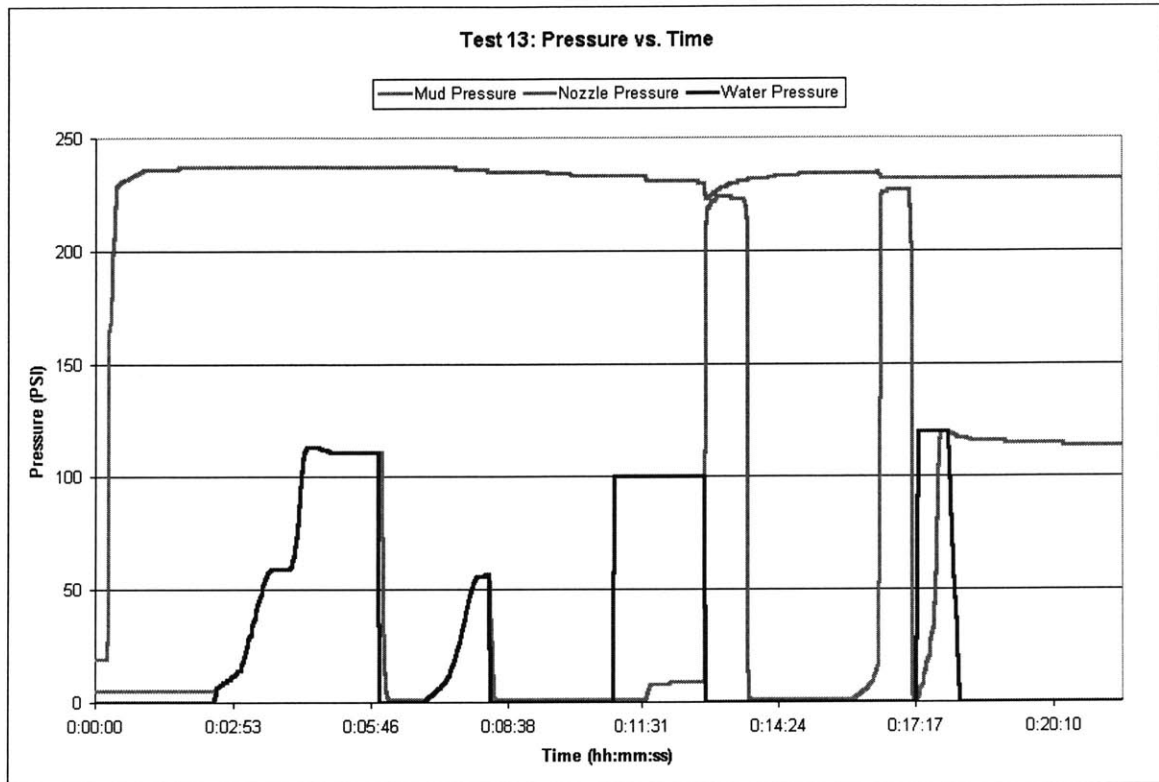


Figure 6.24: Pressure vs. Time Graph of Nozzle Concept Test 13.

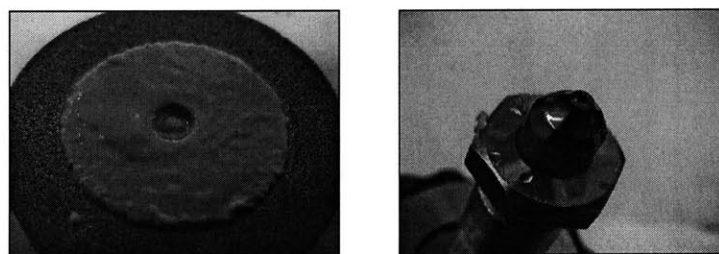


Figure 6.25: Pictures of Nozzle Concept Test 13.

Test 14

Result: Failure Due to destruction of filter

F&H Nozzle: same as in Test 12 and 13

Disc Filters: Used 2 Permaflow disk filters at F40 (largest pore size)

Mud pressure: ~ 200psi
Water pressure: started at 0psi, then varied.
Start test with nozzle at face of core, and filled with water.

Observations: Reason for failure is probably due to destruction of open pore spaces on filter. When the setup was disassembled, the pore spaces where the nozzle hit the filter were flattened so that there was no passage at all. See pictures for Test 14.

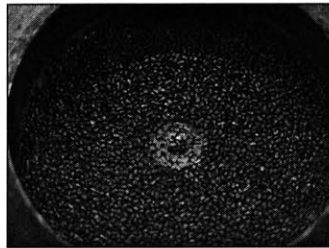


Figure 6.26: Picture of core from Nozzle concept Test 14.

Test 15

Result: Failure due to destruction of pore spaces.

F&H Nozzle: modified long nozzle (same as in test 14), OD= .171" and ID= 0.067"
Disc filters: Used 2 Permaflow filters - F40 (largest pore size)
Mud pressure: ~250 PSI
Water pressure: starting at 0 psi, but then varied.
Start test with nozzle at face of filter and filled with water.

Observations: Unsure of failure during the test. Most likely, failure was due to same thing as in test 14. The nozzle probably plugged and flattened the filter. Should try test with F60 filters which have a smaller pore size.

Reason for failure: Once Test 15 was disassembled the reason for failure was obvious. Because the wall thickness to the nozzle is so thick (same as in test 14 and others), it acted as a punch and flattened out the pore spaces to the filter. Since we are using a relatively large pore space filter, it caused the metal pieces the filter is made up of to be compressed together, leaving no opening or direct passage to the formation pressure. This failure most likely would not happen in an actual down hole test.

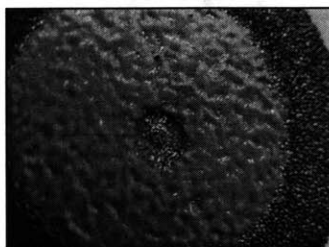


Figure 6.27: Picture of core from Nozzle concept Test 15.

Test 16

Result: Successful

F&H nozzle: L2- 60

Disk Filters: Used two Permaflow bronze disc filters – F60

Mud pressure: ~250psi

Water pressure: 0psi initially and then varied.

Start test with nozzle filled with water.

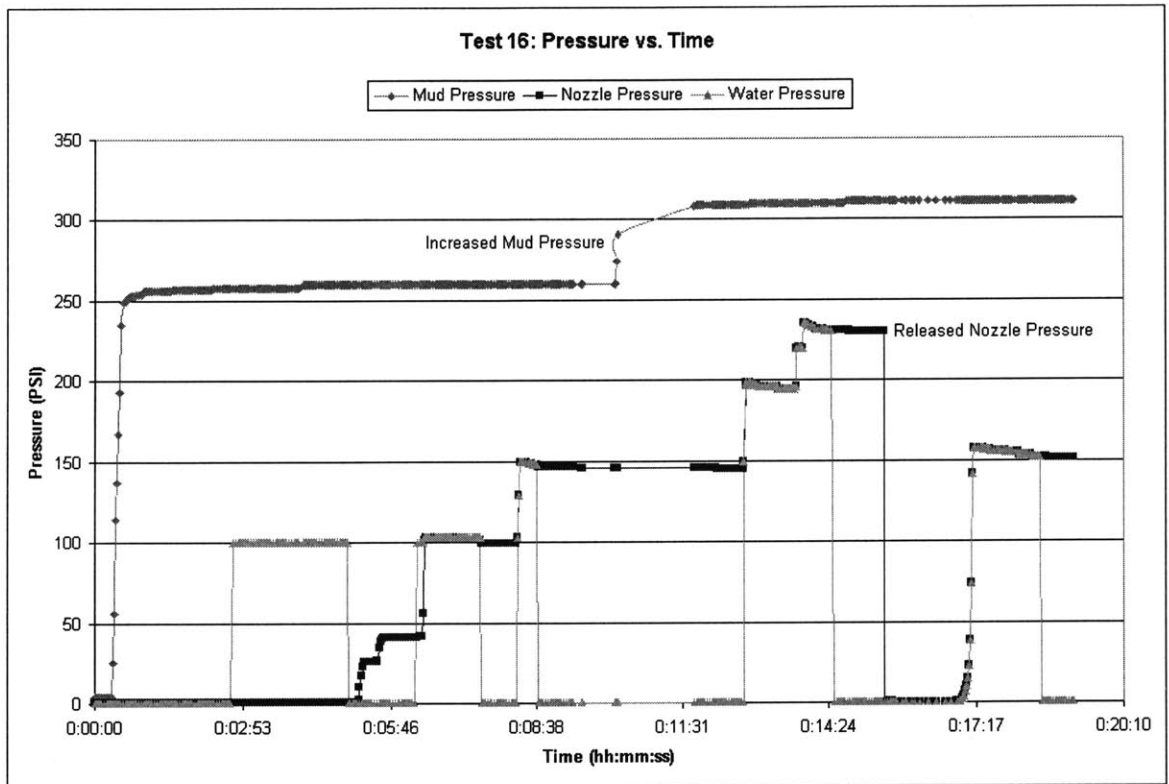


Figure 6.28: Pressure vs. Time graph of Nozzle concept Test 16.

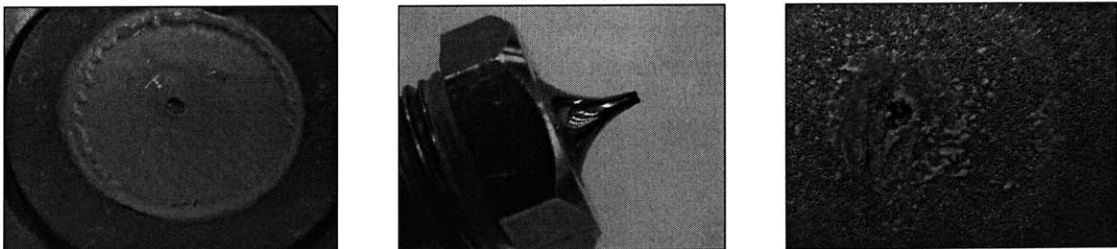


Figure 6.29: Pictures of Nozzle Concept Test 16.

Test 17

Result: Successful

Repeat of test 16 for repeatability assurance

F&H Nozzle: L2- 60

Discs Filters: Used 2 permaflow disk filters (F60)

Mud pressure: ~250psi

Varied water pressure

Start test with water in nozzle and nozzle at face of filter.

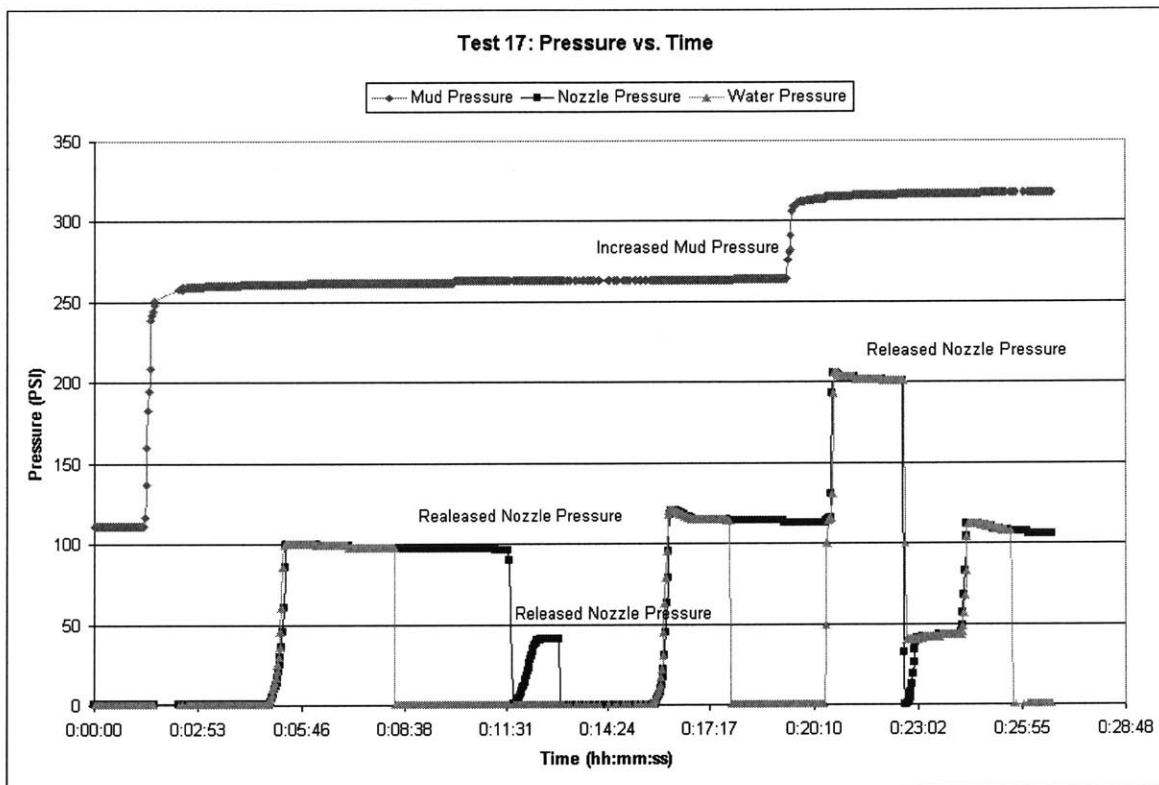


Figure 6.30: Pressure vs. Time graph of Nozzle Concept Test 17.



Figure 6.31: Pictures of Nozzle Concept Test 17.

Test 18

F&H Nozzle: (unlabeled, nozzle orifice= 0.60 mm)

Disc Filters: Used 2 Permaflow disk filters F60

Mud Pressure: ~250psi

Vary water pressure

Start test with water in nozzle and at face of filter.

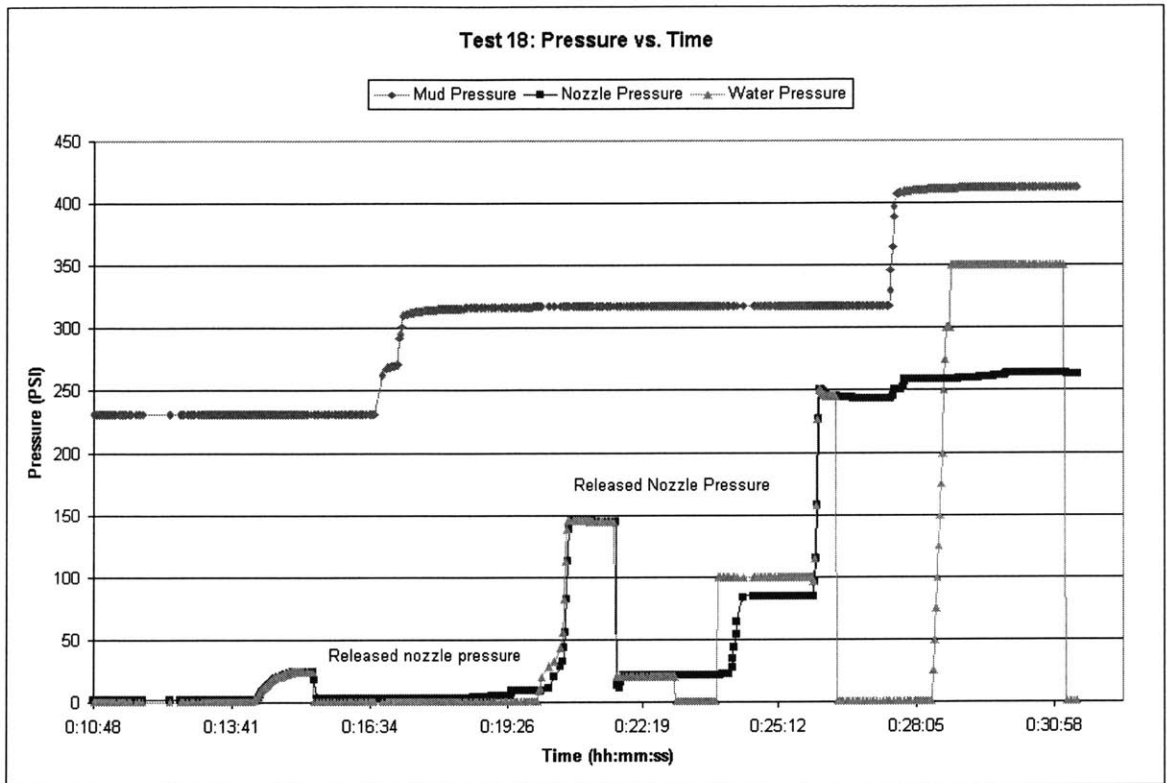


Figure 6.32: Pressure vs. Time graph of Nozzle Concept Test 18.



Figure 6.33: Pictures of Nozzle Concept Test 18.

Test 19

F&H nozzle: unlabeled nozzle (modified to nozzle orifice, OD= 0.108" and ID= 0.054")

Disc Filters: Used 2 Permaflow disk filters F60

Start test with nozzle full of water and on face of filter.

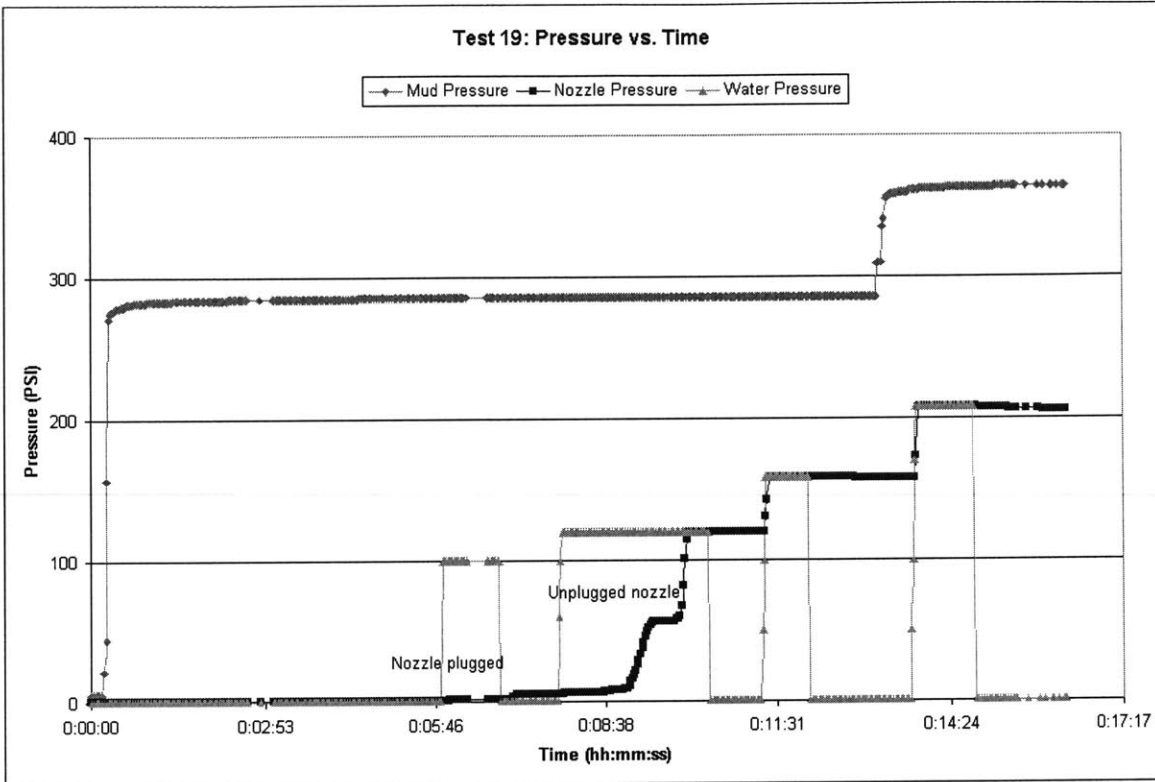


Figure 6.34: Pressure vs. Time graph of Nozzle Concept Test 19.



Figure 6.35: Pictures of Nozzle Concept Test 19.

Test 20

F&H Nozzle: L4 (modified to nozzle tip OD= 0.171" and ID= 0.067") (same as Test 12)

Berea Sandstone core

Mud pressure: ~250psi

Water pressure varied

Start test with nozzle filled with water and at face of core

Observations:

Time for pressure to drop from 100psi to 70psi= 27,236 seconds

Psi/sec= 0.001101483
Sec/psi= 907.8666667

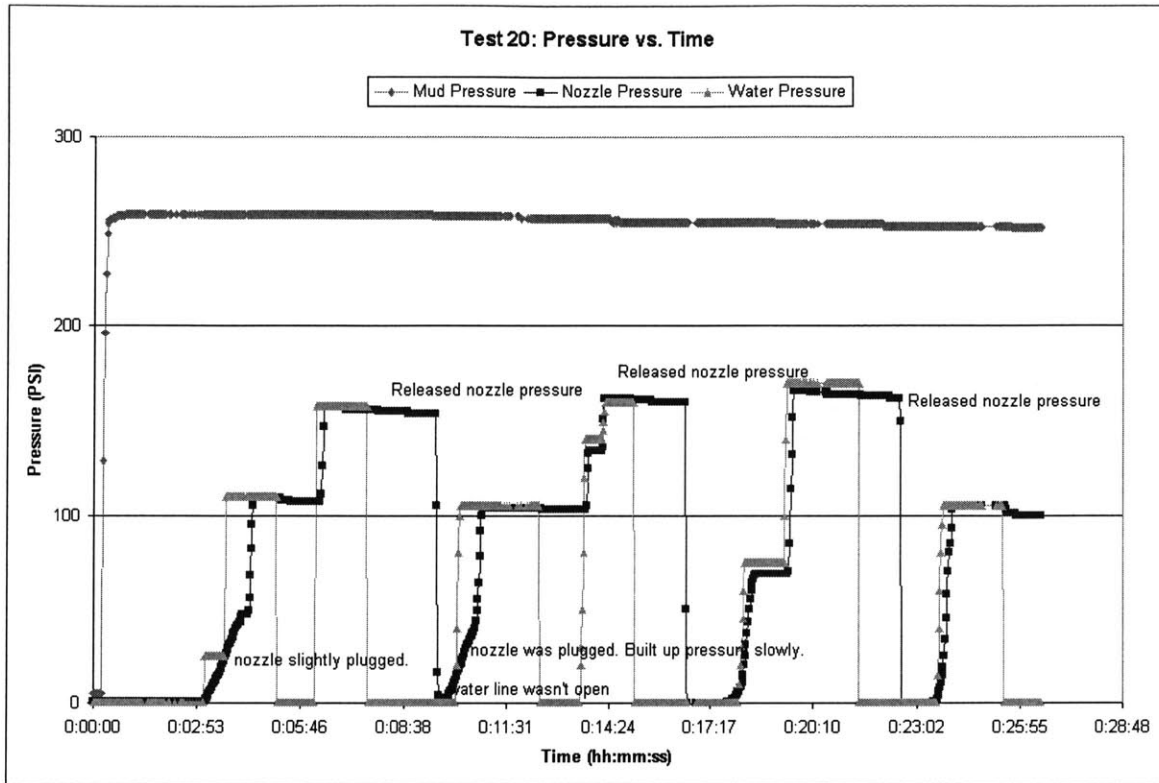


Figure 6.36: Pressure vs. Time Graph of Nozzle Concept Test 20.

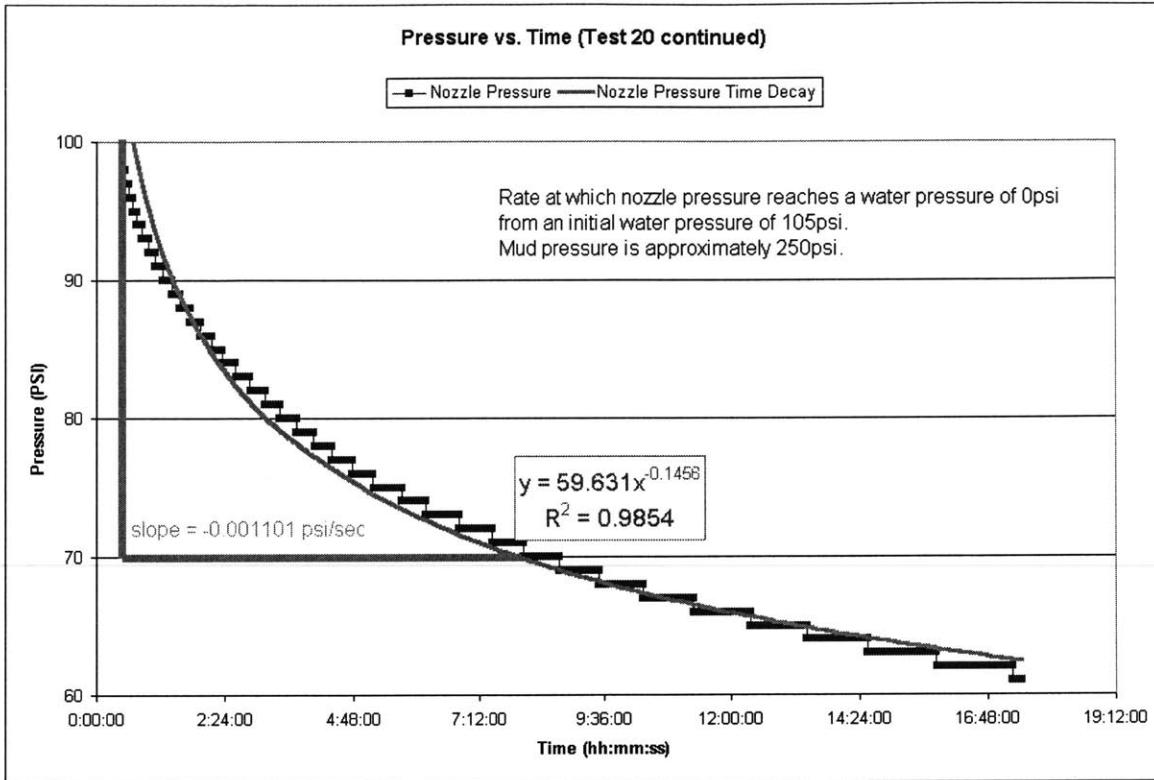


Figure 6.37: Pressure Decay vs. Time graph of Nozzle Concept Test 20.

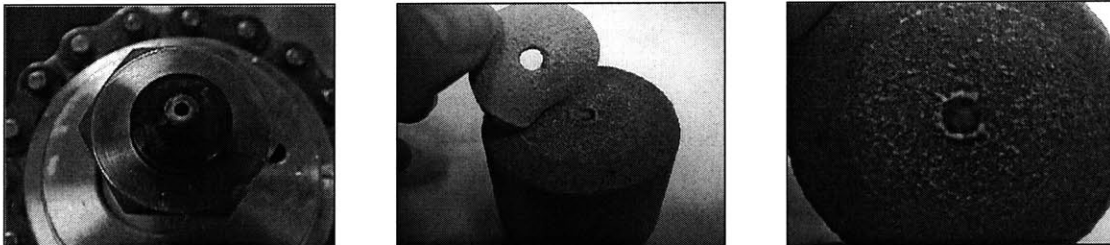


Figure 6.38: Pictures of Nozzle Concept Test 20.

Test 21

F&H Nozzle: L4 (same modifications as in Test 20)
Berea Sandstone core

Filled pressure vessel completely with water to see the nozzle pressure drop off rate.
Pressurize water to 260, and then turn it off to zero. Start with nozzle full of water and at
face of core. No mud was used in this test. Trying to find out leak off rate of nozzle
Time of Decay from 250psi to 300 psi = 1744 seconds
Rate of Decay: 0.028669725 PSI/ sec

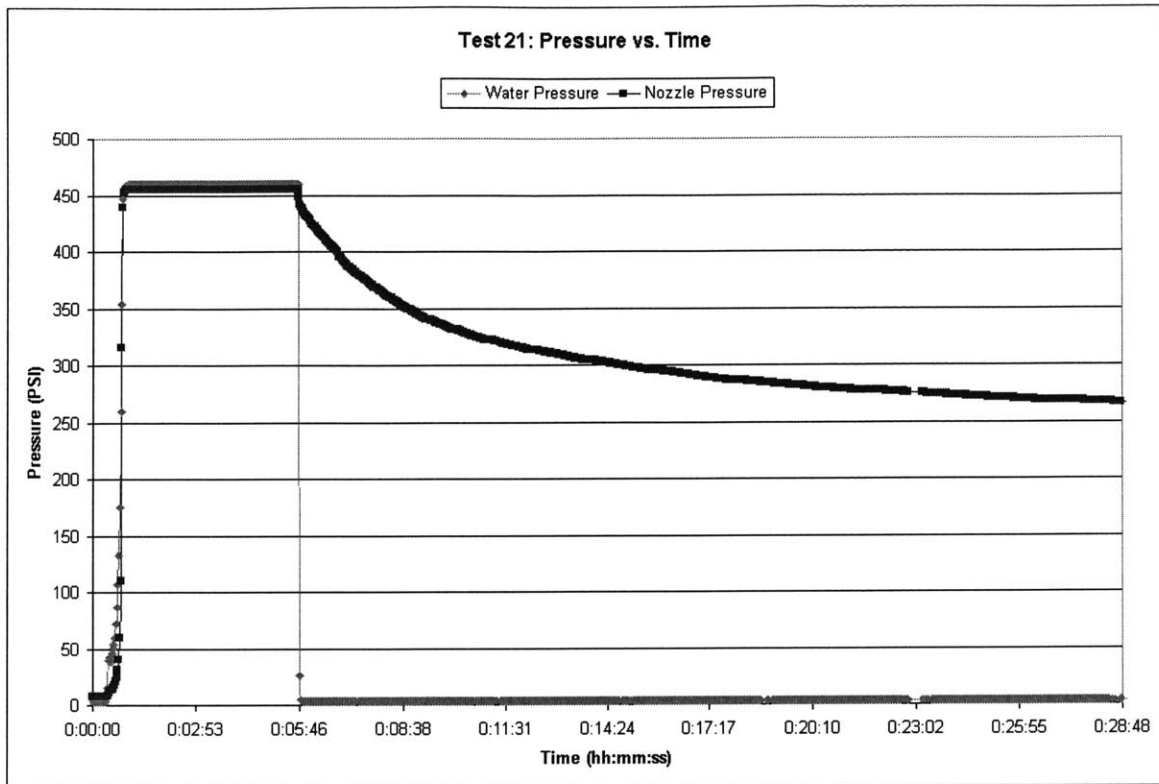


Figure 6.39: Pressure vs. Time graph of Nozzle Conept Test 21.

Test22

F&H Nozzle: L4 with modifications (same as test 22)

Repeat of Test 21, but only bring water pressure up to 350 psi to see if decay rate is the same as Test 21.

Berea sandstone core

Start test with nozzle full of water and at face of rock

Time to go from 300 psi to 250 psi = 723 sec

Rate of Decay: 0.069156293 psi/sec

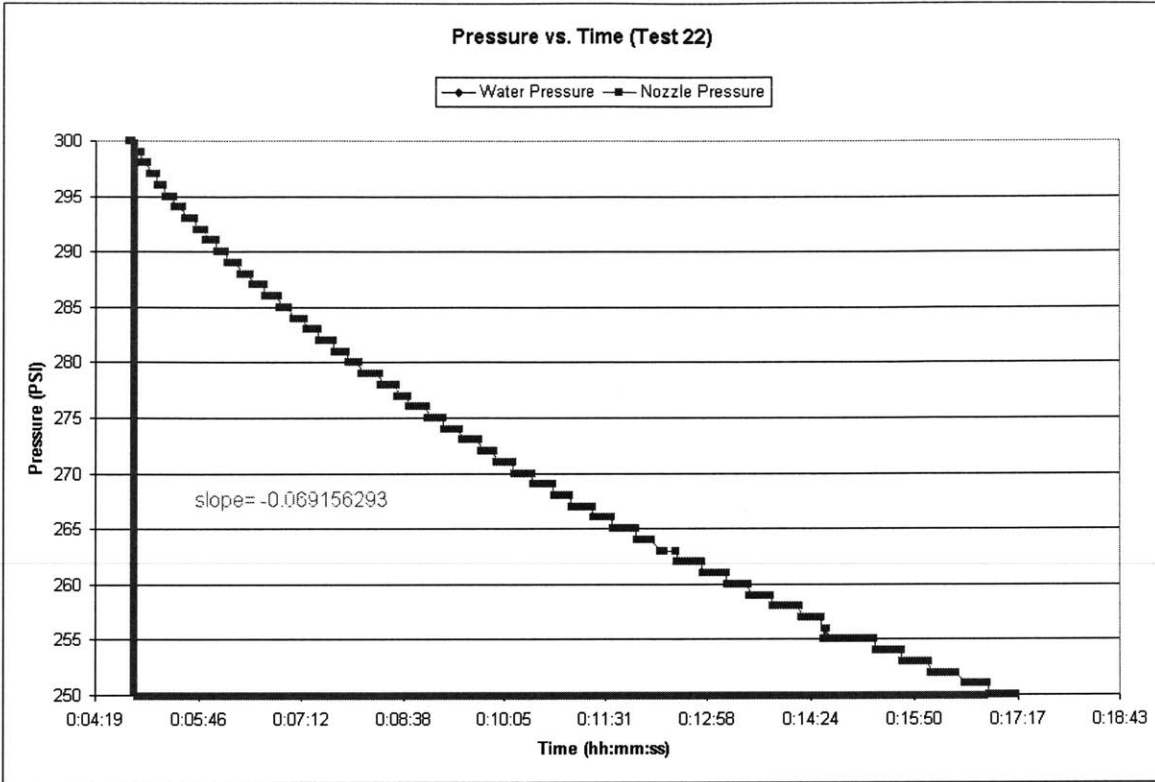


Figure 6.40: Pressure decay vs. Time graph of Nozzle Concept Test 22.

Test 23

Repeat of Test 22

Time to go from 300psi to 250psi: 160seconds

Rate at which pressure falls from 300 to 250psi : 0.3125 psi/sec

Time for pressure to drop 1psi: 3.2 sec/psi

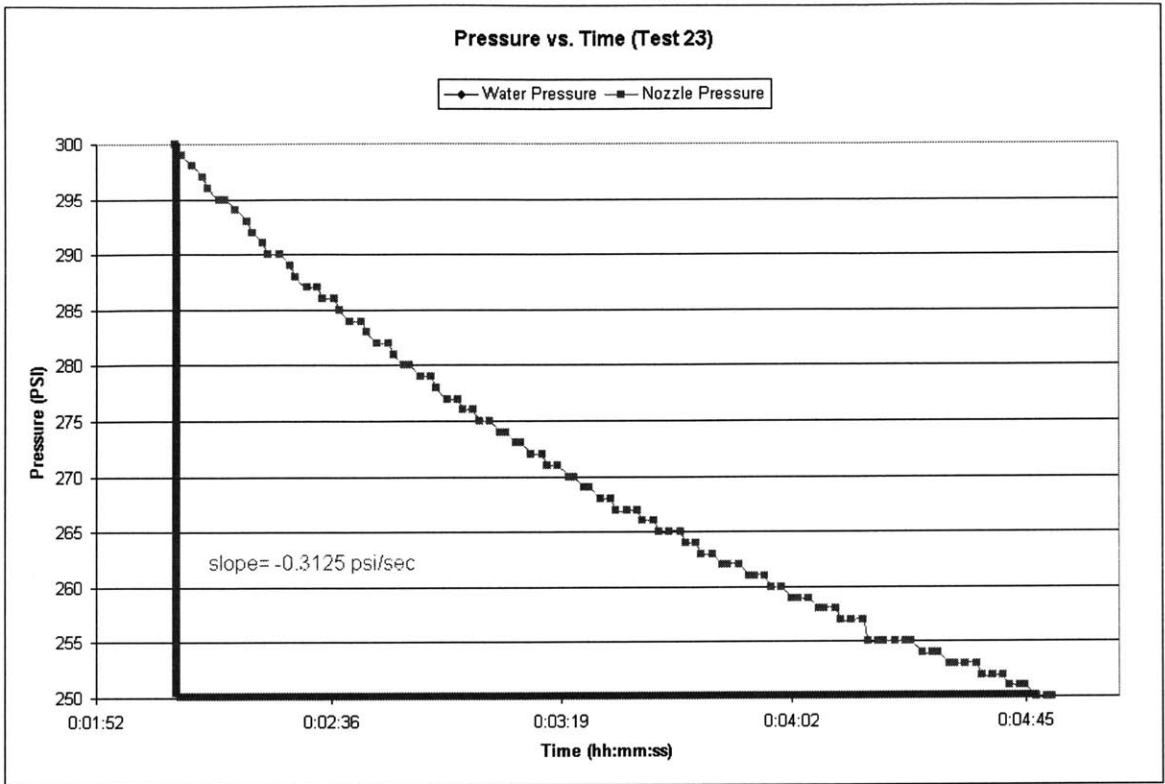


Figure 6.41: Pressure Decay vs. Time graph of Nozzle Concept 23.

Test 24

Repeat of Test 22 and 23

Time to go from 100psi to 70psi= 1329sec

Psi/sec=0.022573363

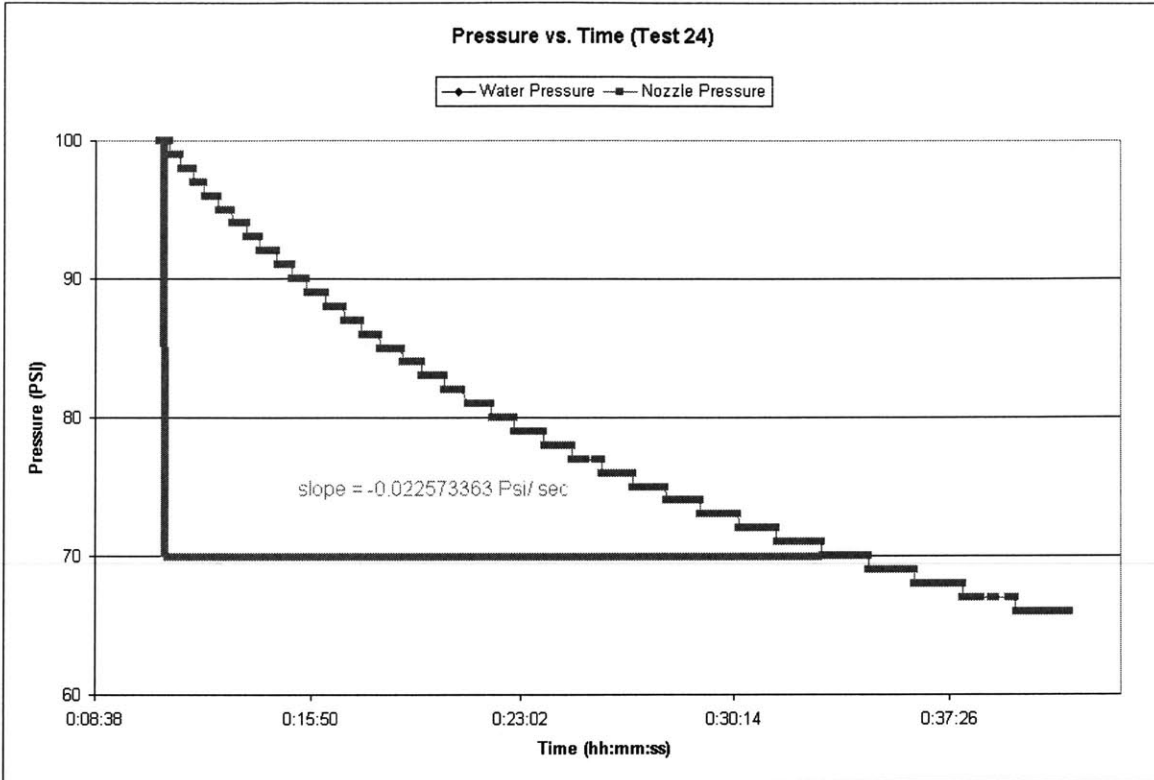


Figure 6.42: Pressure Decay vs. Time graph of Nozzle Concept Test 24.

Test 25

Successful: shows that there is no capillary pressure

F&H nozzle: L4 (with modifications).

Trying to measure capillary pressure leak off rate for the L4 modified F&H Nozzle. No filter in set up. Completely filling the setup with water, and the nozzle with water. Then bringing water pressure to 500psi, and then back down to 0psi instantly.

Observations: Test showed that there are no capillary pressure effects due to the nozzle. It also shows that any "seemingly" capillary effects are in fact due to the pore sizes of the filter when the nozzle is put to the face of the filter.

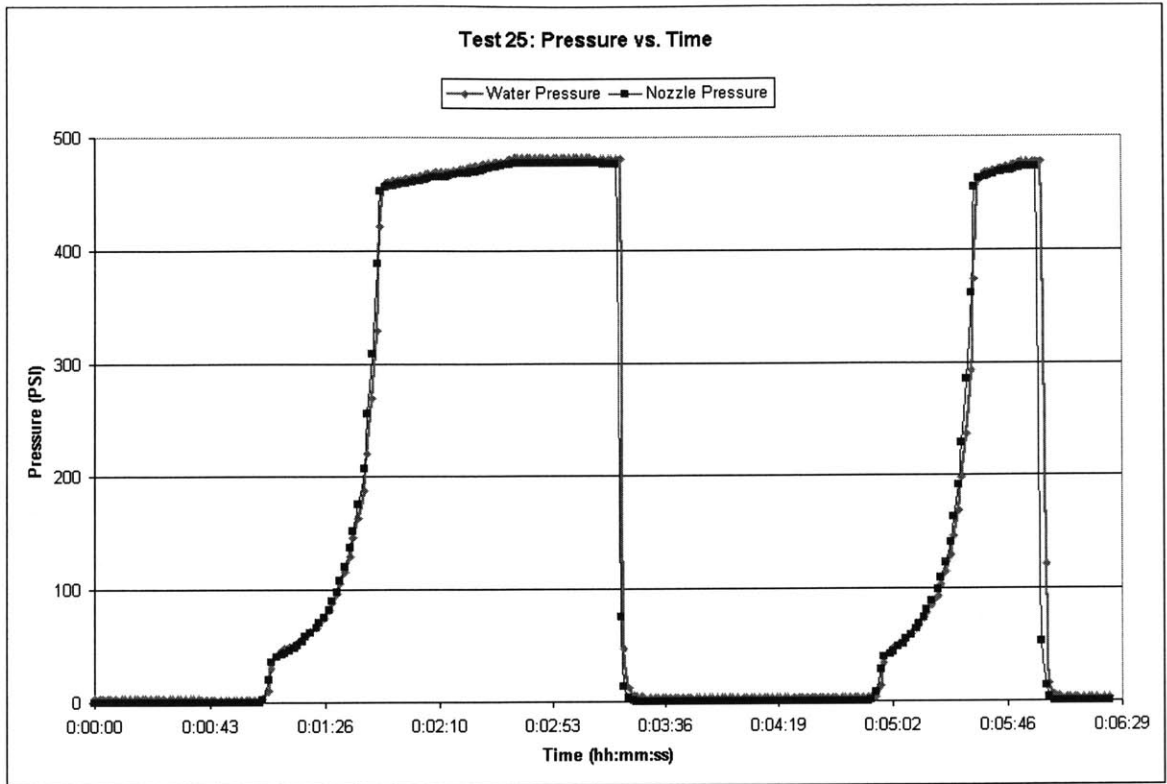


Figure 6.43: Pressure vs. Time Graph of Nozzle Concept Test 25.

Test 26

F&H Nozzle: LS-75 (smallest orifice size)
No filter

Filled the entire apparatus with water in order to try to measure capillary leak off rate from the nozzle.

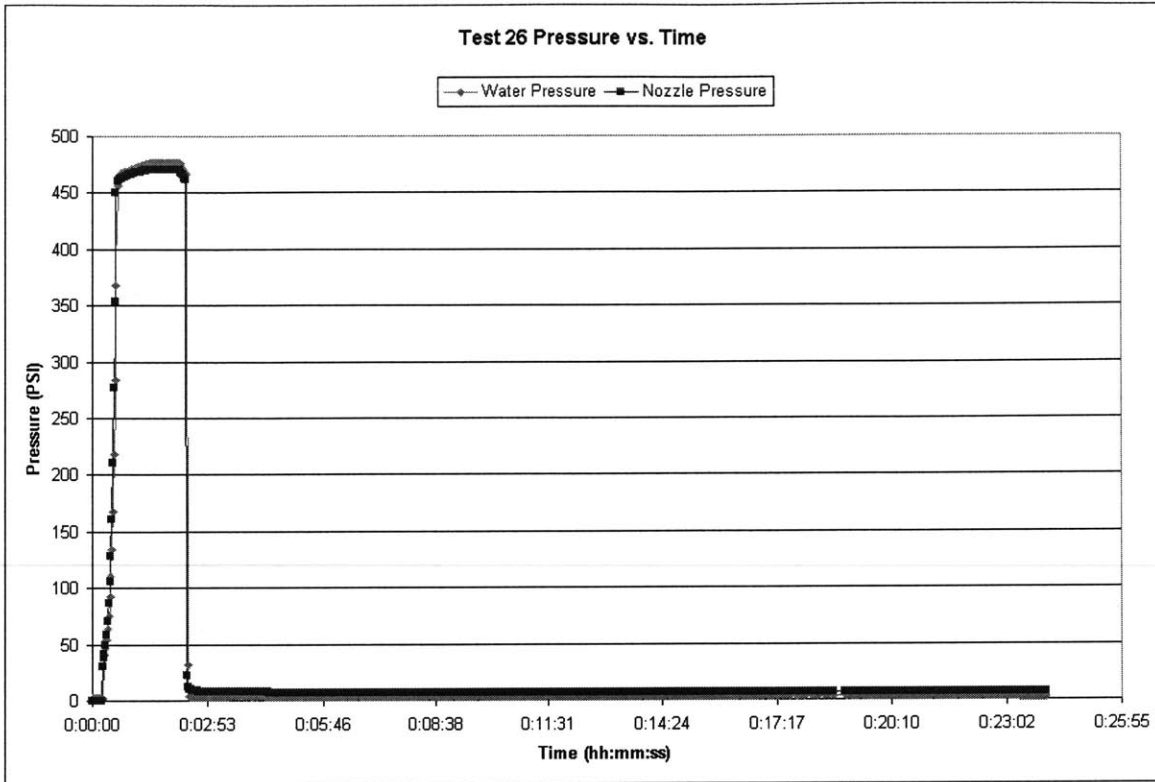


Figure 6.44: Pressure vs. Time graph of Nozzle Concept Test 26.

Test 27

Repeat of Test 26
 F&H Nozzle LS-75
 No core filter

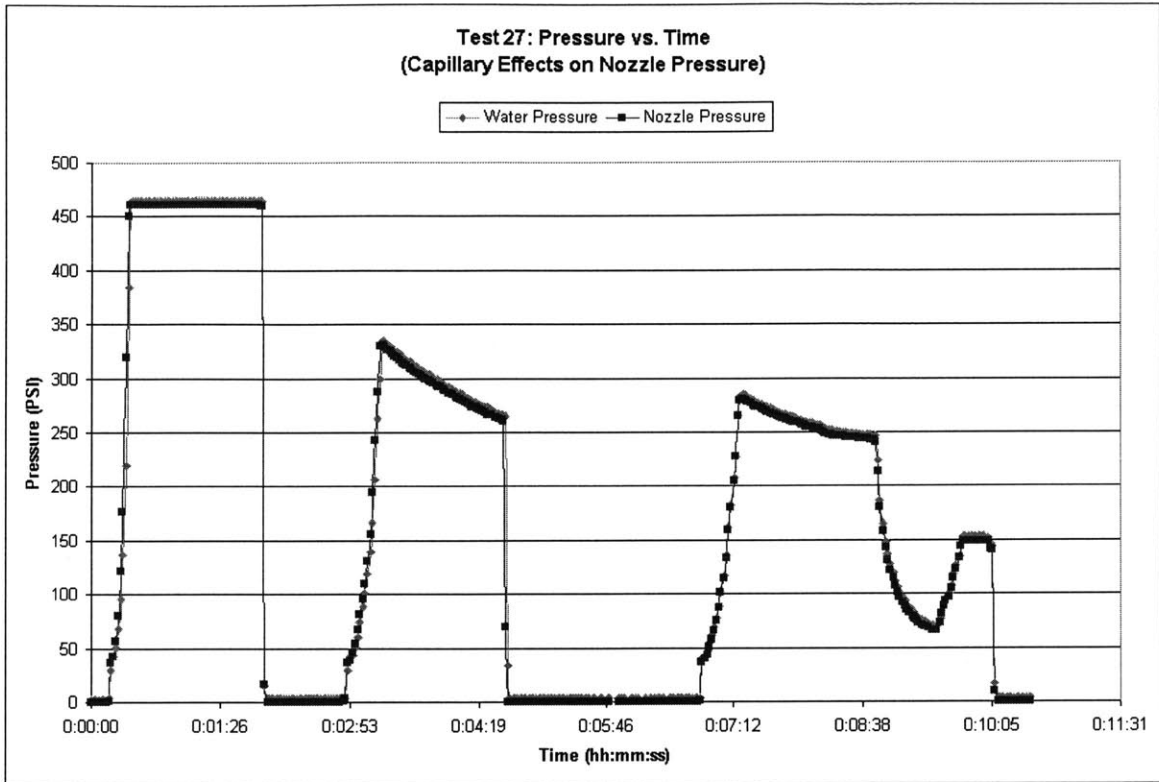


Figure 6.45: Pressure vs. Time graph of Nozzle Concept Test 27.

Test 28

F&H Nozzle: L4 (with a new modification: nozzle orifice OD= 0.195" and ID= 0.085")
 Disc Filters: Used 2 Permaflow disc filters - F60
 Start test with nozzle full of water and at face of filter
 Vary water pressure

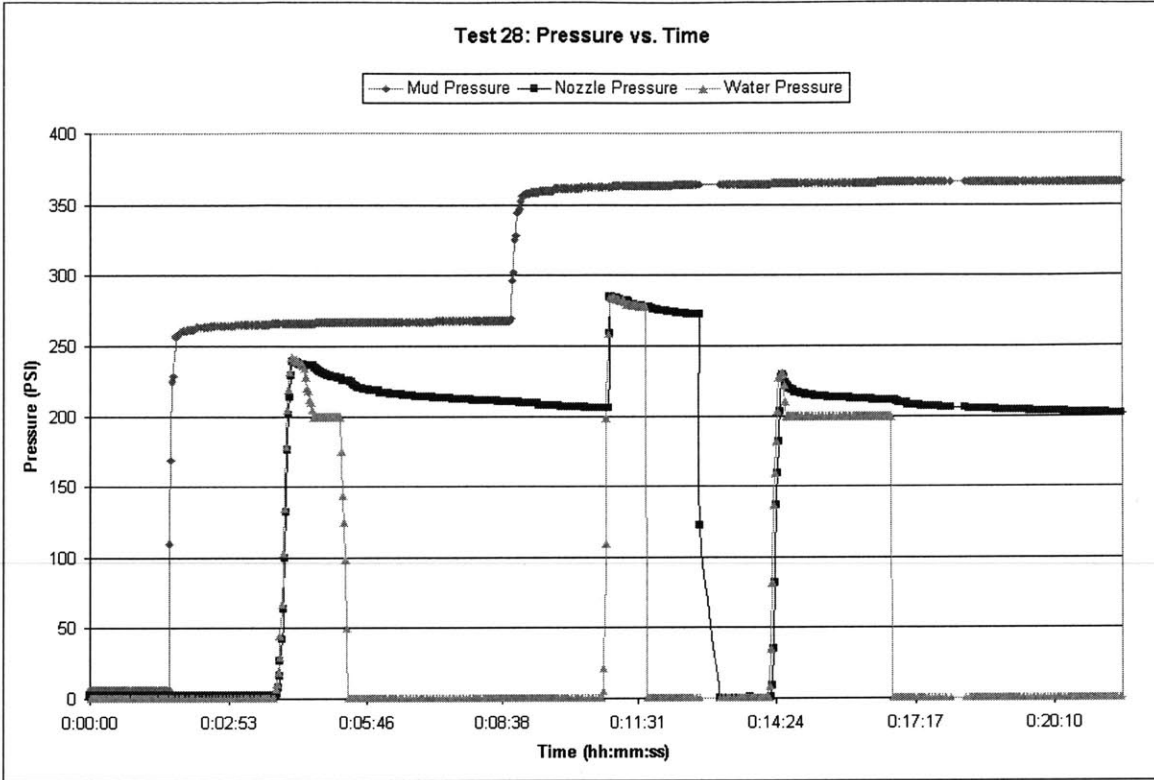


Figure 6.46: Pressure vs. Time Graph of Nozzle Concept Test 28.

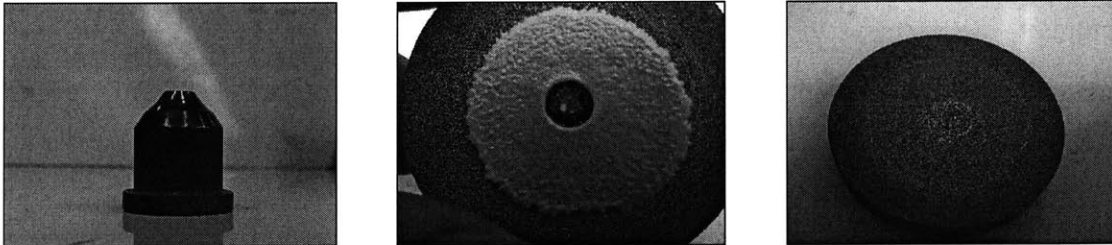


Figure 6.47: Pictures of Nozzle Concept Test 28.

Test 29

F&H Nozzle L4 (with modification III, nozzle orifice with OD= 0.295" and ID= 0.120")
 Disc Filters: Used 2 Permaflow disk filters F60
 Water pressure Varied

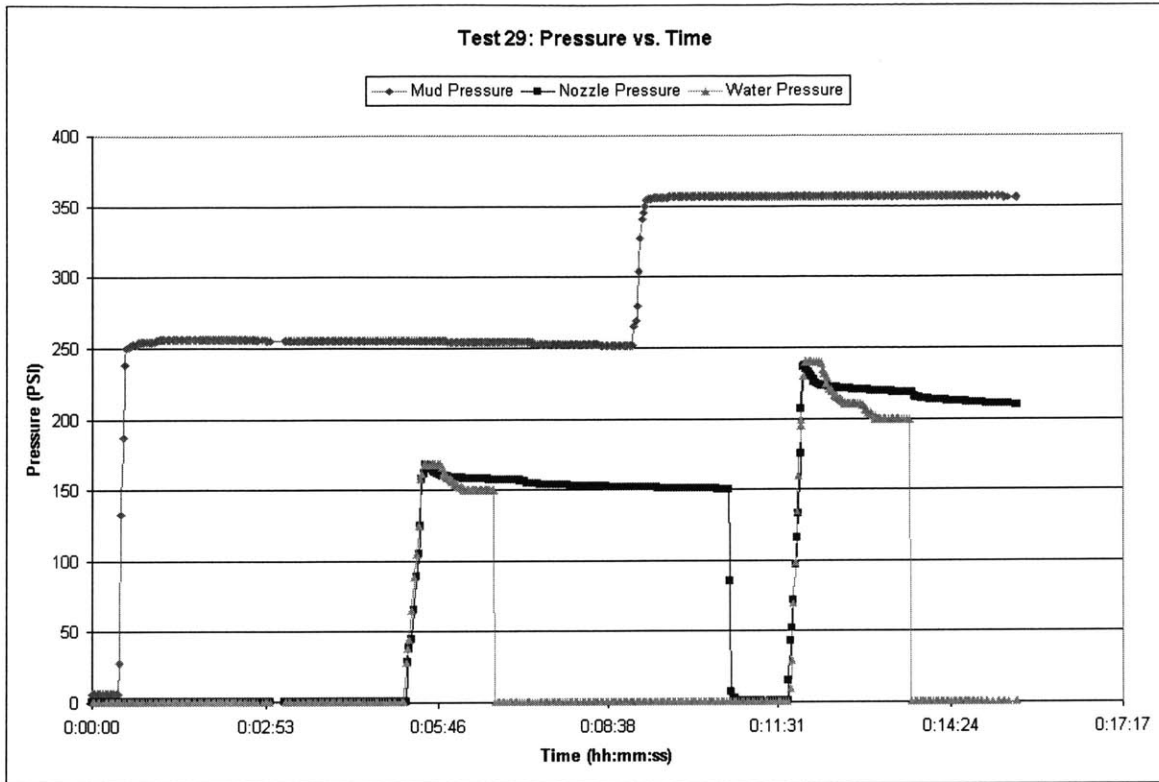


Figure 6.48: Pressure vs. Time graph of Nozzle Concept Test 29.

Pictures:

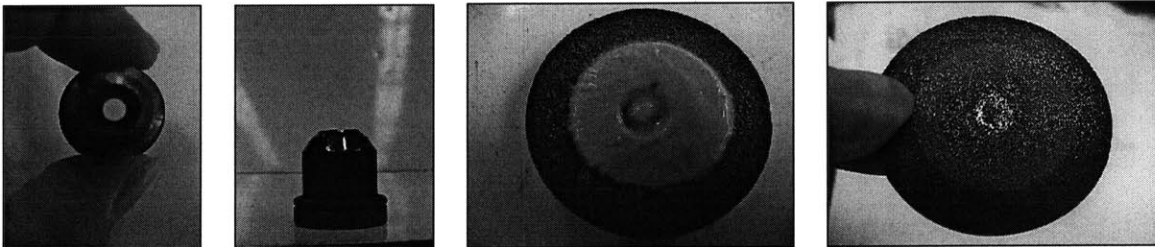


Figure 6.49: Pictures of Nozzle Concept Test 29.

Test 30

F&H Nozzle: L4 (modification IV, nozzle orifice with OD= 0.342" and ID= 0.180")

Disc Filters: Used 2 Permaflow disk filters F60

Varied water pressure

Start test with nozzle filled with water and at face of filter

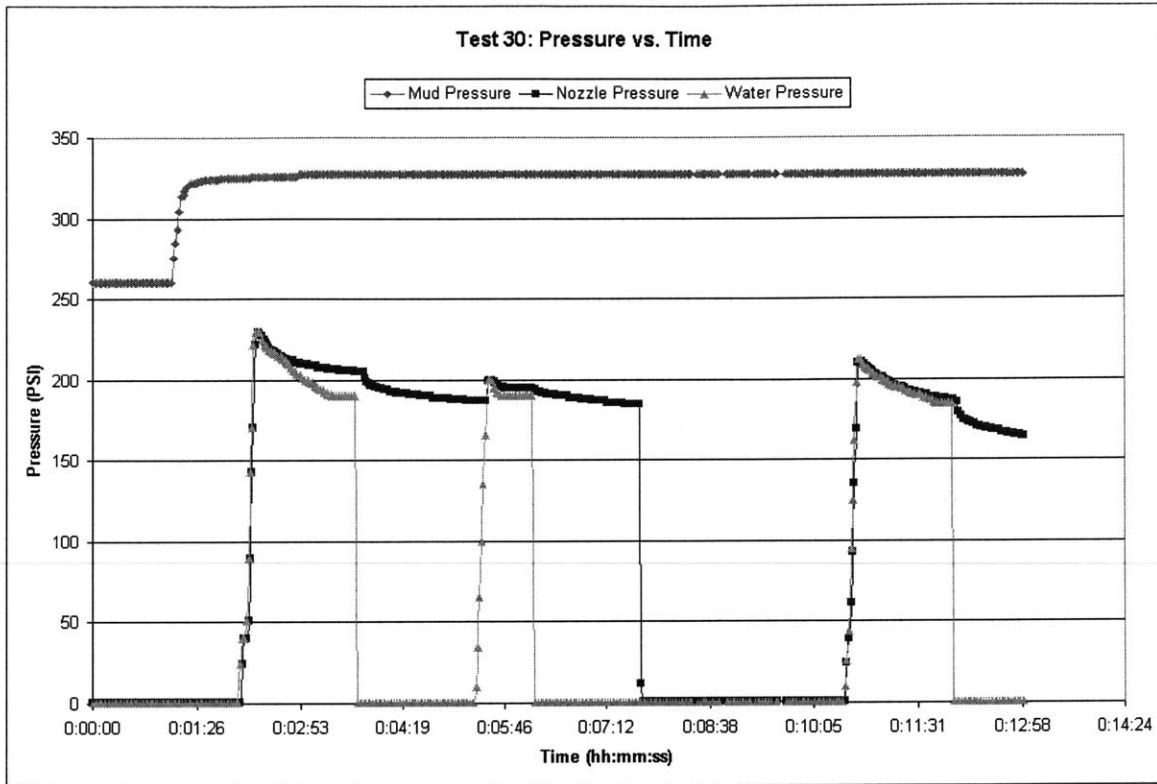


Figure 6.50: Pressure vs. Time Graph of Nozzle Concept Test 30.

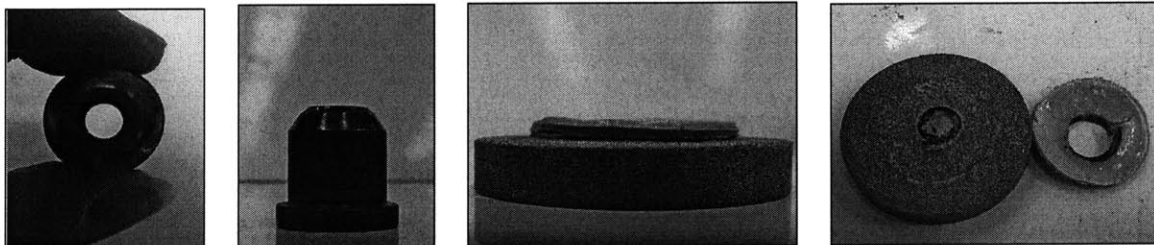


Figure 6.51: Pictures of Nozzle Concept Test 30.

Test 31

Same as test 30, but using a different filter

F&H nozzle L4, (modification IV: nozzle orifice with OD=0.342" and ID= 0.180")

Disc filter: 1 Permaflow disk filter (largest pore size) F40

Start test with nozzle filled with water, and at face of filter.

Compare bleed off rate between test 30 and 31.

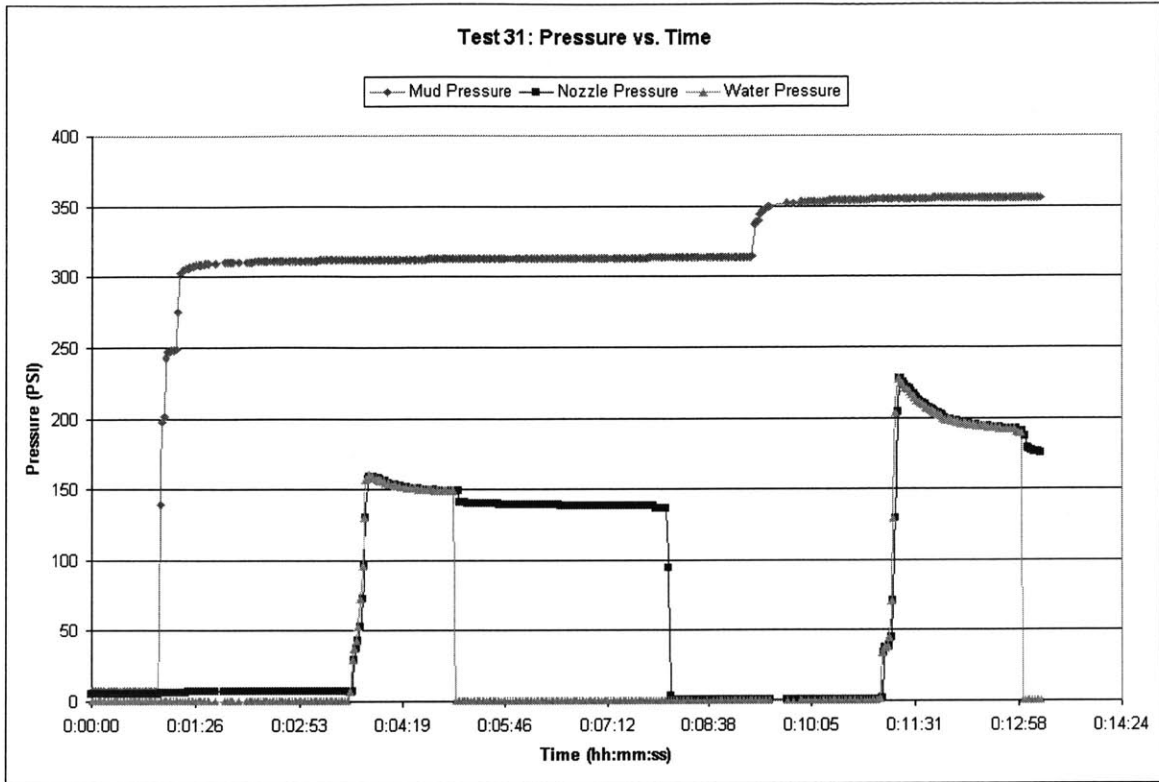


Figure 6.52: Pressure vs. Time Graph of Nozzle Concept Test 31.

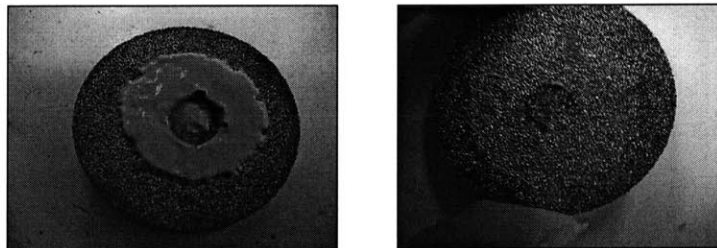


Figure 6.53: Pictures of Nozzle Concept Test 31.

Test 32

F&H Nozzle: L4 (modification V: nozzle orifice, OD= 0.440" and ID= 0.350")
 Disc Filters: Used 4 Mott metal disk filters (equivalent to 2 permafrow disk filters)
 100micron pore size
 Mott CPN:1005010-01-999
 Mott P/N 1000-1.50-125-200

Start test with nozzle full of water and at face of filter

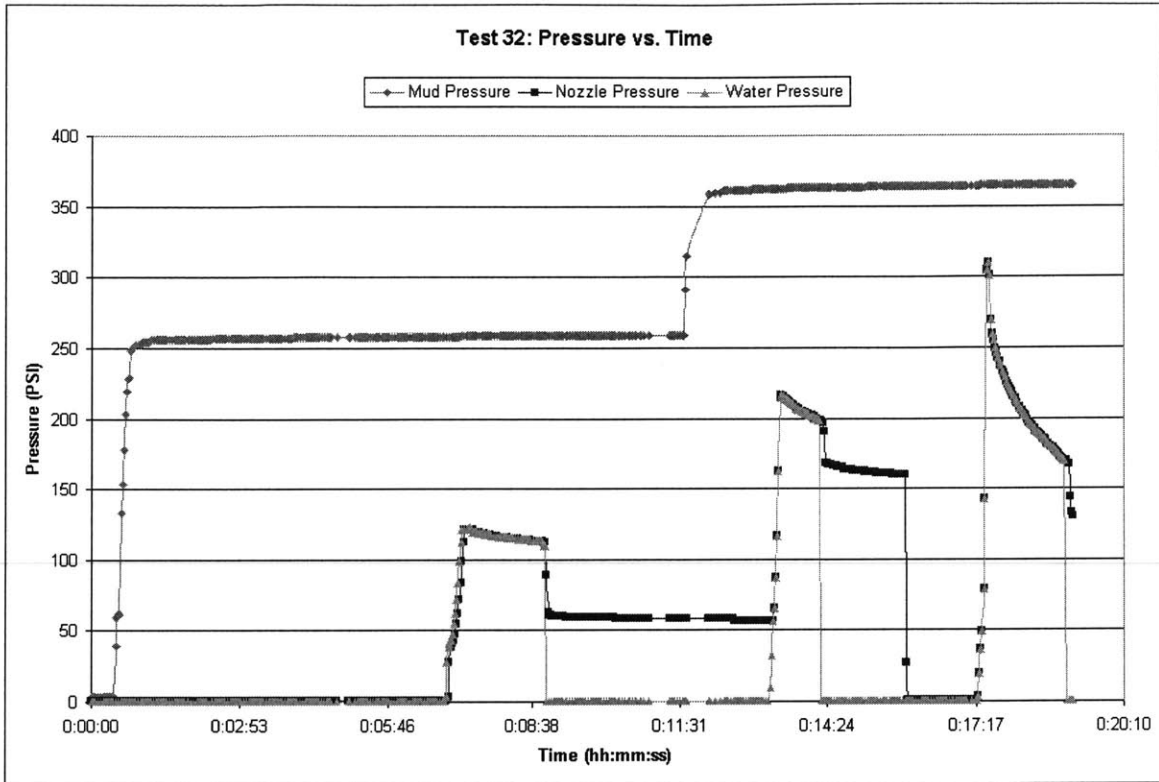


Figure 6.54: Pressure vs. Time graph of Nozzle Concept Test 32.

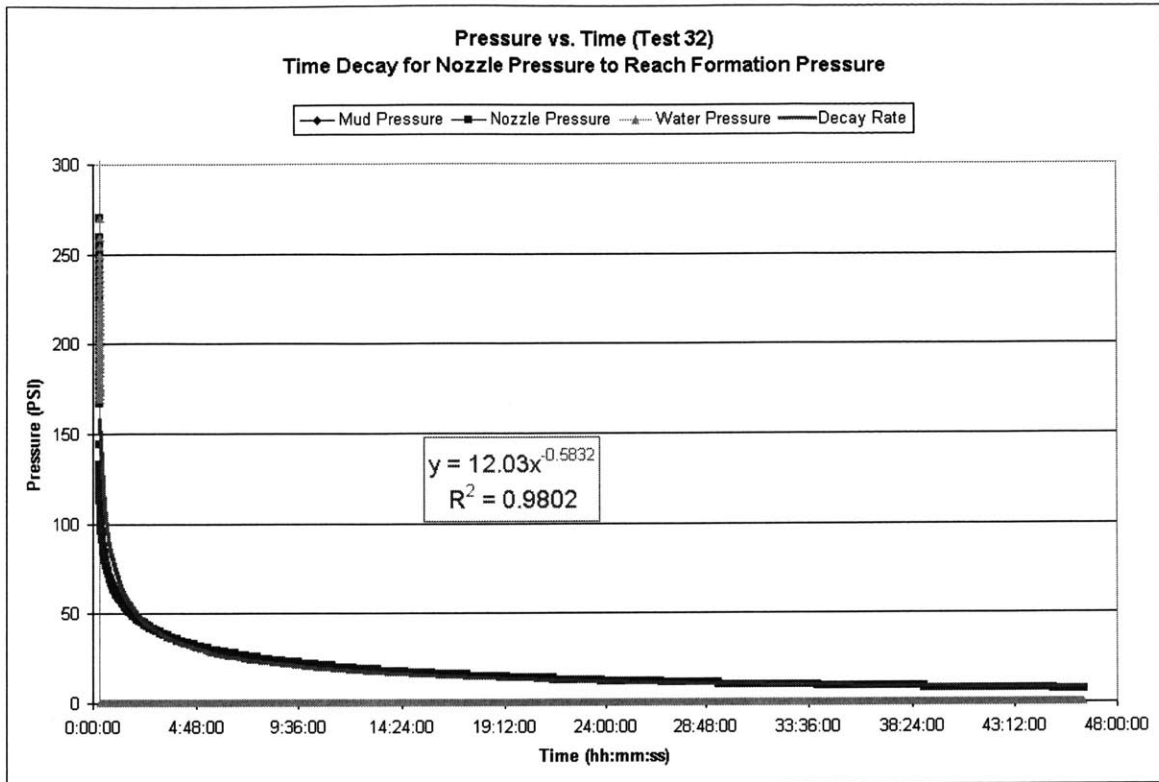


Figure 6.55: Pressure Decay vs. Time Graph of Nozzle Concept Test 32.

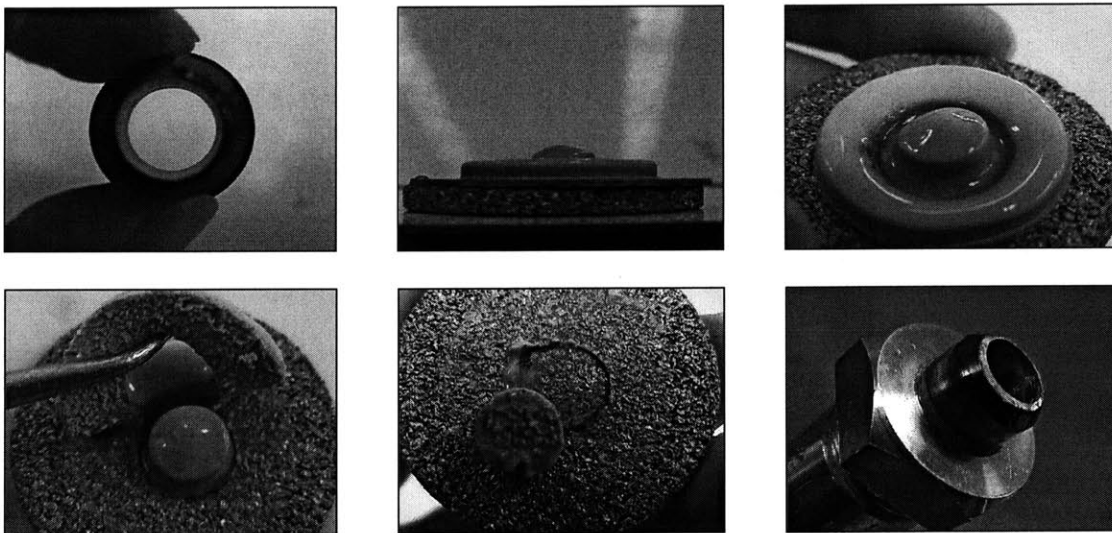


Figure 6.56: Pictures of Nozzle Concept Test 32.

7 Conclusions and Recommendations

7.1 Conclusions

From the Nozzle Concept tests it is concluded that formation pressure can indeed be measured using a small orifice nozzle. The maximum value of the formation pressure can be measured quickly as illustrated in Figure 7.1. Once the nozzle reaches a maximum pressure however, the dissipation rate to any lower pressure is extremely slow (see Figure 7.2). Dissipation rate appears to be formation related. Although the rate of pressure decay is not clearly understood, it appears to be dependent on formation characteristics, pore size of formation, nozzle orifice size and wall thickness and shape since there is variation between dissipation rates (compare Figure 7.2, Figure 7.3, and Figure 7.4). However, it was proven that the decay rate is not dependent upon capillary pressure effects of the nozzle as seen in Figure 7.5.

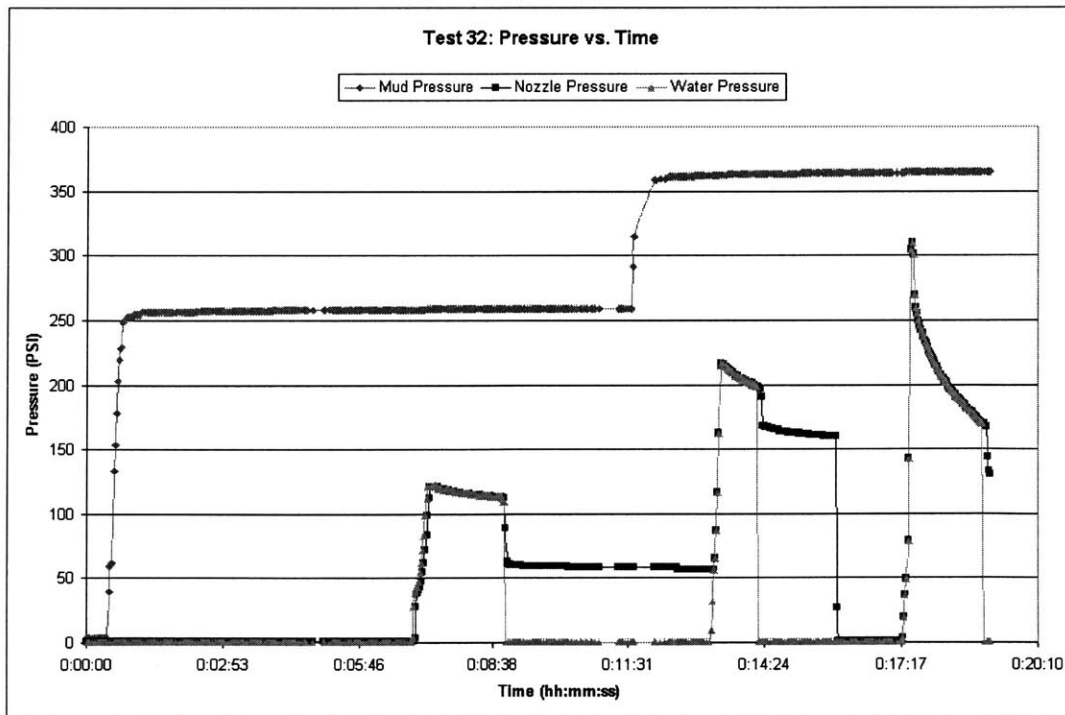


Figure 7.1: Nozzle pressure measures Maximum Water Pressure quickly.

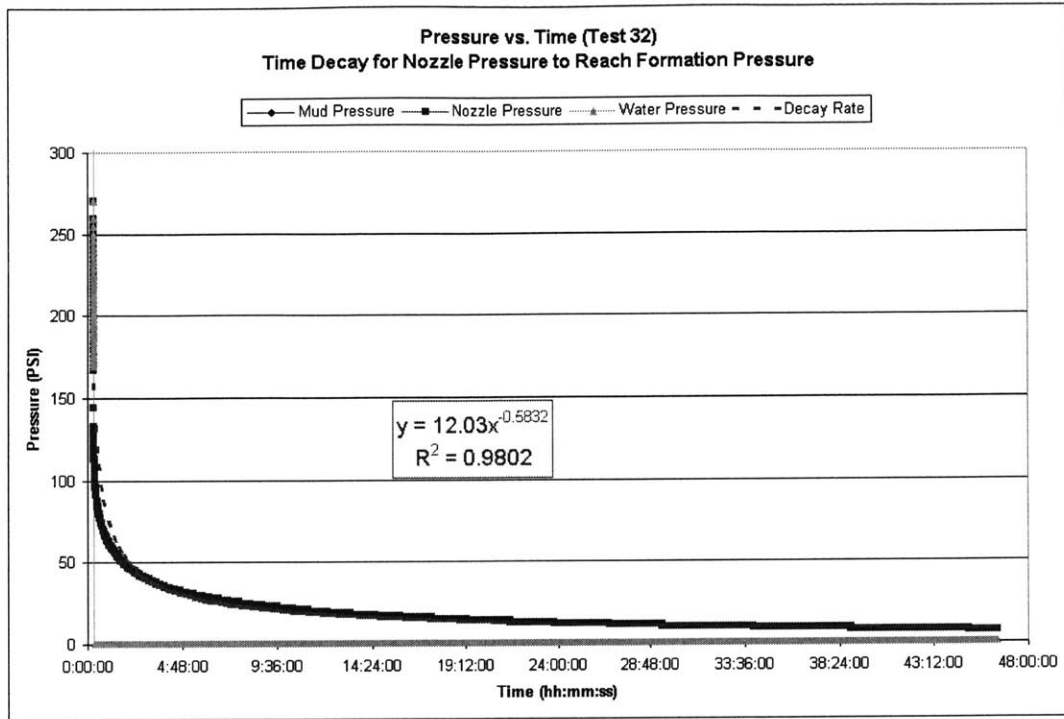


Figure 7.2: Dissipation Rate of nozzle pressure to a lower formation pressure.

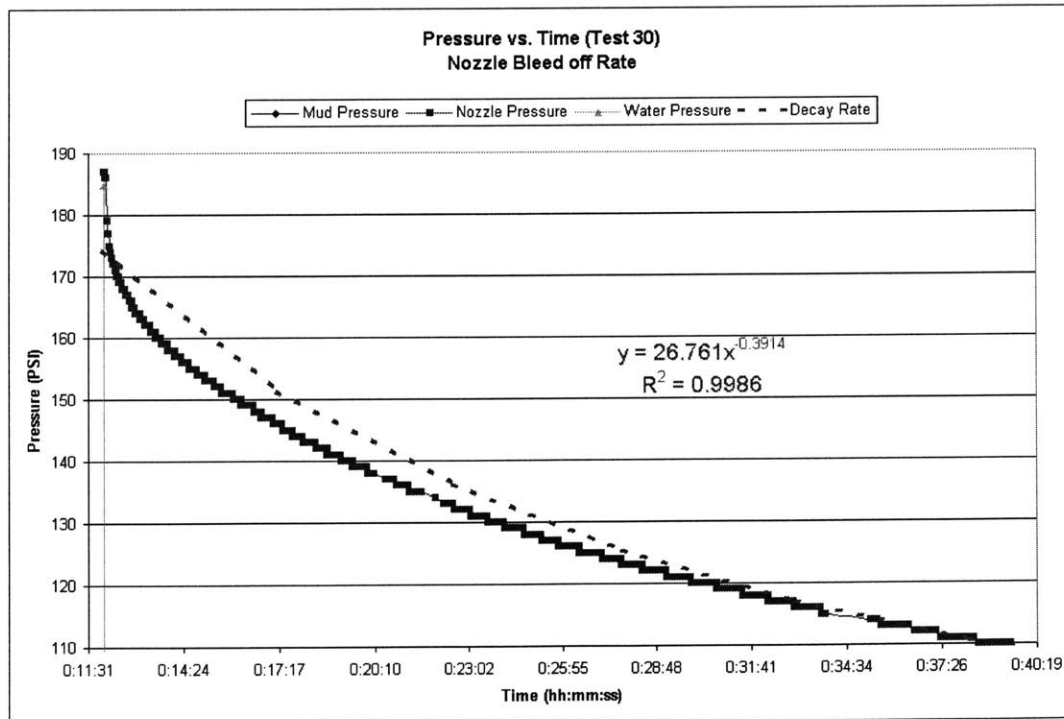


Figure 7.3: Dissipation rate to a lower water pressure.

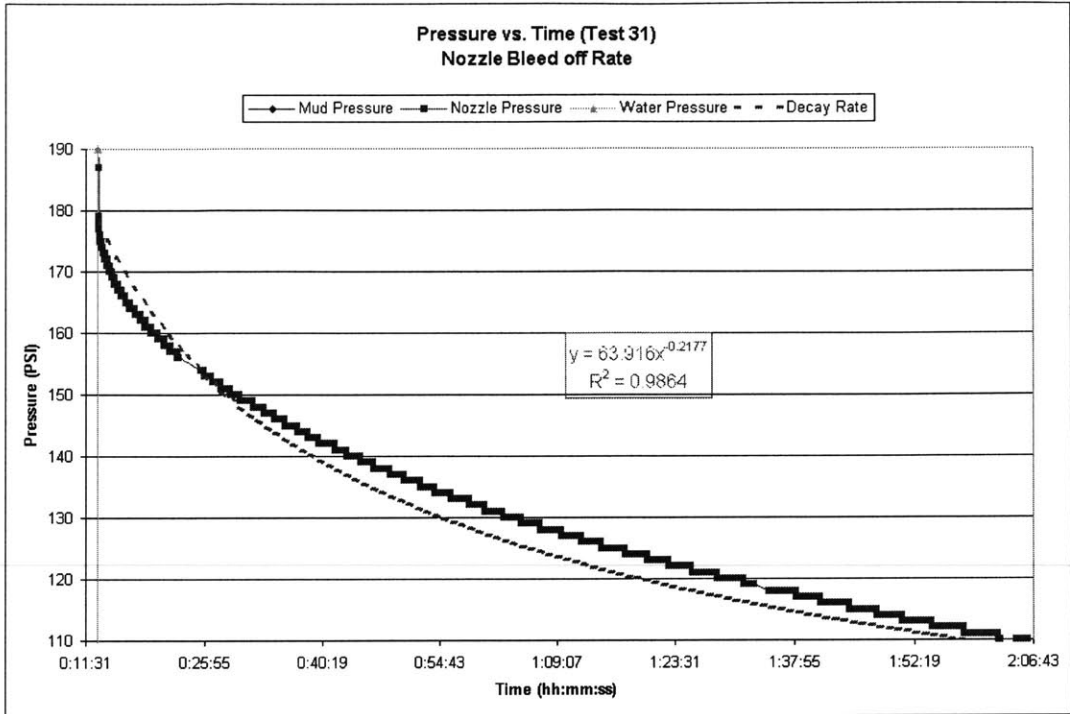


Figure 7.4: Dissipation Rate to a lower water pressure.

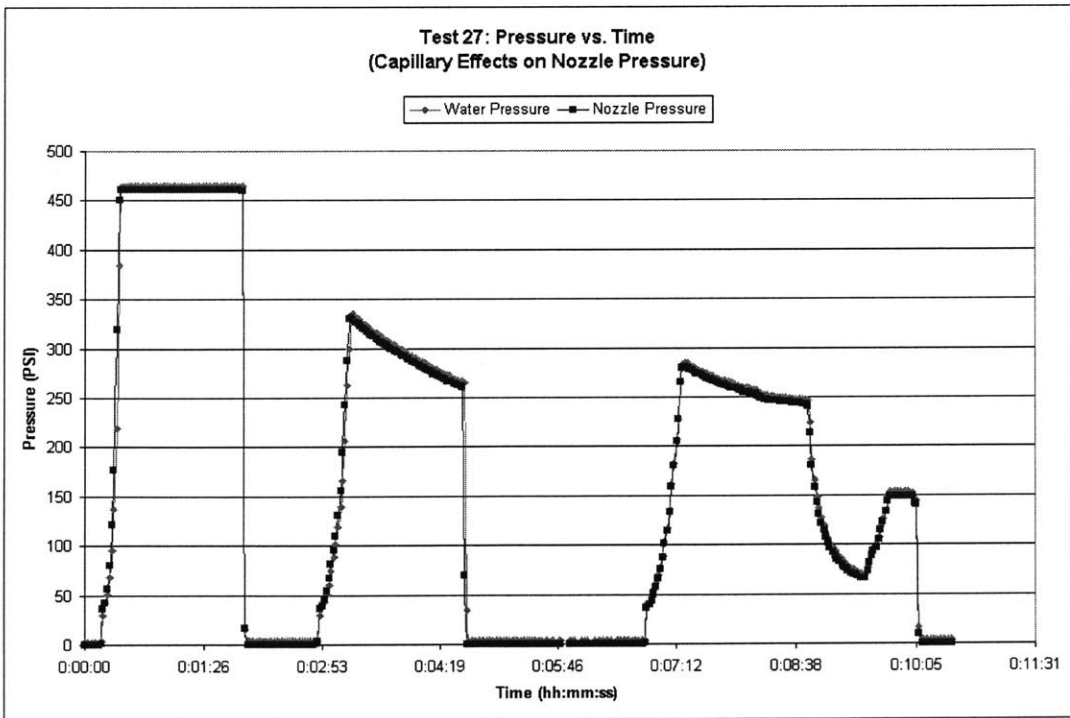


Figure 7.5: Capillary Pressure effects on nozzle pressure (non existent)

In summary, the Nozzle Concept can measure formation pressure

- Measures maximum formation pressure quickly
- Dissipates to a lower formation pressure very slowly
- Mudcake seals the nozzle only if the nozzle is initially at face of formation

7.2 Recommendations for Future Work

This thesis proved the nozzle concept method feasible through preliminary testing methods. Further testing of the Nozzle concept is recommended to gain a better understanding of the results of this testing. It is also recommended that optimization testing be done on the nozzle geometry. Even though several geometries were tested, it is still unclear as to which shape, orifice size, and wall thickness guaranteed the best results. The slow, inconsistent dissipation rate resulting from the tests should also be studied in greater detail.

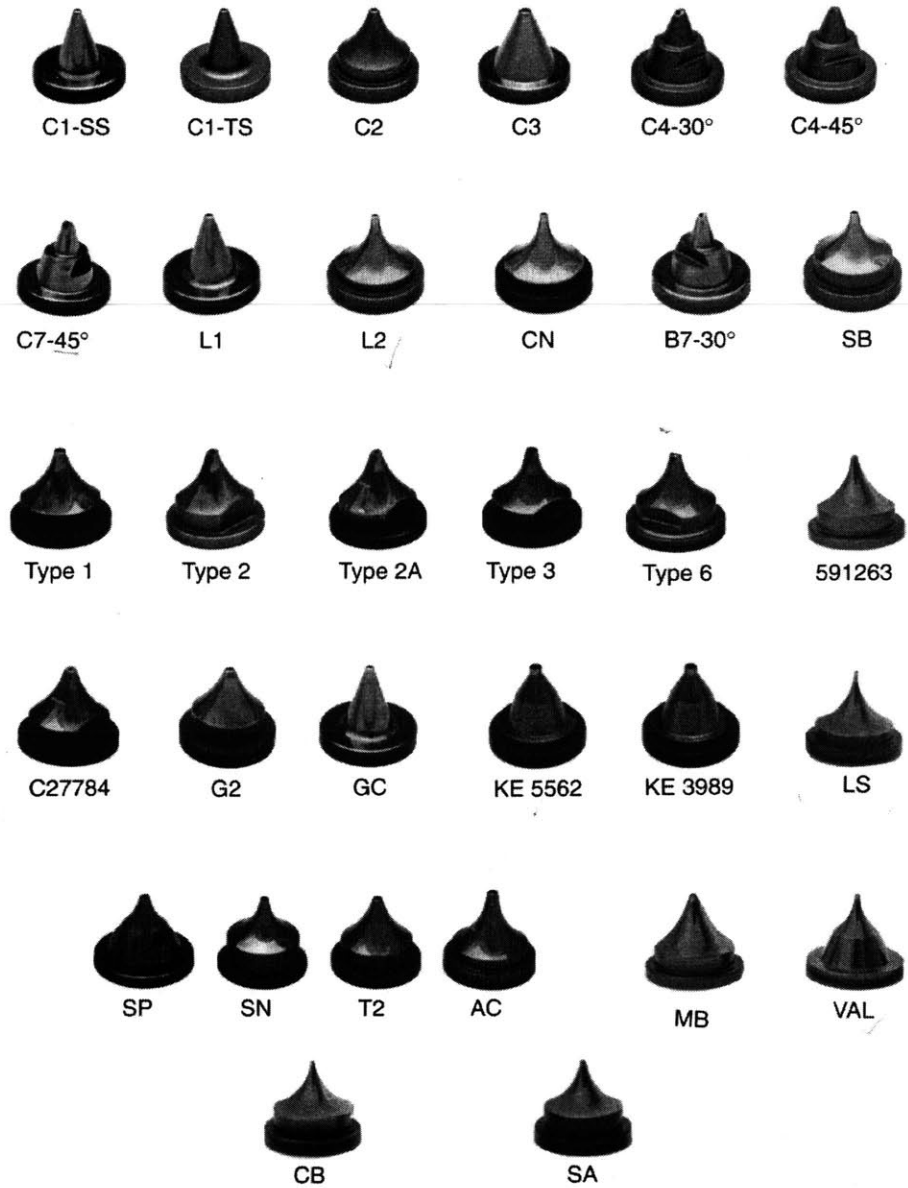
The recommended Phase II testing would involve testing the nozzle concept with a closed-tip nozzle that opens after it penetrates through the mudcake layer. Adding a retractable needle to close of the tip of the nozzle could prevent clogging that occurred during testing.

References

- [1] Oilfield Review. CD-ROM overview of the oilfield industry. Schlumberger, 1996.
- [2] Society of Petroleum Engineers of AIME., *Well completions*. 1978. Dallas, Texas.
- [3] Schlumberger website. www.slb.com. Oilfield Services.
- [4] Schlumberger Dowell Report. Concept Phase. December 1998.
- [5] Annual Book of ASTM Standards, Section 4 Construction. Volume 04.09. Soil and Rock (II): D 4943 –latest; Geosynthetics. D 5778 Standard Test Method for Performing Electronic Friction Cone and Piezocone Penetration Testing of Soils.
- [6] Fugro Geotechnical Company. Pamphlet and website information on CPU technology and applications.
- [7] Recep Yilmaz, VP Fugro Geosciences, Inc. Personal Interview. August 1999.
- [8] Pagani Geotechnical Equipment. Information pamphlet, video.
- [9] Sutabutr, T., “Analysis and Interpretation of Tapered Piezoprobe and Application to Offshore Pile Design”. Doctoral Thesis, MIT. February, 1999.
- [10] Havlinek, K. Report. “Obtaining Formation Pressure using an Ultra-Sonic Horn”. January 1998.
- [11] U.S. Department of Energy, Cone Penetrometer. Innovative Technology Summary Report. April 1996.
- [12] Schlumberger Dowell. Dowell Drilling Fluids: Formation Damage Related to Reservoir Drilling Fluids. Presentation. FMD 1-36. June 1997.
- [13] Underhill, W.B, Schlumberger Sugar Land Product Center, Moore, L., Schlumberger Gulf Coast Special Services and Meeten, G.H., Schlumberger Cambridge Research. “Model-Based Sticking Risk Assessment for Wireline Formation Testing Tools in the U.S. Gulf Coast” SPE 48963. Copyright 1998, Society of Petroleum Engineers, Inc.
- [14] Mark Brady, Schlumberger Dowell. Personal Interview. July 1999.
- [15] Pitoni, E., Copercini, P., ENI-Agip; and Heitmann, N., and Kelly, B., Schlumberger Dowell. “Engineered Drill-in Fluids Deliver No-Skin Wells Offshore Gabon” Fluids Engineering. Copyright Hart Publications Inc., Houston, TX. (Petroleum Engineer – May 1999).
- [16] SRPC-D. Drilling Fluids Systems. STARDRILL: A Fluid System for Openhole Completions. Client Presentation. FMD 1-36. June, 1997.
- [17] J.L.Lummus, A.Park. New Surfactant mixture eases differential sticking, stabilizes hole. Oil and Gas Journal, pages 62-66, November 1962.
- [18] Bushnell, Y.M. and Panesar, S.S., BP Research Center. “Differential Sticking Laboratory Tests Can Improve Mud Design,” SPE 22549. Copyright 1991, Society of Petroleum Engineers, Inc.
- [19] Prieto, C., “Design of a Laboratory System for the Prediction of Wireline Tool Sticking”. Master Thesis, MIT. June 1999.
- [20] Louise Bailey, Edo Boek, Schlumberger Cambridge Research, Simon Jacques, Birkbeck College London, Tony Boassen, Olav Selle, Statoil, Jean-Francois Argillier, Daniel Longeron, Institut Francais du Petrole. “Particulate Invasion From Drilling Fluids” SPE 54762. Copyright 1999, Society of Petroleum Engineers Inc.

Appendix A

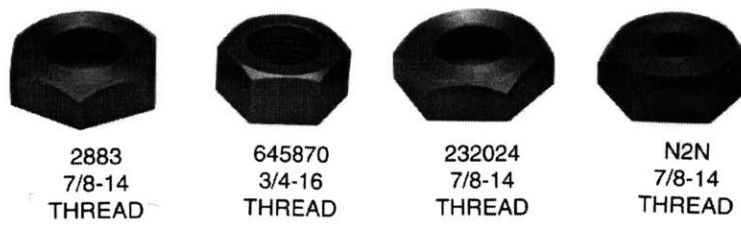
A.1 F&H Nozzles and Retaining Nuts





Nozzle Retaining Nuts

The following pages illustrate some of the various nozzle retaining nuts, as well as, the misting nut produced by F & H Nozzle Specialists, Inc.



A.2 Cores and Disc Filters

Three types of filters were used for the Formation Pressure Tester. Stimlab Berea sandstone cores, Capstan Bronze disc filters, and Mott Steel disc filters.

A.2.1 Capstan Stainless Bronze Disk Filters

Capstan Permaflow Materials



Permaflow offers a complete line of custom-made filters for your specific porous metal applications. Additionally, a standard line of disks, tubes, sheets and threaded elements are readily available.

Porous Metal Filters

MATERIALS	SINTERED BRONZE	SINTERED STAINLESS STEEL
Tensile Strength PSI	3000-7000	4000-8000
Density G/CC	4.5-5.6 (51-64%)	5.2-5.8 (67-72%)
Oxidizing Temp. (°F)	+400	+1000
Max. Operating Temp. (°F)	+800	+1500
Min. Operating Temp. (°F)	-452	-452
Chemical Composition	89-96% Copper, Bal. Tin	Type 316L (18Cr-8Ni-2 Mo)

Capstan Permaflow

16124 S. Figueroa Street
Gardena, CA 90248
T 310-366-5999
F 310-366-7832

Standard Porosity Grades^A

GRADE	Material	Particle Removal Size (Microns)	Bubble Point ^B (in. H ₂ O)	Pressure Drop ^C (PSI for 1 CFM/in ² AIR)	Maximum Pore Size (Microns)
F30	Bronze	65-110	1.1	.04-.07	200-330
F40	Bronze	50-70	1.7	.07-.14	150-210
F60	Bronze	30-45	2.9	.12-.26	90-130
F100	Bronze	15-25	6.1	.43-.90	45-72
FCR25	SS	15-25	6.1	2-8	56-65
FCR510	SS	5-15	11.7	4-12	30-35
FCR1020	SS	3-10	20.7	10-21	16-19
FCR2030	SS	2-5	31.9	17-28	10-13

F100 } 10
F150 } 10

^AOther grades available.

^BAir pressure required on one side of a sample saturated in isopropyl alcohol to form air bubbles on the other side.

^CActual permeability controlled by part density.

Above data is provided for guideline purposes only. Actual results depend on application & part configuration.

Capstan Permaflow Materials



Porous Metal Disks — Stainless Steel

THICKNESS (IN.)	DIAMETER (IN.)											
	1/8	1/4	3/8	1/2	3/4	1	1-1/4	1-1/2	1-3/4	2		
1/16	✓	✓	✓	✓	✓	✓	✓	✓	✓	✓	✓	✓
1/8	✓	✓	✓	✓	✓	✓	✓	✓	✓	✓	✓	✓
1/4	✓	✓	✓	✓	✓	✓	✓	✓	✓	✓	✓	✓

Porous Metal Disks — Bronze

THICKNESS (IN.)	DIAMETER (IN.)																	
	1/8	1/4	3/8	1/2	5/8	3/4	7/8	1	1-1/4	1-1/2	1-3/4	2	2-1/2	3				
1/16	✓	✓	✓	✓	✓	✓	✓	✓	✓	✓	✓	✓	✓	✓	✓	✓	✓	✓
1/8	✓	✓	✓	✓	✓	✓	✓	✓	✓	✓	✓	✓	✓	✓	✓	✓	✓	✓
1/4	✓	✓	✓	✓	✓	✓	✓	✓	✓	✓	✓	✓	✓	✓	✓	✓	✓	✓
3/8																		
1/2																		

Tolerances: Stainless $\pm .005"$ for all dimensions.
 Bronze $+ .000"/- .010"$, for dimensions up to 1"
 $+ .000"/- .020"$, for dimensions up to 2"
 $+ .000"/- .030"$, for dimensions up to 3"

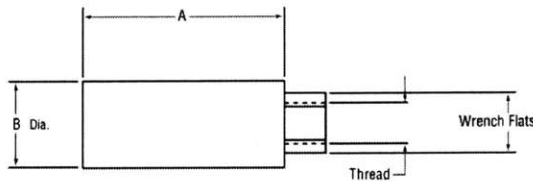
Capstan Permaflow

16124 S. Figueroa Street
 Gardena, CA 90248
 T 310-366-5999
 F 310-366-7832

Porous Bronze — Threaded Elements

PART NUMBER	PIPE THREAD ON FITTING	FILTER DIAMETER (D)	FILTER LENGTH (A)
FAP 100	1/8"	1"	2"
FAP 101	1/4"	1-5/16"	3"
FAP 102	1/2"	1-5/8"	4"
FAP 103	1"	2"	8"

Filter wall thickness is 3/32."



Porous Bronze — Tubes & Sheets

Standard Permaflow Tubes are 8" long with a 3/32" wall thickness.

Standard Diameters ($\pm 1/8"$ O.D.)

1"	3"
1-1/2"	4"
2"	5"
2-1/2"	6"

These tubes are available with both ends open, or with one end closed.

Standard Permaflow Sheets 1/8" or 1/16" thick.

Standard Sizes ($\pm .060"/- .000"$)

3" x 8"
6" x 8"

Flatness Tolerances: $\pm .030"$ on one surface, $\pm .060"$ on the other.

Above data is provided for guideline purposes only. Actual results depend on application & part configuration.

A.2.2 Mott Corporation Steel Disk Filters

Basic shapes.

Standard shapes of Mott porous metal media offer an expedient, cost-effective means of satisfying application requirements. Bulleted (•) items indicate products normally kept in stock for prompt shipment. Many other products are available, some also from stock – consult Mott for more information.

NOTE: Tighter tolerances are available for all products shown. Please contact Mott to speak with our Sales Department if you have more exacting requirements.

For more information about these or other products call Mott at **1-800-BUY-MOTT** or **1-860-747-6333**.

Discs Mott porous 316L SS discs, Series 1000.
Order by Catalog No. 1000-D-T-Micron Grade.



Discs	D, in. (standard tolerance)	T, in. (standard tolerance)	Micron Grade								
			0.2	0.5	2	5	10	20	40	100	
Smallest standard size	0.062 (±0.002)	0.039 (±0.005)									Consult Factory
Largest standard size	1.000 (±0.010)	0.125 (±0.010)									

Also available: discs from 0.031" to 8.375" in diameter, some in stock. Larger discs cut from porous metal sheets are also available.

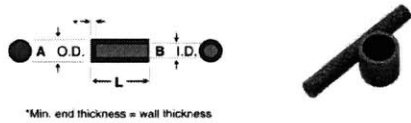
Sheets Mott porous 316L SS sheets, Series 1100.
Order by Catalog No. 1100-W-L-T-Micron Grade.



Sheets	W, in. (standard tolerance)	L, in. (standard tolerance)	T, in. (standard tolerance)	Micron Grade							
				0.2	0.5	2	5	10	20	40	100
Smallest standard size	8.50 (±0.094)	10.00 (±0.094)	0.039/0.062* 0.078/0.093*	•	•	•	•	•	•	•	•
Largest standard size	10.00 (±0.094)	12.00 (±0.094)	0.125*		•	•	•	•	•	•	•

Other sizes and thicknesses are also available, some in stock.

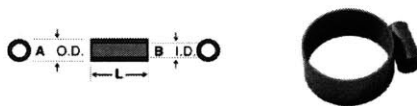
Cups Mott porous 316L SS cups, Series 1200.
Order by Catalog No. 1200-A-B-L-Micron Grade.



Cups	A, in. (standard tolerance)	B, in. (standard tolerance)	L, in. (standard tolerance)	Micron Grade							
				0.2	0.5	2	5	10	20	40	100
Smallest standard size	0.125 (±0.005)	0.062 (±0.005)	0.125 (±0.015)								Consult Factory
Largest standard size	0.812 (±0.008)	0.641 (±0.008)	1.060 (±0.015)								

Also available: cups from .078" to 1.31" O.D., some in stock.

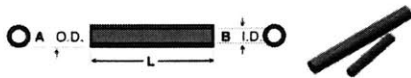
Bushings Mott porous 316L SS bushings, Series 1300.
Order by Catalog No. 1300-A-B-L-Micron Grade.



Bushings	A, in. (standard tolerance)	B, in. (standard tolerance)	L, in. (standard tolerance)	Micron Grade							
				0.5	2	5	10	20	40	100	
Smallest standard size	0.250 (±0.005)	0.125 (±0.005)	1 (±0.015)								Consult Factory
Largest standard size	0.375 (±0.005)	0.250 (±0.005)	1 (±0.015)								

Also available: bushings from 1.38" to 4.528" O.D., some in stock.

Seamless Tubes Mott porous 316L SS seamless tubing, Series 1400. Order Catalog No. 1400-A-B-L-Micron Grade.



Seamless Tubes	A, in. (standard tolerance)	B, in. (standard tolerance)	L, in. (standard tolerance)	Micron Grade						
				0.5	2	5	10	20	40	100
Smallest standard size	0.250 (+0.008) (-0.005)	0.125 (nom.)	6 (±0.031")	•	•	•	•	N/A	N/A	N/A
Largest standard size	1.000 (+0.030) (-0.010)	0.750 (nom.)	12 (±0.031")	•	•	•	•	•	•	•

Lengths in stock: 6", 12", 18", 24". Also available: longer tubes and other diameters, some in stock.

* Depends on µm grade.

Appendix B

B.1 Fann Instrument Company

Fluid Dynamic Filtration Loss Cell

